

## Invited Speaker

**719** Femtosecond extreme-ultraviolet imaging of magnetic domains during ultrafast demagnetization  
Dr. Hung-Tzu Chang<sup>1</sup>, Sergey Zayko<sup>1</sup>, Timo Schmidt<sup>2</sup>, Murat Sivas<sup>1,3</sup>, Manfred Albrecht<sup>2</sup>, Claus Ropers<sup>1,3</sup>

<sup>1</sup>Max Planck Institute for Multidisciplinary Sciences, Göttingen, Germany, <sup>2</sup>Experimental Physics IV, University of Augsburg, Augsburg, Germany, <sup>3</sup>4th Physical Institute, University of Göttingen, Göttingen, Germany

## Oral Presentation

**143** Study of skyrmions in ferromagnetic metallic superlattices using in situ Lorentz magnetic methods

Anaïs Fondet<sup>1</sup>, Dr Thomas Blon<sup>2</sup>, Dr Anne Bernand-Mantel<sup>1</sup>, Dr Christophe Gatel<sup>1</sup>

<sup>1</sup>CEMES-CNRS, Toulouse, France, <sup>2</sup>LPCNO, Toulouse, France

**225** In situ STEM investigations of defect induced memristive switching in off-stoichiometric SrTiO<sub>3</sub>  
Changming Liu<sup>1</sup>, Alexander Meledin<sup>2</sup>, Peng-Han Lu<sup>3</sup>, Wahib Aggoune<sup>4</sup>, Mohamed Abdeldayem<sup>1</sup>, Thilo Remmele<sup>1</sup>, Tobias Schulz<sup>1</sup>, Kaman Yip<sup>2</sup>, Andreas Fiedler<sup>1</sup>, Jutta Schwarzkopf<sup>1</sup>, Rafal Dunin-Borkowski<sup>3</sup>, Matthias Scheffler<sup>4</sup>, Martin Albrecht<sup>1</sup>, Dan Zhou<sup>1</sup>

<sup>1</sup>Leibniz Institut für Kristallzüchtung, Berlin, Germany, <sup>2</sup>Thermo Fisher Scientific Inc., Eindhoven, Netherlands, <sup>3</sup>Ernst Ruska-Center for Microscopy and Spectroscopy with Electrons, Jülich, Germany, <sup>4</sup>Fritz-Haber-Institute of the Max Planck Society, Berlin, Germany

**259** Studying interface charge distribution in HfO<sub>2</sub> and Al<sub>2</sub>O<sub>3</sub> based nanocapacitors by operando electron holography

Dr Leifeng Zhang<sup>1</sup>, Dr Muhammad Hamid Raza<sup>2</sup>, Dr Kilian Gruel<sup>1</sup>, Dr Rong Wu<sup>2</sup>, Dr Catherine Dubourdieu<sup>3</sup>, Dr Martin Hÿtch<sup>1</sup>, Dr Christophe Gatel<sup>4</sup>

<sup>1</sup>CEMES-CNRS, Toulouse, France, <sup>2</sup>Helmholtz-Zentrum Berlin für Materialien und Energie, Berlin, Germany, <sup>3</sup>Freie Universität, Berlin, Germany, <sup>4</sup>CEMES-CNRS, University of Toulouse - Paul Sabatier, Toulouse, France

**403** Multimodal control of the magneto-structural phase transition in FeRh studied by TEM  
Jan Hajducek<sup>1</sup>, Martin Tichý<sup>2</sup>, Jon Ander Arregi<sup>1</sup>, Fabrizio Carbone<sup>3</sup>, Thomas LaGrange<sup>3</sup>, Vojtěch Uhlíř<sup>1,2</sup>

<sup>1</sup>Central European Institute of Technology (CEITEC). Brno University of Technology, Brno, Czech Republic, <sup>2</sup>Institute of Physical Engineering (IPE). Brno University of Technology, Brno, Czech Republic, <sup>3</sup>Laboratory for Ultrafast Microscopy and Electron Scattering (LUMES). École Polytechnique Fédérale de Lausanne, Lausanne, Switzerland

**491** Accessible STEM-DPC Imaging Using ADF Detector Allowing in-situ Magnetic Reversal Studies  
Julie Marie Bekkevold<sup>1,2</sup>, Dr. Magnus Nord<sup>1</sup>

<sup>1</sup>Norwegian University of Science and Technology, Trondheim, Norway, <sup>2</sup>Trinity College Dublin, Dublin, Ireland

**541** Progress in Magnon EELS simulations

Dr. José Ángel Castellanos-Reyes<sup>1</sup>, Dr. Paul Zeiger<sup>1</sup>, Dr. Ján Ruzs<sup>1</sup>

<sup>1</sup>Department of Physics and Astronomy, Uppsala University, Uppsala, Sweden

**610** Electron holography of a vortex-type magnetic domain wall in a cobalt nanotube  
Dr César Magén<sup>1,2</sup>, Dr. Javier Pablo-Navarro<sup>1,2</sup>, Dr. Luis Alfredo Rodríguez<sup>3,4</sup>, Dr. Christophe Gatel<sup>5</sup>, Dr. Ingrid-Marie Andersen<sup>5</sup>, Prof Etienne Snoeck<sup>5</sup>, Prof. José María De Teresa<sup>1,2</sup>

<sup>1</sup>Instituto de Nanociencia y Materiales de Aragón (INMA), Universidad de Zaragoza-CSIC, Zaragoza, Spain, <sup>2</sup>Departamento de Física de la Materia Condensada, Universidad de Zaragoza, Zaragoza, Spain, <sup>3</sup>Grupo de Transiciones de Fase y Materiales Funcionales, Departamento de Física, Universidad del Valle, Cali, Colombia, <sup>4</sup>Centro de Excelencia en Nuevos Materiales (CENM), Departamento de Física,

Universidad del Valle, Cali, , <sup>5</sup>Centre d'Élaboration de Matériaux et d'Études Structurales (CEMES), Toulouse, France

**641** Application of cryogenic in situ biasing (S)TEM holder to study phase transitions in complex oxides

Dr. Yevheniy Pivak<sup>1</sup>, PhD Vasilis Papadimitriou<sup>1</sup>, MSc Tianshu Jiang<sup>2</sup>, PhD Vladimir Roddatis<sup>3</sup>, PhD Leopoldo Molina-Luna<sup>2</sup>, PhD Michele Conroy<sup>4</sup>

<sup>1</sup>DENSsolutions, Delft, The Netherlands, <sup>2</sup>TU Darmstadt, Darmstadt, Germany, <sup>3</sup>GFZ German Research Center for Geosciences, Potsdam, Germany, <sup>4</sup>Imperial College London, London, United Kingdom

**780** Platform for the in-situ measurement of magnetic transport properties in the transmission electron microscope

Sebastian Schneider<sup>1,2</sup>, Steven Waddy<sup>1</sup>, Takanori Sato<sup>1</sup>, Vijay Bhatia<sup>1</sup>, Yevheniy Pivak<sup>3</sup>, David J. Reilly<sup>1</sup>, Bernd Rellinghaus<sup>2</sup>, Julie M. Cairney<sup>1</sup>, Magnus Garbrecht<sup>1</sup>

<sup>1</sup>The University Of Sydney, Sydney Microscopy And Microanalysis, Sydney, Australia, <sup>2</sup>Dresden Center for Nanoanalysis (DCN), TU Dresden, Dresden, Germany, <sup>3</sup>DENSsolutions, , Netherlands

**871** STEM-EELS and Image simulations of inelastic spin-scattering of magnons in confined geometries Julio Do Nascimento<sup>1,2</sup>, Dr. Demie Kepaptsoglou<sup>1,4</sup>, Prof. Quentin Ramasse<sup>2,4</sup>, Prof. Vlado Lazarov<sup>1,2</sup>

<sup>1</sup>School of Physics, Engineering and Technology, University of York, York, United Kingdom, <sup>2</sup>York-JEOL Nanocentre, University of York, York, United Kingdom, <sup>3</sup>SuperSTEM Laboratory, SciTech Daresbury, Daresbury, United Kingdom, <sup>4</sup>School of Chemical and Process Engineering & School of Physics and Astronomy, University of Leeds, Leeds, United Kingdom

**1094** Quantitative EMCD analysis of Fe thin films on MgOx substrates

Mr. Sharath Kumar Manjeshwar Sathyanath<sup>1</sup>, Dr Anna L. Ravensburg<sup>2</sup>, Professor Vassilios Kapaklis<sup>2</sup>, Professor Björgvin Hjörvarsson<sup>2</sup>, Professor Klaus Leifer<sup>1</sup>

<sup>1</sup>Department of Materials Science and Engineering, Uppsala University, Uppsala, Sweden, <sup>2</sup>Department of Physics and Astronomy, Uppsala University, Uppsala, Sweden

**1143** Imaging Chiral Spin Textures with Electron Interferometry and Polarimetry

Professor Benjamin McMorran<sup>1</sup>, Dr. Sergio Montoya<sup>2</sup>, Prof. Eric E. Fullerton<sup>2</sup>

<sup>1</sup>University of Oregon, Eugene, USA, <sup>2</sup>Center for Memory and Recording Research, University of California, San Diego, USA

## Poster Presentation

**34** Chemical and structural investigations of epitaxial Fe-Cr-O thin films

Dr Benedicte Warot-Fonrose<sup>1</sup>, Dr Pamela Vasconcelos Borges Pinho<sup>2</sup>, Dr Alain Chartier<sup>2</sup>, Dr Antoine Barbier<sup>3</sup>, Dr Denis Menut<sup>4</sup>, Dr Myrtille Hunault<sup>4</sup>, Dr Cecile Marcelot<sup>1</sup>, Dr Frederic Miserque<sup>2</sup>, Dr Jean-Baptiste Moussy<sup>3</sup>

<sup>1</sup>CEMES-CNRS, Toulouse, France, <sup>2</sup>Université Paris-Saclay, CEA, Service de recherche en Corrosion et Comportement des Matériaux, Saclay, France, <sup>3</sup>Université Paris-Saclay, CEA, CNRS, SPEC, Saclay, France, <sup>4</sup>Synchrotron SOLEIL, Gif sur Yvette, France

**37** Manipulating topological magnetic structures by in-situ Lorentz microscopy

Dongsheng Song<sup>1</sup>

<sup>1</sup>Institutes of Physical Science and Information Technology, Anhui University, Hefei 230601, China, Hefei, China

**96** Characterisation of Skyrmion Spin Textures in CoB/CoFeB Multilayers

Colin Kirkbride<sup>1</sup>, Dr Razan Aboljadayel<sup>2</sup>, Dr Kayla Fallon<sup>1</sup>, Ms Sara Villa<sup>1</sup>, Dr Trevor Almeida<sup>1</sup>, Prof. Marrows CH<sup>2</sup>, Prof. Stephen McVitie<sup>1</sup>

<sup>1</sup>University of Glasgow, Glasgow, United Kingdom, <sup>2</sup>University of Leeds, Leeds, United Kingdom

**147** Deformation mapping in Lorentz transmission electron microscopy images of magnetic skyrmion lattices

Dr. Thibaud Denneulin<sup>1</sup>, Dr. András Kovács<sup>1</sup>, Pr. Rafal E. Dunin-Borkowski<sup>1</sup>

<sup>1</sup>Ernst Ruska-Centre for Microscopy and Spectroscopy with Electrons and Peter Grünberg Institute, Forschungszentrum Jülich, Jülich, Germany

**172** Quantitative Analysis of Magnetic Spin Textures in Fe<sub>3-x</sub>CoxGeTe<sub>2</sub> Compositions using 4D-STEM  
Mr. Aidan Horne<sup>1</sup>, Dr. Daniel Mayoh<sup>1</sup>, Dr. Damien McGrouther<sup>2</sup>, Prof. Geetha Balakrishnan<sup>1</sup>, Dr. Peng Wang<sup>1</sup>

<sup>1</sup>Department of Physics, University of Warwick, Coventry, United Kingdom, <sup>2</sup>JEOL (UK) Ltd., Welwyn Garden City, United Kingdom

**209** Fine structure tuning for strongly correlated functionalities in high entropy oxides  
Dr. Di Wang<sup>1,2</sup>, Mr. Abhishek Sarkar<sup>1,3</sup>, Mr. Gleb Iankevich<sup>1,4</sup>, Mr. Zhibo Zhao<sup>1</sup>, Mr. Horst Hahn<sup>1,3,4</sup>, Mr. Robert Kruk<sup>1</sup>, Mr. Christian Kuebel<sup>1,2</sup>

<sup>1</sup>Karlsruhe Institute of Technology, Institute of Nanotechnology, Karlsruhe, Germany, <sup>2</sup>Karlsruhe Institute of Technology, Karlsruhe Nano Micro Facility (KNMFi), Karlsruhe, Germany, <sup>3</sup>KIT-TUD Joint Research Laboratory Nanomaterials – Technical University of Darmstadt, Darmstadt, Germany, <sup>4</sup>Karlsruhe Institute of Technology, Institute for Quantum Materials and Technologies, Karlsruhe, Germany

**240** Vacancy-driven electron spin engineering to promote Li-S redox reactions  
PhD JING YU<sup>1,2</sup>, Mr. Andreu Cabot<sup>2</sup>, Mr. Jordi Arbiol<sup>1</sup>

<sup>1</sup>Catalan Institute of Nanoscience and Nanotechnology (ICN2), Bellaterra, 08193, Spain, <sup>2</sup>Catalonia Institute for Energy Research (IREC), Sant Adrià de Besòs, 08930, Spain

**248** Investigating multiferroic phase change dynamics using in-situ electron counted spectrum imaging with synchronized holder control

Liam Spillane<sup>1</sup>, Dr Michele Conroy<sup>2</sup>

<sup>1</sup>Gatan Inc., Pleasanton, USA, <sup>2</sup>Department of Materials, London Centre of Nanotechnology, Henry Royce Institute, Imperial College London, London, UK

**265** Ex situ observation of ferroelectric domain evolution in wurtzite-type AlScN thin films  
Dr. Niklas Wolff<sup>1</sup>, Tim Grieb<sup>2</sup>, Georg Schönweger<sup>3</sup>, Md. Redwanul Islam<sup>1</sup>, Florian F. Krause<sup>2</sup>, Andreas Rosenauer<sup>2</sup>, Stefano Leone<sup>5</sup>, Isabel Streicher<sup>5</sup>, Simon Fichtner<sup>1,4</sup>, Lorenz Kienle<sup>1</sup>

<sup>1</sup>Department of Material Science, Kiel University, Kiel, Germany, <sup>2</sup>Department for Solid State Physics, Bremen University, Bremen, Germany, <sup>3</sup>Department of Electrical and Information Engineering, Kiel University, Kiel, Germany, <sup>4</sup>Fraunhofer Institute for Silicon Technology (ISIT), Itzehoe, Germany, <sup>5</sup>Fraunhofer Institute for Applied Solid State Physics, Freiburg, Germany

**335** L-TEM characterization of controlled skyrmion nucleation in synthetic antiferromagnetic multilayers

Sara Villa<sup>1</sup>, Dr Christopher Barker<sup>2</sup>, Dr Kayla Fallon<sup>1</sup>, Mr Colin Kirkbride<sup>1</sup>, Dr Trevor Almeida<sup>1</sup>, Prof. Christopher Marrows<sup>3</sup>, Prof. Stephen McVitie<sup>1</sup>

<sup>1</sup>School of Physics and Astronomy, University of Glasgow, Glasgow, United Kingdom, <sup>2</sup>National Physics Laboratory (NPL), Teddington, United Kingdom, <sup>3</sup>School of Physics and Astronomy, University of Leeds, Leeds, United Kingdom

**355** Observation of novel ferroelectric domain configurations in PbTiO<sub>3</sub>/DyScO<sub>3</sub> epitaxial films  
Pau Torruella-Besa<sup>1</sup>, Chih-Ying Hsu<sup>1,2</sup>, Ludovica Tovaglieri<sup>2</sup>, Iaroslav Gaponenko<sup>2</sup>, Cécile Hébert<sup>1</sup>, Jean-Marc Triscone<sup>2</sup>, Céline Lichtensteiger<sup>2</sup>, Duncan T. L. Alexander<sup>1</sup>

<sup>1</sup>Electron Spectrometry and Microscopy Laboratory (LSME), Institute of Physics (IPHYS), Ecole Polytechnique Fédérale de Lausanne (EPFL), Lausanne, Switzerland, <sup>2</sup>Department of Quantum Matter Physics, University of Geneva, Geneva, Switzerland

**401** Magnetic behavior of steel studied by in-situ Lorentz microscopy, magnetic force microscopy and micromagnetic simulations

Mari Honkanen<sup>1</sup>, Suvu Santa-aho<sup>2</sup>, Sami Kaappa<sup>3</sup>, Lucio Azzari<sup>1</sup>, Henri Lukinmaa<sup>4,5</sup>, Jaakko Kajan<sup>4</sup>, Samuli Savolainen<sup>4</sup>, Mikko Palosaari<sup>4</sup>, Lasse Laurson<sup>3</sup>, Minnamari Vippola<sup>1,2</sup>

<sup>1</sup>Tampere Microscopy Center / Tampere University, Tampere, Finland, <sup>2</sup>Materials Science and Environmental Engineering / Tampere University, Tampere, Finland, <sup>3</sup>Computational Physics

Laboratory / Tampere University, Tampere, Finland, <sup>4</sup>Stresstech Oy, Jyväskylä, Finland, <sup>5</sup>Verity, Zurich, Switzerland

**458** Nanoscale Chemical Segregation to Twin Interfaces in  $\tau$ -MnAl-C and Resulting Effects on the Magnetic Properties

Mr. Panpan Zhao<sup>1</sup>, Markus Gusenbauer<sup>3</sup>, Harald Oezelt<sup>3</sup>, Daniel Wolf<sup>1</sup>, Thomas Gemming<sup>1</sup>, Thomas Schrefl<sup>3</sup>, Kornelius Nielsch<sup>1,2</sup>, Thomas George Woodcock<sup>1</sup>

<sup>1</sup>Leibniz IFW Dresden, Dresden, Germany, <sup>2</sup>TU Dresden, Dresden, Germany, <sup>3</sup>Department for Integrated Sensor Systems, Danube University Krems, Krems an der Donau, Austria

**468** Twinning in HfO<sub>2</sub> nanocrystals

Hongchu Du<sup>1</sup>, Prof. Dr. Joachim Mayer<sup>1,2,3</sup>

<sup>1</sup>Forschungszentrum Jülich GmbH, Jülich, Germany, <sup>2</sup>RWTH Aachen University, Aachen, Germany, <sup>3</sup>Jülich Aachen Research Alliance, Jülich, Germany

**476** Atomically Sharp Domain Walls in an Antiferromagnet

Jan Michalička<sup>1</sup>, Filip Křížek<sup>2</sup>, Sonka Reimers<sup>3</sup>, Zdenek Kašpar<sup>2</sup>, Ondrej Man<sup>1</sup>, Jan Ruzs<sup>4</sup>, Juan Carlos Idrobo<sup>5</sup>, Peter Wadley<sup>3</sup>, Tomas Jungwirth<sup>1,3</sup>

<sup>1</sup>CEITEC - Brno University of Technology, Brno, Czech Republic, <sup>2</sup>Institute of Physics of CAS, Prague, Czech Republic, <sup>3</sup>School of Physics and Astronomy, University of Nottingham, Nottingham, United Kingdom, <sup>4</sup>Department of Physics and Astronomy, Uppsala University, Uppsala, Sweden, <sup>5</sup>Center for Nanophase Materials Sciences, ORNL, Oak Ridge, USA

**478** Observing Magnetic Skyrmions in Pt/Co/Cu Multilayers using in-situ Lorentz Transmission Microscopy

Nuria Bagues<sup>1,2,3</sup>, Binbin Wang<sup>1,2,4</sup>, Shuyu Cheng<sup>5</sup>, Shekhar Das Das<sup>5</sup>, Ziling Li<sup>5</sup>, Jacob Freyermuth<sup>5</sup>, Camelia Selcu<sup>5</sup>, Denis V. Pelekhov<sup>5</sup>, Chris Hammel<sup>5</sup>, Mohit Randeria<sup>5</sup>, Roland Kawakami<sup>5</sup>, David W McComb<sup>1,2</sup>

<sup>1</sup>Center for Electron Microscopy and Analysis, The Ohio State University, Columbus, US, <sup>2</sup>Department of Material Science and Engineering, The Ohio State University, Columbus, US, <sup>3</sup>Present address: Alba Synchrotron Light Facility, CELLS, Cerdanyola del Vallès, Spain, <sup>4</sup>Present address: Intel Corporation, Hillsboro, US, <sup>5</sup>Department of Physics, The Ohio State University, Columbus, US

**538** Polar textures in multiferroic BiFeO<sub>3</sub>-based superlattices

Dr. Razvan Burcea<sup>1</sup>, Oana Condurache<sup>1</sup>, Mouna Khiari<sup>2</sup>, Maxime Vallet<sup>1</sup>, Stephane Roux<sup>3</sup>, Pascal Ruello<sup>4</sup>, Brahim Dkhil<sup>1</sup>, Houssny Bouyanfif<sup>2</sup>

<sup>1</sup>Université de Paris-Saclay, CentraleSupélec, SPMS, Gif-sur-Yvette, France, <sup>2</sup>LPMC EA2081, Université de Picardie Jules Verne, Amiens, France, <sup>3</sup>Université de Paris-Saclay, ENS Paris-Saclay, LMPS, Gif-sur-Yvette, France, <sup>4</sup>IMMN, Le Mans Université, France

**606** Atomic-resolution STEM analysis of polar states in Sr<sub>1-x</sub>BaxMnO<sub>3</sub> thin films

Dr César Magén<sup>1,2</sup>, Mr Panagiotis Koutsogiannis<sup>1,2</sup>, Prof. PA Algarabel<sup>1,2</sup>, Ms. MP Morales<sup>1</sup>, Dr. JA Pardo<sup>3</sup>

<sup>1</sup>Instituto de Nanociencia y Materiales de Aragón (INMA), Universidad de Zaragoza-CSIC, Zaragoza, Spain, <sup>2</sup>Departamento de Física de la Materia Condensada, Universidad de Zaragoza, Zaragoza, Spain, <sup>3</sup>Departamento de Ciencia y Tecnología de Materiales y Fluidos, Universidad de Zaragoza, Zaragoza, Spain

**614** Investigation of Ferroelectricity using Advanced Microscopy

Xinxin Hu<sup>1</sup>, Felip Sandiumenge<sup>2</sup>, Umair Saeed<sup>1</sup>, Rohini Kumara Cordero Eduards<sup>1</sup>, Gustau Catalan<sup>1,3</sup>, Jordi Arbiol<sup>1,3</sup>

<sup>1</sup>Catalan Institute of Nanoscience and Nanotechnology (ICN2), CSIC and The Barcelona Institute of Science and Technology (BIST), Barcelona, Spain, <sup>2</sup>Institute of Materials Science of Barcelona (ICMAB-CSIC), Barcelona, Spain, <sup>3</sup>ICREA, Barcelona, Spain

**625** Revealing atomic structure and composition in ultrahigh energy storage density ferroelectric thin-films

Prof Shery Chang<sup>1,2</sup>, Dr Daniel Stroppa<sup>3</sup>, Dr Richard Webster<sup>1</sup>, Prof Danyang Wang<sup>2</sup>



<sup>1</sup>Electron Microscope Unit, Mark Wainwright Analytical Centre, University of New South Wales, Sydney, Australia, <sup>2</sup>School of Materials Science and Engineering, University of New South Wales, Sydney, Australia, <sup>3</sup>Dectris Ltd, Baden-Daetwil, Switzerland

**648** Magnetic layers reversal in new MRAM devices measured with operando Electron Holography  
Augustin Nogier<sup>1</sup>, Bernard Dieny<sup>1</sup>, Ricardo Sousa<sup>1</sup>, Christophe Gatel<sup>2</sup>, Eric Gautier<sup>1</sup>, Aurélien Masseboeuf<sup>1</sup>, Kévin Garello<sup>1</sup>

<sup>1</sup>SPINTEC, Grenoble, France, <sup>2</sup>CEMES, Toulouse, France

**659** Domain structures in ferroelectric epitaxial WO<sub>3</sub> thin films

Ewout Van Der Veer<sup>1</sup>, Stijn Feringa<sup>1</sup>, Jack Eckstein<sup>2</sup>, Bart Kooi<sup>1</sup>, Beatriz Noheda<sup>1</sup>

<sup>1</sup>University of Groningen, Groningen, The Netherlands, <sup>2</sup>Cambridge University, Cambridge, United Kingdom

**711** Unveiling moiré-induced topological polar structures in freestanding ferroelectric membranes

Dr Gabriel Sanchez Santolino<sup>1</sup>, Victor Rouco<sup>1</sup>, Sergio Puebla<sup>2</sup>, Hugo Aramberri<sup>3</sup>, Victor Zamora<sup>1</sup>, Fabian Cuellar<sup>1</sup>, Carmen Munuera<sup>2,4</sup>, Federico Monpean<sup>2,4</sup>, Mar García-Hernandez<sup>2,4</sup>, Andrés Castellanos-Gomez<sup>2,4</sup>, Jorge Íñiguez<sup>3,5</sup>, Carlos León<sup>1,4</sup>, Jacobo Santamaría<sup>1,4</sup>

<sup>1</sup>GFMC. Dept. Física de Materiales. Facultad de Física. Universidad Complutense. 28040 Madrid, Spain, , , <sup>2</sup>Instituto de Ciencia de Materiales de Madrid ICMM-CSIC 28049 Cantoblanco. Spain, , ,

<sup>3</sup>Materials Research and Technology Department, Luxembourg Institute of Science and Technology (LIST), Avenue des Hauts-Fourneaux 5, L-4362 Esch/Alzette, Luxembourg, , , <sup>4</sup>Unidad Asociada UCM/CSIC, "Laboratorio de Heteroestructuras con aplicación en spintrónica", , , <sup>5</sup>Department of Physics and Materials Science, University of Luxembourg, 41 Rue du Brill, L-4422 Belvaux, Luxembourg, ,

**958** TEM studies of polarization nanodomains in (BaTiO<sub>3</sub>/SrTiO<sub>3</sub>)<sub>10</sub> superlattices on silicon

Dr Ines Haeusler<sup>1</sup>, Valentin Väinö Hevelke<sup>1</sup>, Adnan Hammud<sup>2</sup>, Prof. Dr. Christoph Koch<sup>3</sup>, Dong Jik Kim<sup>1</sup>, Prof. Dr. Catherine Dubourdieu<sup>1</sup>

<sup>1</sup>Helmholtz-Zentrum Berlin für Materialien und Energie, Institute Functional Oxides for Energy Efficient Information Technology, 14109 Berlin, Germany, <sup>2</sup>Fritz-Haber Institut der Max-Planck-Gesellschaft, 14195 Berlin, Germany, <sup>3</sup>Humboldt-Universität zu Berlin, Department of Physics, 12489 Berlin, Germany

**978** In situ growth and phase engineering of manganese arsenide nanostructures in environmental TEM

Hedda Christine Soland<sup>1,2</sup>, Mikelis Marnauza<sup>1,2</sup>, Pau Ternero<sup>2,3</sup>, Professor Kimberly A. Dick<sup>1,2</sup>

<sup>1</sup>Centre for Analysis and Synthesis, Lund University, Lund, Sweden, <sup>2</sup>NanoLund, Lund University, Lund, Sweden, <sup>3</sup>Solid State Physics, Lund University, Lund, Sweden

**1028** Characterizing Magnetic Properties of Nanoparticle Systems: Insights from Electron Tomography and Micromagnetic Simulations

Cristian Radu<sup>1,2</sup>, Andrei Cristian Kuncser<sup>1</sup>

<sup>1</sup>National Institute of Materials Physics, Atomistilor 405A, 077125, , Romania, <sup>2</sup>Faculty of Physics, University of Bucharest, Atomistilor 405, 077125, , Romania

**1053** Exploring Local Order/Disorder in Relaxor Ferroelectric Materials via TEM and STEM Methods

Beatriz Vargas Carosi<sup>1</sup>, PRanjali Nandi<sup>1</sup>, Lluís Yedra<sup>1</sup>, Sonia Estradé<sup>1</sup>, Angélica M. Benitez-Castro<sup>2,3</sup>, Juan Muñoz-Saldaña<sup>3</sup>, Bernat Mundet<sup>4</sup>, Lluís López-Conesa<sup>1</sup>, Francesca Peiró<sup>1</sup>

<sup>1</sup>LENS, Department of Electronics and Biomedical Engineering and Institute of Nanoscience and Nanotechnology (IN2UB), University of Barcelona (UB), Barcelona, Spain, <sup>2</sup>Institute of Glass and Ceramics, Department of Materials Science and Engineering, Friedeich-Alexander-Universität Erlangen-Nürnberg, Erlangen, Germany, <sup>3</sup>Centro de Investigación y de Estudios Avanzados del IPN, Lib. Norponiente 2000, Querétaro, Mexico, <sup>4</sup>Catalan Institute of Nanoscience and Nanotechnology (ICN2), CSIC and BIST, Campus UAB, Bellaterra, Spain

**1084** Geometric phase analysis-based characterization of skyrmion lattice equilibria

M.Sc Vinko Sršan<sup>1,2</sup>, Asst. Prof. Matej Komelj<sup>2</sup>, Prof. Sašo Šturm<sup>1,2,3</sup>

<sup>1</sup>Jožef Stefan International Postgraduate School, Ljubljana, Slovenia, <sup>2</sup>Department for Nanostructured Materials, Jožef Stefan Institute, Ljubljana, Slovenia, <sup>3</sup>Department of Geology, Faculty of Natural Sciences and Engineering, University of Ljubljana, Ljubljana, Slovenia

**1105** Correlative microscopy for the discovery of novel nano-grains in spintronic materials.

Dr Adam Kerrigan<sup>1</sup>, Dr Irene Azaceta<sup>2</sup>, Dr Ercin Duran<sup>3</sup>, Dr Stuart Cavill<sup>2</sup>, Dr Alex Eggeman<sup>3</sup>, Prof Vlado Lazarov<sup>1,2</sup>

<sup>1</sup>The York-JEOL Nanocentre, University of York, York, United Kingdom, <sup>2</sup>School of Physics, Engineering and Technology, University of York, York, United Kingdom, <sup>3</sup>Department of Materials, University of Manchester, Manchester, United Kingdom

**1165** Exploring polar ordering in lead-free K<sub>0.5</sub>Na<sub>0.5</sub>NbO<sub>3</sub> ferroelectrics using in situ biasing and 4D STEM techniques

prof. Goran Dražić<sup>1,2,3</sup>, Ms. Katarina Žiberna<sup>2,3</sup>, Dr. Oana Condurache<sup>2,3</sup>, prof. Andreja Benčan Golob<sup>2,3</sup>

<sup>1</sup>Department for materials chemistry, National institute of chemistry, Ljubljana, Slovenia, <sup>2</sup>Electronic ceramics department, Jožef Stefan Institute, Ljubljana, Slovenia, <sup>3</sup>Jožef Stefan international postgraduate school, Ljubljana, Slovenia

## Late Poster Presentation

**1272** Unveiling the Mechanisms of Structural Reconstruction and Magnetic Evolution in NiFe<sub>2</sub>O<sub>4</sub> During Phase Transition

Dr. Qi Wang<sup>1,2,3</sup>, Prof. Xiaoyan ZHONG<sup>1,2,3</sup>

<sup>1</sup>Department of Materials Science and Engineering, City University of Hong Kong, Hong Kong, People's Republic of China, <sup>2</sup>City University of Hong Kong Matter Science Research Institute (Futian), Shenzhen, People's Republic of China, <sup>3</sup>Nanomanufacturing Laboratory (NML), City University of Hong Kong Shenzhen Research Institute, Shenzhen, People's Republic of China

719

## Femtosecond extreme-ultraviolet imaging of magnetic domains during ultrafast demagnetization

Dr. Hung-Tzu Chang<sup>1</sup>, Sergey Zayko<sup>1</sup>, Timo Schmidt<sup>2</sup>, Murat Sivas<sup>1,3</sup>, Manfred Albrecht<sup>2</sup>, Claus Ropers<sup>1,3</sup>

<sup>1</sup>Max Planck Institute for Multidisciplinary Sciences, Göttingen, Germany, <sup>2</sup>Experimental Physics IV, University of Augsburg, Augsburg, Germany, <sup>3</sup>4th Physical Institute, University of Göttingen, Göttingen, Germany

PS-08 (2), Lecture Theater 2, august 27, 2024, 14:00 - 16:00

### Background incl. aims

Understanding femtosecond dynamics of magnetic domains such as photoinduced ultrafast demagnetization and magneto-optical switching is important for the development of optoelectronics such as ultrafast optical-magnetic memory devices. Despite intensive research, the extraction and elucidation of those ultrafast magnetization dynamics remains highly challenging due to the multitude of the electronic, phonon, and spin processes involved. Direct observation of nanometer magnetic domain dynamics in real space, in particular, the domain wall profile, can yield valuable information for determining the mechanism of magnetization dynamics (1, 2) yet it remains elusive due to the simultaneous requirement of nanometer and femtosecond spatiotemporal resolution. In this work, we utilize femtosecond extreme ultraviolet (XUV) imaging with high-harmonic light source (3) to visualize the magnetic domain dynamics during the demagnetization of a Co<sub>0.75</sub>Tb<sub>0.25</sub> ferrimagnetic thin film in real time and extract the local changes of the domain walls at each wall position.

### Methods

Coherent diffractive imaging of the Co<sub>0.75</sub>Tb<sub>0.25</sub> thin film produced with magnetron sputtering is conducted with circularly polarized femtosecond XUV pulses at 59 eV (Co M<sub>2,3</sub> edge), which is time-delayed with a 35 fs laser pulse centered at 800 nm exciting the sample. The circularly polarized XUV pulses are produced with high harmonic generation of bi-circular 800 nm and 400 nm laser pulses in He with a MAZEL-TOV configuration (4). The amplitude and phase of the transmitted XUV field is reconstructed using an iterative phase retrieval algorithm and the local magnetization is extracted from the phase difference between the left and right circularly polarized field exiting the sample (5).

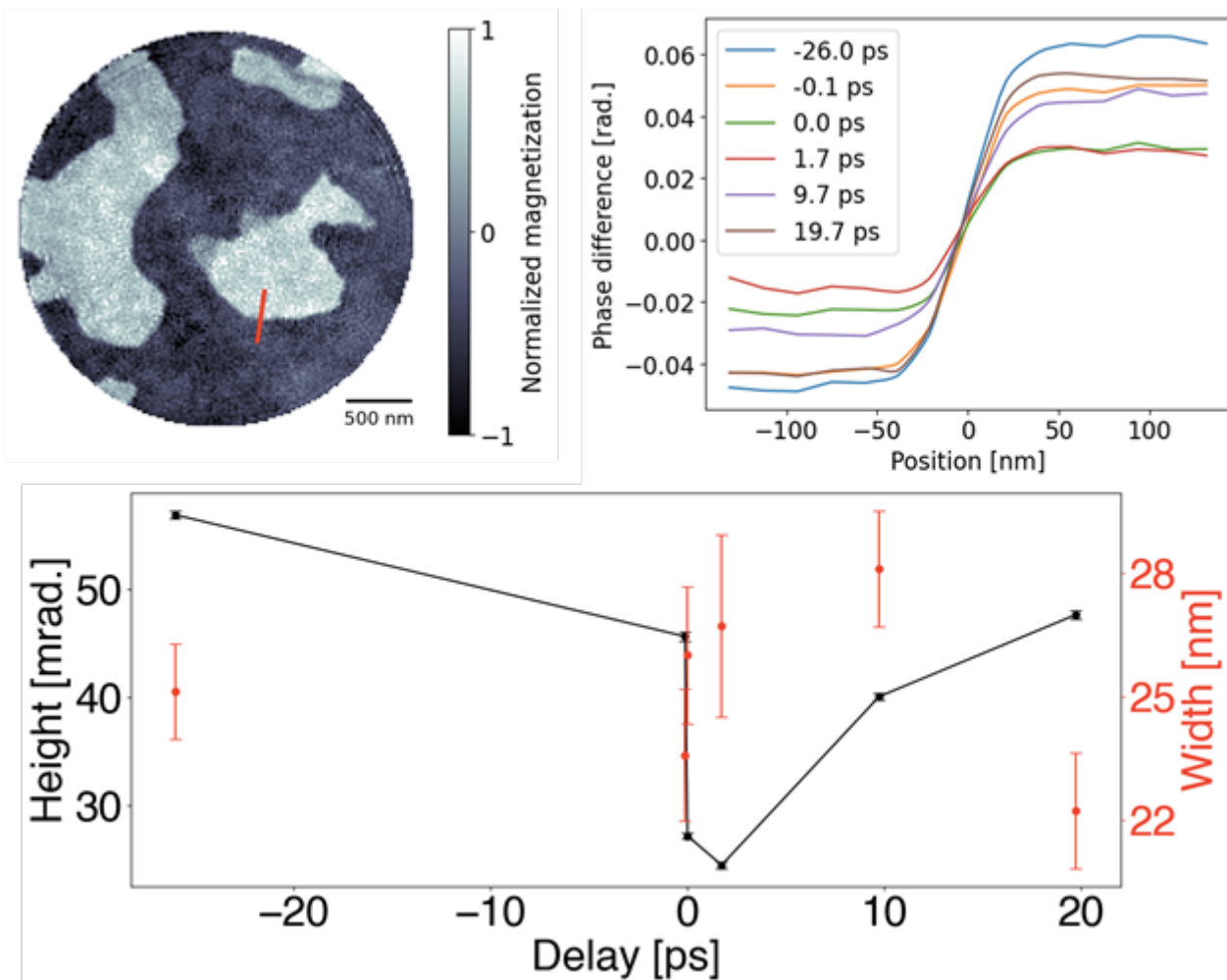
### Results

Using femtosecond imaging at the Co M<sub>2,3</sub> edge with circularly polarized XUV pulses we obtained images of the magnetic domains in Co<sub>0.75</sub>Tb<sub>0.25</sub> thin films with 13.5 nm spatial resolution, which is confirmed with analysis of the phase retrieval transfer function. The positions of the domain walls are determined by the local maxima of magnetization gradient. At each domain wall position, the wall width is extracted by fitting the magnetization as a Bloch-type domain wall function of a cutout perpendicular to the domain wall. By fitting the domain wall profile as a function of time delays between the optical pump and XUV probe, we show that while the domain wall height exhibits a subpicosecond decrease and recovery due to demagnetization, the widths of the domain walls remain largely unchanged throughout 0-20 ps delays with an average of approximately 25 nm.

### Conclusion

In summary, we demonstrate femtosecond XUV imaging of magnetic domain dynamics of a Co<sub>0.75</sub>Tb<sub>0.25</sub> alloy thin film with 13.5 nm spatial resolution and for the first time extract the real-time changes of domain wall widths. The observed real-space domain dynamics can be further utilized to elucidate the mechanisms of the demagnetization process. Our method can be readily

applied to other magnetic thin film materials to understand and control ultrafast magnetization dynamics.



**Keywords:**

Ultrafast magnetization dynamics, EUV imaging

**Reference:**

1. P. Baláž, K. Carva, U. Ritzmann, P. Maldonado, P. M. Oppeneer, Phys. Rev. B. 101, 174418 (2020).
2. R. Jangid et al., Phys. Rev. Lett. 131, 256702 (2023).
3. S. Zayko et al., Nat. Commun. 12, 6337 (2021).
4. O. Kfir et al., Appl. Phys. Lett. 108, 211106 (2016).
5. O. Kfir et al., Sci. Adv. 3, eaao4641 (2017).

143

## Study of skyrmions in ferromagnetic metallic superlattices using in situ Lorentz magnetic methods

Anaïs Fondet<sup>1</sup>, Dr Thomas Blon<sup>2</sup>, Dr Anne Bernard-Mantel<sup>1</sup>, Dr Christophe Gatel<sup>1</sup>

<sup>1</sup>CEMES-CNRS, Toulouse, France, <sup>2</sup>LPCNO, Toulouse, France

PS-08 (1), Lecture Theater 2, august 27, 2024, 10:30 - 12:30

### Background incl. aims

Magnetic skyrmions, which consist of local swirls of spins, are a prime example of topologically nontrivial spin textures. Nanoscale isolated skyrmions exist at low temperature in bulk chiral materials, while in thin films and multilayers, room temperature (RT) stable skyrmions exhibit intermediate sizes ranging between 50 nm to a few  $\mu\text{m}$ . Ferromagnetic metallic superlattices are materials which are promising for the development of RT nanoscale skyrmions due to the high tunability of their properties. There exist a large number of experimental studies reporting the observation of stripe domains and skyrmion bubbles in metallic multilayers, for example Pt/Fe/Ir[1] and Ta/Co/Pt[2]. It is well understood that these skyrmions and stripes are created by a combined action of the stray field effect and the Dzyaloshinskii-Moria interaction (DMI)[3]. These non-collinear spin structures can also be easily simulated numerically [2]. However, in a system with a high number of degrees of freedom, the quest remains open regarding how to optimize the parameters to obtain the most compact and stable skyrmion and the development of adequate analytical tools could lead to breakthrough and transform this quest from a random walk to a guided tour. Many experimental techniques have been used throughout the years in order to study skyrmions, including Magnetic Force Microscopy[4], soft-x-ray microscopy[1] and Magneto-Optical Kerr Effect (MOKE) microscopy [5] among others. But quantitative nanoscale studies on the conditions of skyrmion nucleation remains of primary importance. In this study we chose to study skyrmions in a classical [Pt/Co/Ta] $n$  metallic superlattices system,  $n$  being the number of repetition of the tri-layer.

### Methods

Samples were fabricated by magnetron sputtering, and studied using Lorentz Transmission Electron Microscopy (LTEM) in Fresnel mode combined with electron holography (EH). LTEM in Fresnel mode offers an easy and straightforward method for a semi-quantitative study of the local magnetization, well suited to the observation of skyrmions. We aimed to explore the magnetic phase diagrams of our multilayered magnetic system by developing an automatized process to record magnetic images with in situ application of magnetic field through the control of the objective lens and modulation of the temperature using a dedicated sample holder. In parallel, we used electron holography (EH) which allows to reach higher spatial resolution (up to 0.5 nm) and obtain quantitative magnetic measurements. Our approach is combined with MOKE, theoretical models and numerical simulations (using Mumax3).

### Results

In this system, RT skyrmionic bubbles as small as 50 nm have been observed when the Co thickness was tuned close to the spin reorientation transition[2]. In our study, we fixed the Co thickness at 0.8 nm and we tuned the thickness of the total system by varying the number of repetitions  $n$  of the Pt/Co/Ta tri-layer. This allows us to tune selectively the effect of the stray field while keeping roughly constant the system intrinsic parameters (magneto-crystalline anisotropy, saturation magnetisation, DMI). We were able to image the magnetic micro-structures of [Pt/Co/Ta] $n$  multilayers with various different number of repetitions in LTEM and MOKE (Figure 1a). We conducted an experimental study of the stripe domain structures as a function of the multilayer total thickness, see Figure 1b, and when applying a magnetic field (using the objective lens), we studied the formation process of



magnetic skyrmions, the stripe-skyrmion transition, and the presence of skyrmion lattice or isolated skyrmions in certain samples. We could correlate the magnetic contrast observations with applied field to the magnetic hysteresis obtained from VSM measurements. We also studied the influence of the temperature on the stripe pattern and on the formation of skyrmions, from which we could elaborate experimental phase diagrams coupled to theoretical diagrams, based on skyrmionic bubble model (Figure 2). Finally, we performed EH experiments at the state-of-the-art, combining high spatial resolution with a dedicated Lorentz stage, direct electron detector with the K3 camera and long exposure time up to 4 mn thanks to the dynamical correction of instabilities. We were able to recover the magnetic phase of the Néel type skyrmions up to few nanometers of spatial resolution, and to observe the detailed stripe-to-skyrmion transition with external applied magnetic field (Figure 3). We will detail the magnetic processes which has been deduced from such observations combined with simulations.

### Conclusions

Our experimental study focused on  $[\text{Pt}/\text{Co}/\text{Ta}]_n$  metallic superlattices, investigating the manipulation of their properties by varying the number of repetitions ( $n$ ) of the tri-layer. Through spatially resolved magnetic measurements using magneto-optic techniques and transmission electron microscopy methods combined with in situ experiments, we could explore the stripe domain structures and skyrmion formation as a function of total thickness, the applied magnetic field and varying the temperature. Our findings give new insights of the stripe-skyrmion transition and temperature's influence on these phenomena, supported by experimental phase diagrams and theoretical models. Additionally, we studied Néel-type skyrmions structure using advanced EH observations, achieving a very high spatial resolution and observing detailed transitions from stripe to skyrmion configurations under external magnetic fields. Our study provides significant contributions to understanding the magnetic behaviors of skyrmions in metallic superlattices by combining TEM magnetic imaging and MOKE, correlated to micromagnetic simulations, stripe domain and skyrmion models.

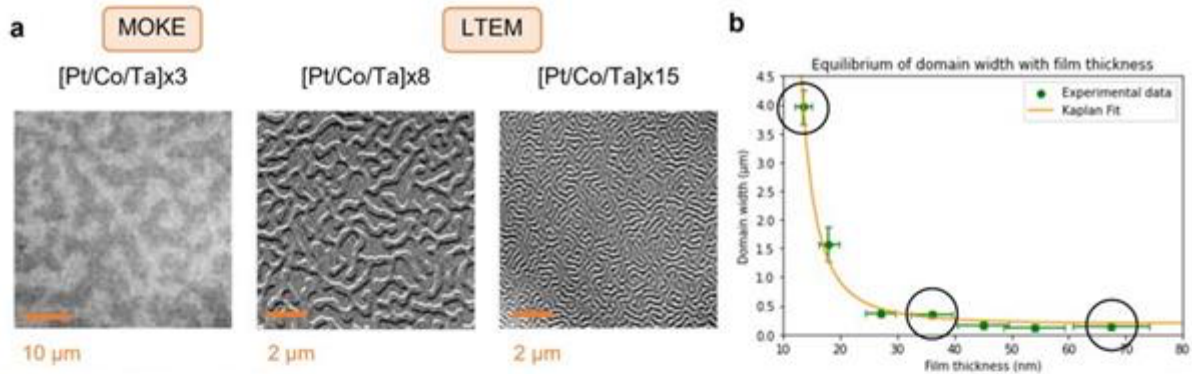


Figure 1 : (a) MOKE and LTEM observations of stripe domains at zero applied field for different numbers of repetition  $n$ , and (b) the stripe domain width as a function of the multilayer thickness in [Pt/Co/Ta] $_n$  multilayers with circled points extracted from images of (a), fitted with Kaplan stripe domains model.

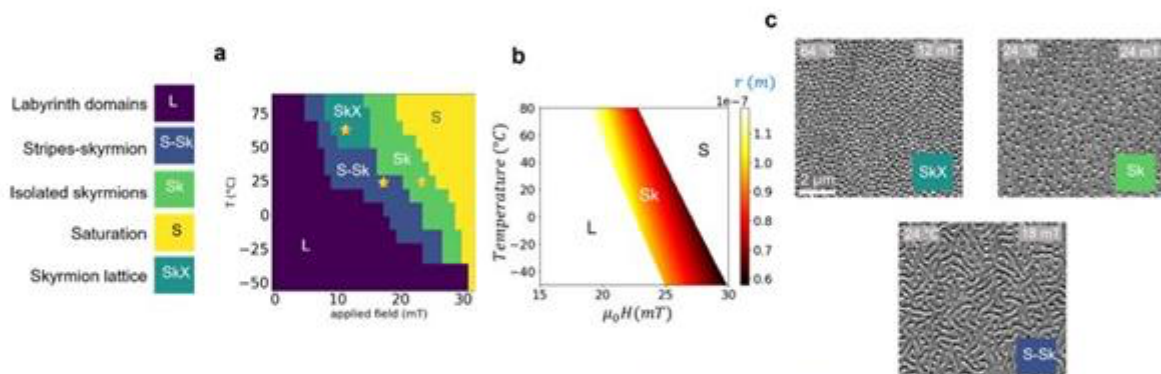


Figure 2 : (a) Experimental phase diagram constructed from series of LTEM images and (b) theoretical skyrmion phase diagram computed from skyrmion model, for [Pt/Co/Ta] $\times$ 12. The images in (c) are LTEM images showing the three different skyrmion phases observed and identified in the phase diagram (a) by the stars, with the temperature ( $^{\circ}\text{C}$ ) and applied magnetic field (mT) indicated in the upper corners.

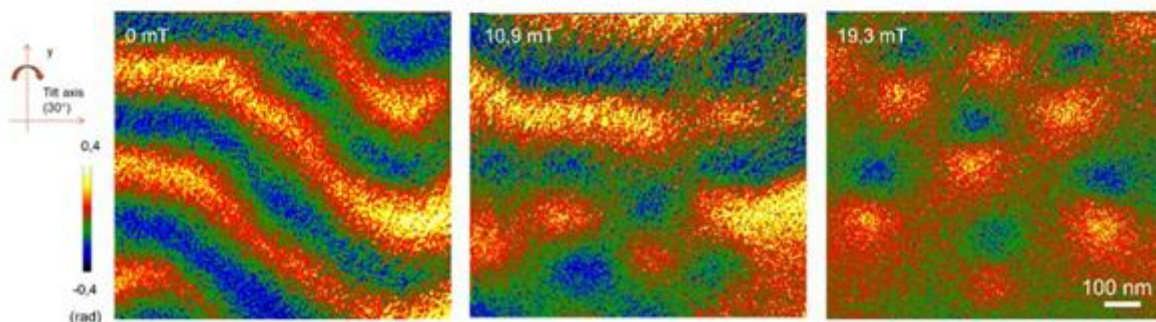


Figure 3 : Magnetic phase images of [Pt/Co/Ta] $\times$ 10 sample extracted from respective holograms at different *in-situ* applied fields, with the sample tilted by 30°. A circular mask has been applied in Fourier space leading to 7 nm spatial resolution.

**Keywords:**

LTEM, EH, skyrmion, MOKE, nanomagnetism

**Reference:**

[1]Moreau-Luchaire, C.et Al. (2016) Additive interfacial chiral interaction in multilayers for stabilization of small individual skyrmions at room temperature, Nature Nanotechnology,11(5), 444-448.

[2]Wang, L., et Al., (2019) Construction of a Room-Temperature Pt/Co/Ta Multilayer Film with Ultrahigh-Density Skyrmions for Memory Application, ACS Applied Materials & Interfaces, 11(12), 12098-12104.

[3]Bernand-Mantel, A.et Al. (2018) The skyrmion-bubble transition in a ferromagnetic thin film, SciPost Physics, 4(5), 027.

[4]Hrabec, A.et Al. (2017), Current-induced skyrmion generation and dynamics in symmetric bilayers, 8(1), 15765.

[5]Schott, M.et Al. (2017), The Skyrmion Switch : Turning Magnetic Skyrmion Bubbles on and off with an Electric Field, Nano Letters,17(5), 3006-3012.

## In situ STEM investigations of defect induced memristive switching in off-stoichiometric SrTiO<sub>3</sub>

Changming Liu<sup>1</sup>, Alexander Meledin<sup>2</sup>, Peng-Han Lu<sup>3</sup>, Wahib Aggoune<sup>4</sup>, Mohamed Abdeldayem<sup>1</sup>, Thilo Remmele<sup>1</sup>, Tobias Schulz<sup>1</sup>, Kaman Yip<sup>2</sup>, Andreas Fiedler<sup>1</sup>, Jutta Schwarzkopf<sup>1</sup>, Rafal Dunin-Borkowski<sup>3</sup>, Matthias Scheffler<sup>4</sup>, Martin Albrecht<sup>1</sup>, Dan Zhou<sup>1</sup>

<sup>1</sup>Leibniz Institut für Kristallzüchtung, Berlin, Germany, <sup>2</sup>Thermo Fisher Scientific Inc., Eindhoven, Netherlands, <sup>3</sup>Ernst Ruska-Center for Microscopy and Spectroscopy with Electrons, Jülich, Germany, <sup>4</sup>Fritz-Haber-Institute of the Max Planck Society, Berlin, Germany

PS-08 (1), Lecture Theater 2, august 27, 2024, 10:30 - 12:30

### Background

In the pursuit of neuromorphic computing, which seeks to emulate the human brain's intricate computational capabilities, the transition of digital memory to an analogue state is crucial. A central scientific question revolves around directing materials to incorporate synaptic plasticity. Among the most promising and technologically advanced strategies for achieving this are resistive random access memory (ReRAM) devices. Traditional ReRAMs operate through the stochastic formation and breakage of conductive filaments within an insulator storage medium, making control challenging. By deliberately introducing an A-site cation (Sr) deficiency in SrTiO<sub>3</sub> of up to about 16% through metal organic vapor phase epitaxy (MOVPE), we have successfully realized resistive switching without the need for filament formation, achieving on/off ratios as high as 10<sup>3</sup> [1].

In this study, we integrated various techniques of in situ scanning transmission electron microscopy, including differential phase contrast (DPC) imaging, integrated-DPC imaging, energy-dispersive X-ray spectroscopy (EDS), electron energy-loss spectroscopy (EELS), precession electron diffraction, along with I-V curve measurements. This comprehensive approach enabled us to gain insights into the underlying mechanisms and holds potential for developing more controllable memristive materials for ReRAM devices.

### Methods

The theoretical crystal and electronic structures were calculated by the Heyd-Scuseria-Ernzerhof (HSE) hybrid functional method within density functional theory (DFT). The STEM simulations were performed with the structure concluded from the HSE calculations and with the simulation code adapted from Kirkland[2]. The high-resolution STEM imaging and spectroscopy were acquired from a probe-corrected Thermo Fisher Scientific Spectra Ultra operated at 300 kV, while the precession-assisted 4D STEM were obtained on Tescan Tensor STEM operated at 100 kV.

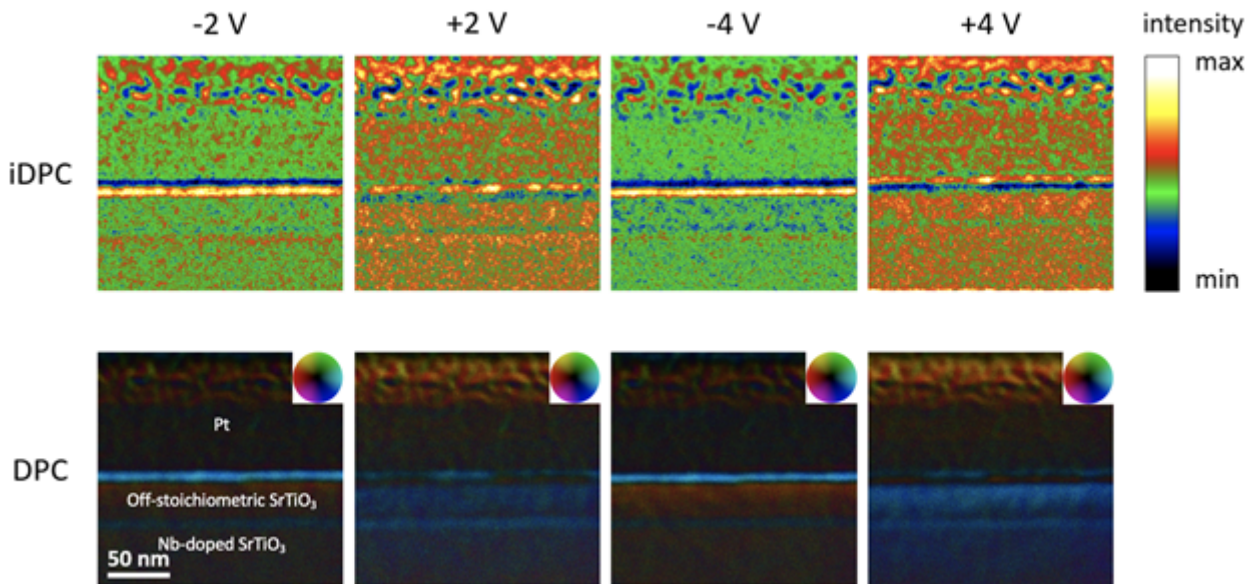
### Results

As shown in the figure, a reversible switching of electrical field direction was observed from iDPC and DPC imaging of the off-stoichiometric SrTiO<sub>3</sub> TEM sample upon in situ switching between positive to negative bias. Reducing the voltage to 0 V results in a stable state, albeit with the polarization erased, returning the local film to a high-resistance state. The results from EDS and EELS mapping tells that approximately 16% of the V<sub>Sr</sub> sites are occupied by Ti. The observed resistive switching phenomena can be attributed to trap-assisted tunneling through Ti antisite defects, which induce a switchable polarization characterized by negative spherical aberration imaging (NCSI).

Additional details, including scanning precession electron diffraction, which maps nanoscale strain and electric field with high precision, EELS mapping, which discerns different valence states of Ti, and a few others, will be presented on site.

## Conclusion

The correlation between structure, composition, bias and electric field distribution from in situ STEM biasing experiments gives direct evidence of antisite defects induced memristive switching in the off-stoichiometric SrTiO<sub>3</sub> sample. The findings offer bottom-up perspective on the promising prospects for future neuromorphic computing applications. The workflow presented here facilitates new insights in developing similar materials.



## Keywords:

Resistive switching, antisite defects, DPC, in-situ biasing TEM

## Reference:

- [1] A. Baki, J. Stöver, T. Schulz, et al. Influence of Sr deficiency on structural and electrical properties of SrTiO<sub>3</sub> thin films grown by metal–organic vapor phase epitaxy. *Sci Rep* 11, 7497 (2021).
- [2] Earl J. Kirkland, Book: *Advanced Computing in Electron Microscopy*, Springer, 2010.



## Studying interface charge distribution in HfO<sub>2</sub> and Al<sub>2</sub>O<sub>3</sub> based nanocapacitors by operando electron holography

Dr Leifeng Zhang<sup>1</sup>, Dr Muhammad Hamid Raza<sup>2</sup>, Dr Kilian Gruel<sup>1</sup>, Dr Rong Wu<sup>2</sup>, Dr Catherine Dubourdieu<sup>3</sup>, Dr Martin Hÿtch<sup>1</sup>, Dr Christophe Gatel<sup>4</sup>

<sup>1</sup>CEMES-CNRS, Toulouse, France, <sup>2</sup>Helmholtz-Zentrum Berlin für Materialien und Energie, Berlin, Germany, <sup>3</sup>Freie Universität, Berlin, Germany, <sup>4</sup>CEMES-CNRS, University of Toulouse - Paul Sabatier, Toulouse, France

PS-08 (1), Lecture Theater 2, august 27, 2024, 10:30 - 12:30

### Background

Among dielectric materials, HfO<sub>2</sub> and Al<sub>2</sub>O<sub>3</sub> are widely studied for micro and nanoelectronic applications. They present very interesting properties for several types of devices such as a higher dielectric constant compared to SiO<sub>2</sub>, high thermal stability and a compatibility with complementary metal oxide semiconductor (CMOS) technologies. For instance, resistive random-access memory (RRAM) devices [1, 2] or memristor devices [3] containing high- $\kappa$  HfO<sub>2</sub> and Al<sub>2</sub>O<sub>3</sub> dielectrics are promising candidates in neuromorphic computing. However, the exact location of the charge stored in such devices is subject of debate and hence the mechanisms for charge trapping remain unclear. Particularly, the influence of interface charges has rarely been addressed because of the lack of suitable characterization techniques.

Whilst dielectric properties can be readily measured macroscopically using electrical methods, the task is difficult at the nanoscale. What is missing is a local and direct measurement of the electrical potential distribution within such devices upon biasing. Indeed, the phase of the electron hologram can be directly related to the electrostatic potential encountered by the fast electron along its trajectory. Recently, we were able to perform operando electron holography experiments in the same region under different biases and to successfully map the electric potential across a working SiO<sub>2</sub>-based MOS nanocapacitor with unprecedented sensitivity [4]. We observed an unexpected charging of the dielectric at both interfaces with the electrodes, over a distance extending up to few nanometers, a value much larger than the structural or chemical width of each interface [4]. In this study, we aim to take one step further to quantify the trapped charge at several interfaces, including insulator-insulator interfaces and metal-insulator interfaces, for which we have designed two thin tri-layer nanocapacitors: TiN/HfO<sub>2</sub>/Al<sub>2</sub>O<sub>3</sub>/HfO<sub>2</sub>/TiN (T-1) and TiN/Al<sub>2</sub>O<sub>3</sub>/HfO<sub>2</sub>/Al<sub>2</sub>O<sub>3</sub>/TiN (T-2) as shown in Fig. 1(a) & (b).

### Methods

The tri-layer nanocapacitors were fabricated by atomic layer deposition (ALD). Each HfO<sub>2</sub> or Al<sub>2</sub>O<sub>3</sub> layer has a nominal thickness of 20 nm. TiN layers were deposited by sputtering before and after the insulating layer to serve as top and bottom electrodes during electrical biasing. In situ biasing TEM experiments necessitate a specific and complex sample preparation that minimizes preparation artifacts whilst ensuring the electrical functionality of the specimen itself. Specimens were prepared by FIB (FEI Helios 600i), on a Hummingbird chip-based biasing holder. Holography experiments were carried out using a Hitachi HF-3300 (I2TEM) microscope operating at 300 kV in Lorentz mode enabling a large field of view with a spatial resolution of 0.5 nm. Holograms were acquired during long exposure time using dynamical automation for compensating instabilities under different applied bias [5]. Finite element method (FEM) modelling was performed using COMSOL software to interpret the phase profiles quantitatively, including factors such as specimen geometry, preparation artefacts and stray fields around the sample device.

### Results

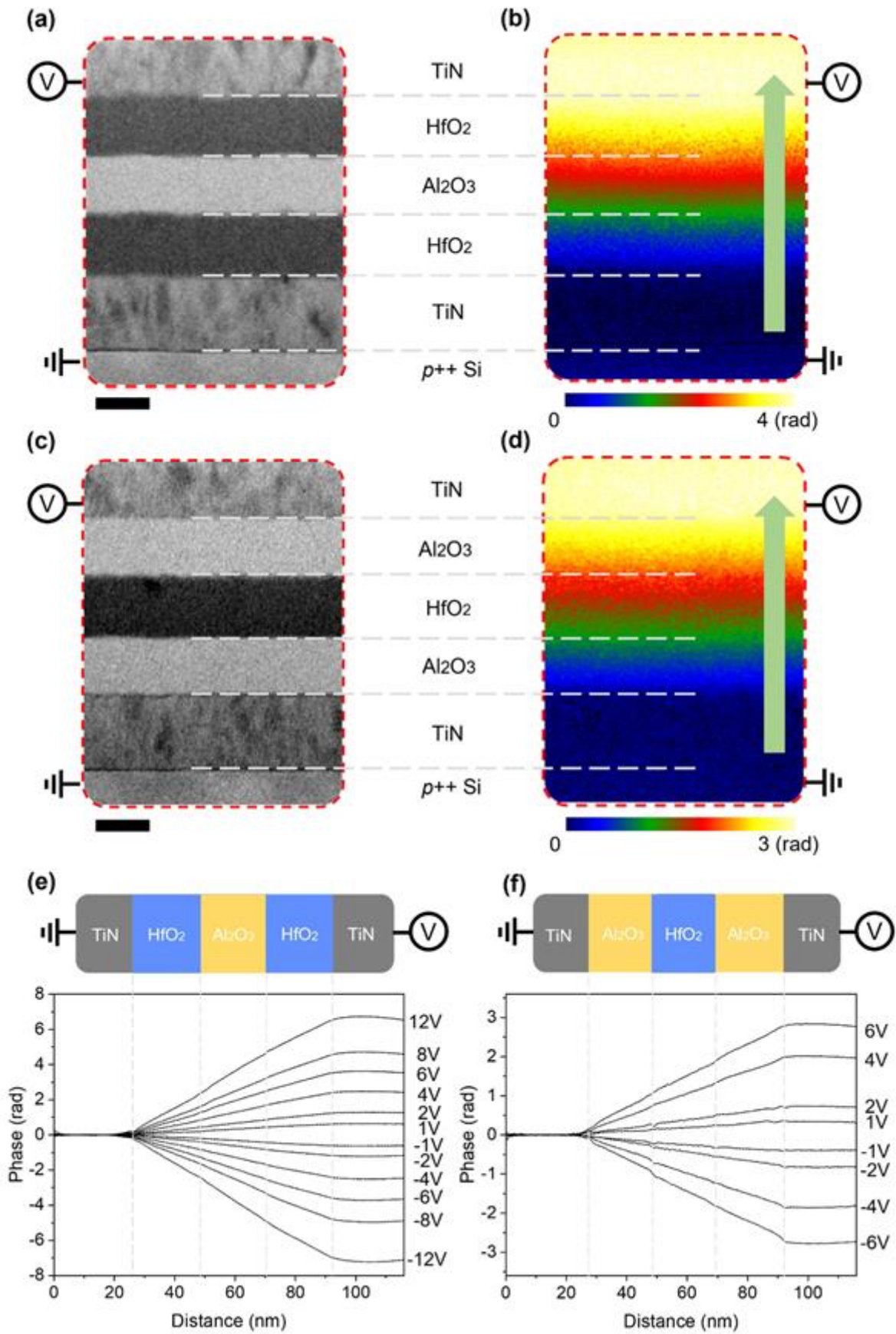
Figures (a) and (b) show the studied regions for T-1 and T-2, respectively while the corresponding phase maps extracted from holograms acquired under a bias of 6V are given in Figure (b) and (d), respectively. The phase map has been corrected by the reference hologram at 0 V, by which the experimental artifacts were removed and the remaining signal can be attributed to the applied electrical biasing. The artifacts comprise the possible variable lamella thickness, damage layers, diffraction contrast, and electron-beam-induced charging.

The amplitude of the measured phase profiles across the tri-layer insulators (Figures (e) and (f)) extracted from phase images rise with increased bias, and appear symmetric when switching the sign of the bias, for example, 6 V and -6 V. However, the potential distributions as well as the measured electrical fields are quite different from those expected theoretically. Considering a relative permittivity of 7.4 for Al<sub>2</sub>O<sub>3</sub> and 18 for HfO<sub>2</sub>, both measured by C-V tests at 100 kHz for their macro devices, the electric field should be 2.44 times higher in Al<sub>2</sub>O<sub>3</sub> than HfO<sub>2</sub>, which consequently should result in a 2.44 times higher potential drop in Al<sub>2</sub>O<sub>3</sub>. In contrast, the experimental phase profiles highlight a homogenous electric field in all the layers for both T-1 and T-2 due to the appearance of charged layers at insulator-insulator interfaces as well as metal-insulator interfaces. Combined with extensive FEM simulations, we successfully quantified the charge densities of each interface for both capacitors as a function of the applied bias responsible of the homogenous electric field. These charges densities linearly vary with the applied bias and present a thickness between 3 and 5 nm width. Scanning TEM electron energy loss spectroscopy (STEM-EELS) measurements have been carried out to understand the origin of these charged interfaces.

Figure. (a) Device structure for T-1; (b) phase map of projected electric potential obtained by electron holography for T-2; (c) Device structure of T-2; (d) phase map of T-2. Here, (b) and (d) correspond to the same regions as (a) and (c) for T-1 and T-2, respectively. Scale bars are 20 nm in (a) and (c). (e) and (f) are the phase profiles extracted from the green arrows as a function of applied biasing for T-1 and T-2, respectively.

## Conclusion

We used operando electron holography to evidence and quantify charges occurring at the different interfaces in tri-layer HfO<sub>2</sub>/Al<sub>2</sub>O<sub>3</sub>/HfO<sub>2</sub> and Al<sub>2</sub>O<sub>3</sub>/HfO<sub>2</sub>/Al<sub>2</sub>O<sub>3</sub> nanocapacitors with TiN electrodes. An equivalent uniform electric field distribution throughout the whole dielectric stack in HfO<sub>2</sub> and Al<sub>2</sub>O<sub>3</sub> is observed even though HfO<sub>2</sub> has a much larger dielectric permittivity than Al<sub>2</sub>O<sub>3</sub>. The electric field distribution originates from the presence of charges trapped at each interface. It is revealed that there is a linear relationship between the surface charge density and the applied bias, and, at each bias, the interfaces between HfO<sub>2</sub> and Al<sub>2</sub>O<sub>3</sub> have an equivalent trapped charge density. With unprecedented sensitivity and spatial resolution, the information gained with operando electron holography on the location of the trapped charges and on their densities provide unique insights on the functioning of nanocapacitors. Further work could be devoted to the interface charging behaviour in ferroelectric-dielectric devices.



**Keywords:**

Electric field mapping, electron holography

**Reference:**

- [1] C. Li, et al., *Advanced Materials*, 29, 1602976 (2017)
- [2] E. A. Khera, et al., *RSC advances*, 12, 11649 (2022)
- [3] M. Rao, et al., *Nature*, 615, 823-829 (2023)
- [4] C. Gatel, et al., *Physical Review Letters*, 129, 137701 (2022)
- [5] C. Gatel, et al., *Appl. Phys. Lett*, 113, 133102 (2018)

403

## Multimodal control of the magneto-structural phase transition in FeRh studied by TEM

Jan Hajducek<sup>1</sup>, Martin Tichý<sup>2</sup>, Jon Ander Arregi<sup>1</sup>, Fabrizio Carbone<sup>3</sup>, Thomas LaGrange<sup>3</sup>, Vojtěch Uhlíř<sup>1,2</sup>

<sup>1</sup>Central European Institute of Technology (CEITEC). Brno University of Technology, Brno, Czech Republic, <sup>2</sup>Institute of Physical Engineering (IPE). Brno University of Technology, Brno, Czech Republic, <sup>3</sup>Laboratory for Ultrafast Microscopy and Electron Scattering (LUMES). École Polytechnique Fédérale de Lausanne, Lausanne, Switzerland

PS-08 (1), Lecture Theater 2, august 27, 2024, 10:30 - 12:30

### Background incl. aims

The onset and properties of long-range ordering in solids come from a fine interplay between different order parameters. Materials featuring magneto-structural phase transitions constitute optimal systems for investigating the interplay of structural, electronic, and magnetic order parameters. The equiatomic FeRh alloy is a prototypical system undergoing a first-order magneto-structural phase transition from antiferromagnetic (AF) to ferromagnetic (FM) order upon heating (350 – 380 K), that is accompanied by a lattice parameter expansion [1]. Broad options for the tunability of the transition temperature via doping, strain, magnetic field, or controlled disorder make the system attractive for micro- and nanoscale spintronics [2], magnetocalorics, and sensors. The fulfillment of the application potential however requires the understanding of the phase coexistence, phase boundary properties, and transition dynamics at nanoscale. Here we demonstrate broad possibilities of controlling and sensing different ordering parameters of the FeRh phase transition using TEM.

### Methods

TEM investigations are performed in free-standing FeRh thin films which were epitaxially grown on MgO substrates via magnetron sputtering and subsequently released by chemically dissolving the MgO substrate. Different external stimuli are applied in-situ in TEM to drive the FeRh transition, namely, magnetic field, stage-induced static heating, or fs-laser-induced heating [3]. Other stimuli are applied ex-situ to locally tune the transition properties, such as ion irradiation. The induced structural and magnetic order modifications in FeRh are then explored using different TEM-based techniques, such as Lorentz TEM (LTEM), Transfer of Intensity (TIE) reconstruction of LTEM [4], Differential Phase Contrast (DPC), Electron Magnetic Circular Dichroism (EMCD) [5], or Selected Area Electron Diffraction (SAED).

### Results

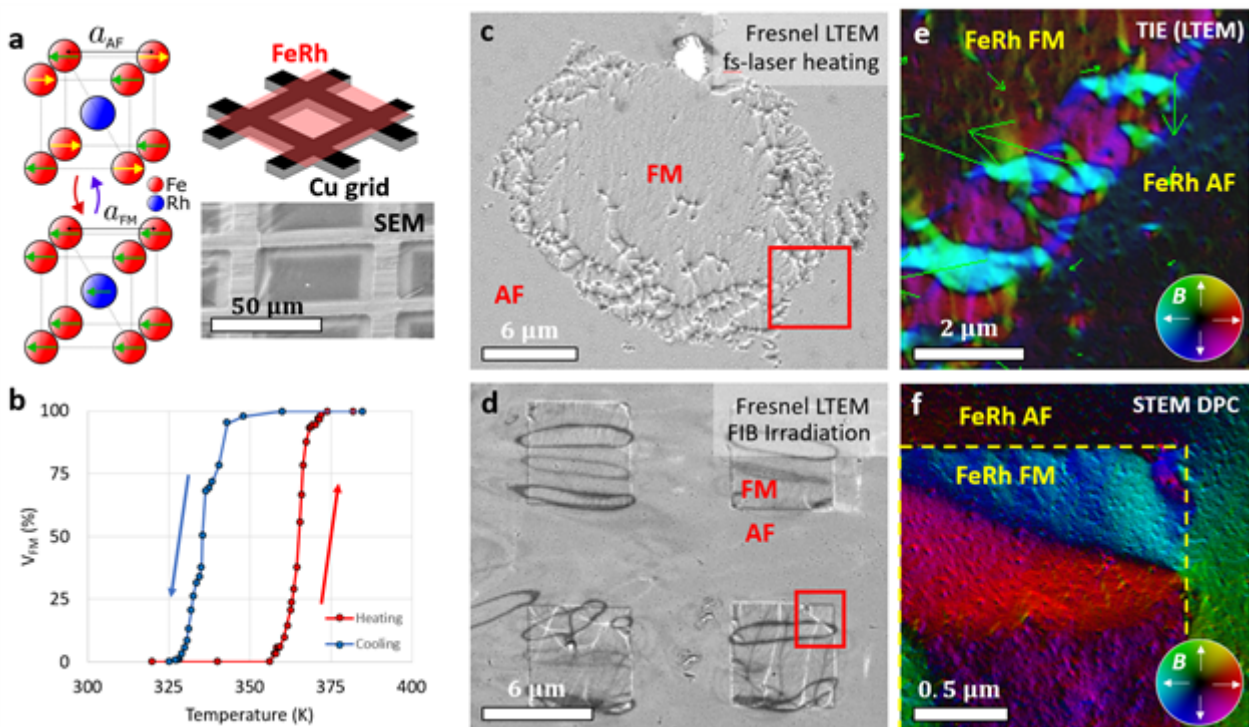
The studied free-standing FeRh film exhibits a well-defined phase transition as evidenced by the thermal evolution of the magnetic and structural ordering parameters that vary between AF and FM phases, as shown in Fig 1(a). TEM enables unprecedented nanoscale visualization of the evolution of the phase transition upon following magnetization via LTEM or lattice parameter from SAED. For instance, Fig 1(b) shows the temperature dependence of the FM phase domain content as measured via LTEM. Apart from stage-driven static heating, the AF-FM transition in FeRh can be driven by fs-laser light or locally by ion irradiation as can be seen in Fig 1(c) and 1(d), respectively. High-resolution vectorial magnetic reconstruction can be done either using TIE-LTEM or DPC as shown in Fig 1(e) and (f), respectively.

### Conclusion



Overall, we demonstrate that multimodal TEM represents a unique experimental platform to tackle state-of-the-art challenges in probing the interplay between different order parameters in magnetic systems at the nanoscale. In particular, we show that in combination with different stimuli, nanoscale phase coexistence of structural and magnetic orders in FeRh can be uniquely probed and disentangled. Furthermore, high-resolution magnetic imaging using STEM-DPC represents a unique tool for investigating magnetic phases and their boundaries at the nanoscale.

Figure 1: (a) Schematics of the phase transition in FeRh and the sample geometry for TEM. (b) Temperature-dependent FM phase fraction in FeRh as obtained from LTEM. (c-d) LTEM imaging of the FM phase induced by fs-laser induced heating, and by localized ion irradiation using gallium FIB, respectively. (e) High-resolution image of the laser-induced FM phase using TIE reconstruction. (f) High-resolution image of the ion irradiation-induced FM phase using STEM DPC.



### Keywords:

FeRh, TEM, magnetic imaging

### Reference:

- [1]: Maat, S., et al. Phys. Rev. B 72(21), 214432 (2005).
- [2]: Chen, X. Z., et al. Nat. Commun. 8: 449 (2017).
- [3]: Hajduček, J., et al. In preparation. (2024).
- [4]: De Graef, M., et al. J. Appl. Phys. 89, 7177–7179 (2001).
- [5]: LaGrange, T., et al. In preparation. (2024).

491

## Accessible STEM-DPC Imaging Using ADF Detector Allowing in-situ Magnetic Reversal Studies

Julie Marie Bekkevold<sup>1,2</sup>, Dr. Magnus Nord<sup>1</sup>

<sup>1</sup>Norwegian University of Science and Technology, Trondheim, Norway, <sup>2</sup>Trinity College Dublin, Dublin, Ireland

PS-08 (1), Lecture Theater 2, august 27, 2024, 10:30 - 12:30

Scanning transmission electron microscopy (STEM) is a powerful tool for both structural and functional characterisation of materials. Phase contrast techniques such as differential phase contrast (DPC) are commonly used to observe functional properties, for example magnetic fields inside samples. However, phase contrast imaging typically requires specialised equipment such as segmented or pixelated detectors[1]. In this work we have imaged nanomagnet arrays to demonstrate the feasibility of a simplified and accessible method for DPC using a monolithic annular dark field (ADF) detector. Using the post-specimen deflector lenses, the electron beam is shifted onto an edge of the ADF detector to translate magnetic deflection into intensity variations in the image[2]. By acquiring such images at four opposing edges of the ADF detector we were able to qualitatively image the magnetic landscape of our nanomagnet structures. The images were corrected for de-scan background intensity variation and then processed like data from an annular four-segmented detector. The resulting DPC image is very well in agreement with that acquired from a center-of-mass calculation from a pixelated detector. Additionally, we show that the increased speed and lowered data set size of this accessible STEM-DPC method, when compared with 4D-STEM, allows for characterisation of the magnetic hysteresis of nanomagnet arrays with different geometries. DPC images of a nanomagnet array in three different magnetic configurations can be seen in Fig. 1. In conclusion, this method makes qualitative DPC available in most STEM-capable TEMs, enables fast and easy in-situ magnetic experiments, and paves an accessible route to correlation of observed function with structural properties.

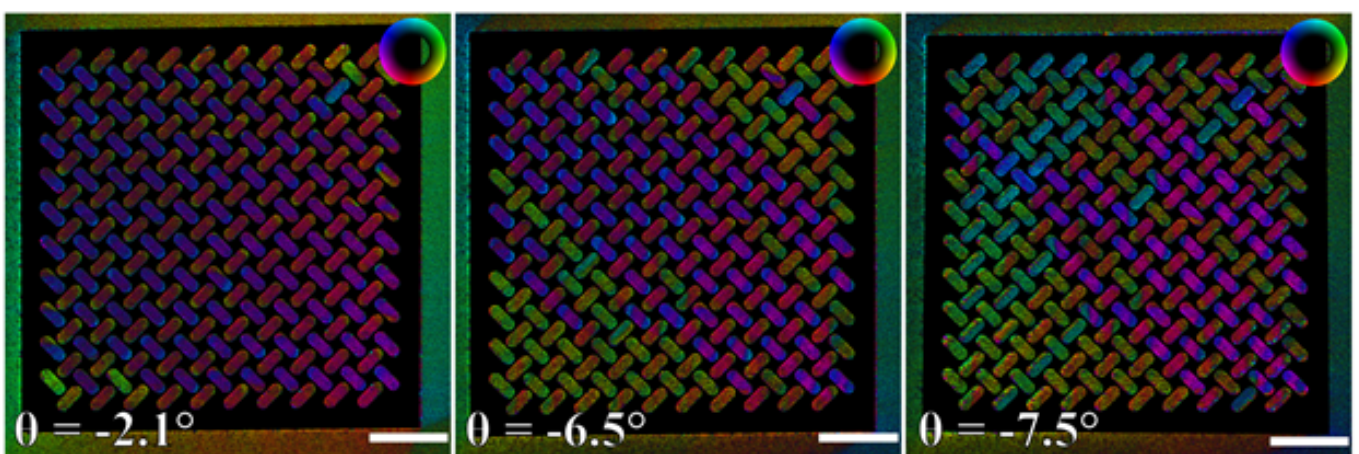


Figure 1: Nanomagnet array in three different magnetic configurations during an in-situ magnetic reversal experiment. DPC images calculated from four images acquired with the monolithic ADF detector.

### Keywords:

DPC, in-situ, magnetic hysteresis

**Reference:**

1. Yang, H., Pennycook, T. J. & Nellist, P. D. Efficient phase contrast imaging in STEM using a pixelated detector. Part II: Optimisation of imaging conditions. *Ultramicroscopy* 151, 232–239 (2015).
2. Kraut, S. & Cowley, J. M. A simplified mode of differential phase contrast lorentz microscopy. *Microsc. Res. Tech.* 25, 341–345 (1993).

541

## Progress in Magnon EELS simulations

Dr. José Ángel Castellanos-Reyes<sup>1</sup>, Dr. Paul Zeiger<sup>1</sup>, Dr. Ján Ruzs<sup>1</sup>

<sup>1</sup>Department of Physics and Astronomy, Uppsala University, Uppsala, Sweden

PS-08 (1), Lecture Theater 2, august 27, 2024, 10:30 - 12:30

### Background incl. Aims

Magnons, the quanta of spin waves, play a pivotal role in various solid-state phenomena, including memory and information processing [1]. Understanding their behavior at the nanoscale is crucial for advancing magnetic technologies. Electron energy loss spectroscopy (EELS) holds promise for probing these excitations with high spatial resolution [2, 3], potentially enabling the exploration of magnon dispersions down to the atomic scale. However, experiments face substantial challenges due to the overlap in excitation energy ranges between phonons and magnons, with phonon signals typically overshadowing magnon signals significantly [3]. Hence, elucidating optimal conditions for discerning magnon EELS signals remains crucial.

In this work, we present our progress in simulating inelastic electron scattering signals of magnons in Scanning Transmission Electron Microscopy, discussing the feasibility of Magnon EELS detection.

### Methods

We implement a new methodology [4] to compute magnon EELS from Pauli-multislice simulations. In particular, this methodology integrates state-of-the-art simulation techniques to model magnon spectra, including the Frozen Magnon Multislice Method with absorptive-potential-based phonon scattering [3].

### Results

We present findings suggesting the potential for detecting statistically significant magnon signals by selecting combinations of temperature and sample thickness [3]. Additionally, we show the capabilities of our methodology by presenting angle-resolved magnon EELS simulations.

### Conclusion

Our simulations suggest the existence of feasible conditions to differentiate magnon inelastic signals from phonon signals. Also, we show the potential of our developed methodology to simulate angle-resolved magnon EELS signals.

### Keywords:

Magnons Phonons EELS Multislice

### Reference:

- [1] A. Barman et al., *J. Phys.: Condens. Matter* 33, 413001 (2021).
- [2] K. Lyon et al., *Phys. Rev. B* 104, 214418 (2021).
- [3] J. Á. Castellanos-Reyes et al., *Phys. Rev. B* 108, 134435 (2023).
- [4] J. Á. Castellanos-Reyes, P. Zeiger, and J. Ruzs, arXiv:2401.15599 [cond-mat.mtrl-sci] (2024).

610

## Electron holography of a vortex-type magnetic domain wall in a cobalt nanotube

Dr César Magén<sup>1,2</sup>, Dr. Javier Pablo-Navarro<sup>1,2</sup>, Dr. Luis Alfredo Rodríguez<sup>3,4</sup>, Dr. Christophe Gatel<sup>5</sup>, Dr. Ingrid-Marie Andersen<sup>5</sup>, Prof Etienne Snoeck<sup>5</sup>, Prof. José María De Teresa<sup>1,2</sup>

<sup>1</sup>Instituto de Nanociencia y Materiales de Aragón (INMA), Universidad de Zaragoza-CSIC, Zaragoza, Spain, <sup>2</sup>Departamento de Física de la Materia Condensada, Universidad de Zaragoza, Zaragoza, Spain, <sup>3</sup>Grupo de Transiciones de Fase y Materiales Funcionales, Departamento de Física, Universidad del Valle, Cali, Colombia, <sup>4</sup>Centro de Excelencia en Nuevos Materiales (CENM), Departamento de Física, Universidad del Valle, Cali, , <sup>5</sup>Centre d'Élaboration de Matériaux et d'Etudes Structurales (CEMES), Toulouse, France

PS-08 (2), Lecture Theater 2, august 27, 2024, 14:00 - 16:00

### Background incl. aims

Three-dimensional nanomagnets and curved magnetism are nowadays exciting topics in Nanomagnetism. The appearance of novel spin textures and topologically protected magnetization states may be the key to develop 3D spintronic devices for magnetic data storage, magnetic logics and sensing [1]. One of these exciting architectures are ferromagnetic nanotubes (NTs), in which the predicted core-less spin states are ideal for stable and fast domain wall (DW) motion beyond the Walker limit [2]. Even though they have modelled and predicted theoretically, a detailed experimental observation of these DWs is missing. In this work we aim at revealing the nature of magnetic DWs in cobalt NTs.

### Methods

Focused electron beam induced deposition (FEED) [3] has been used to synthesize 3D cobalt NTs. FEED is an exceptional nanolithography technique to produce high-quality magnetic architectures. It is a direct one-step nanolithography technique that allows 2D and 3D growth of architectures of almost arbitrary shape on virtually any substrate or surface geometry. It is based on the decomposition of an organometallic gas precursor by the electron beam to produce a deposit. In the case of 3D nanostructures of magnetic materials, such as cobalt or iron, the deposits are mixed with carbon and oxygen residues of the precursor. This contamination reduces its purity and therefore its magnetization. Thermal annealing procedures in high vacuum of an environmental SEM have been performed to increase the metallic content of as-grown cobalt layer [4]. Structural and chemical characterization of the as-grown and annealed NTs have been carried out by STEM-EELS in a probe-corrected Titan. Quantitative magnetic imaging of the remanent state and DW structure of a 3D ferromagnetic cylindrical NT has been achieved by off-axis Electron Holography (EH) in aberration-corrected Lorentz (field-free) transmission electron microscope (TEM) Hitachi I2TEM. Magnetic and electrostatic phase images have been obtained through holograms obtained before and after flipping the specimen. Micromagnetic simulations of the cobalt NTs have been carried out using the OOMMF software.

### Results

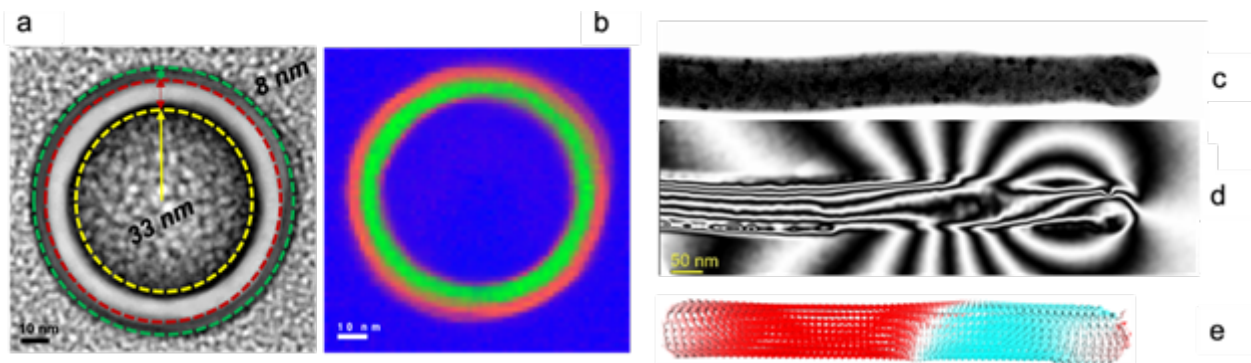
12-nm-thick cobalt layers have been deposited on non-magnetic vertical Pt-C nanowire templates with a diameter of  $\approx 70$  nm, and then annealed at 450 °C in high vacuum to produce high-purity, chemically and structurally homogeneous cobalt NTs (see Fig. 1a,b). They present a good cylindrical symmetry and homogeneous cobalt coverage over the Pt-C template, with a very thin (1-3 nm) oxidation layer at the surface caused by exposure to ambient atmosphere. While as-grown NTs present a low cobalt content (< 70% at.), the thermally annealed ones present very high purity (approx. 95% at.). The magnetization state of the FEED cobalt NTs determined by EH evidences a



magnetic induction value near bulk values ( $>1.55$  T), comparable to the magnetic induction measured in homogeneous cobalt nanowires annealed in similar conditions [3]. The thermally annealed cylindrical NTs give evidence for the nucleation and pinning of a DW during the magnetization reversal process induced by a excitation of the objective lens of the microscope. A quantitative analysis of the magnetic phase image and its comparison with detailed OOMMF micromagnetic simulations have confirmed that the magnetic contrast corresponds to a core-less head-to-head vortex DW, as shown in Fig. 1c-e. In this coreless magnetic structure, the magnetization is confined in the nanotube plane with the spins rotating perpendicular to radial direction of the cylindrical structure.

### Conclusion

Thermally annealed NTs with high-purity cobalt have been successfully grown by FEBID. EH performed in an aberration-corrected Lorentz TEM gives evidence for a high magnetization of the NTs in agreement with the increased metallic content achieved by high vacuum thermal annealing. A DW has been nucleated, imaged and quantitatively characterized for the first time. A comparison of phase images with micromagnetic simulations demonstrates the formation of a head-to-head vortex DW, as predicted in the literature according to the nanotube geometrical dimensions.



### Keywords:

Holography, magnetism, nanotubes, vortex, spintronics

### Reference:

- [1] A. Fernández-Pacheco et al. *Nature Comm.* 8 (2017) 15756.
- [2] M. Staño, O. Fruchart, *Handbook of Magnetic Materials* 27 (2018) 155.
- [3] J. Pablo-Navarro, et al. *Nanotechnology* 27 (2016) 285302; *ACS Appl. Nano Mater.* 1 (2018) 38.
- [4] J. Pablo-Navarro et al. in preparation (2024).

641

## Application of cryogenic in situ biasing (S)TEM holder to study phase transitions in complex oxides

Dr. Yevheniy Pivak<sup>1</sup>, PhD Vasilis Papadimitriou<sup>1</sup>, MSc Tianshu Jiang<sup>2</sup>, PhD Vladimir Roddatis<sup>3</sup>, PhD Leopoldo Molina-Luna<sup>2</sup>, PhD Michele Conroy<sup>4</sup>

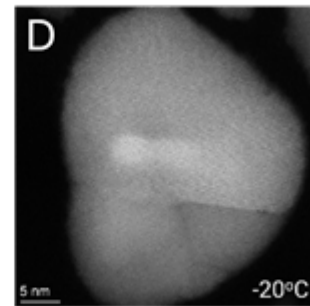
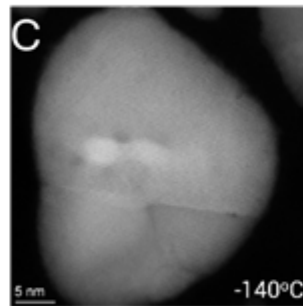
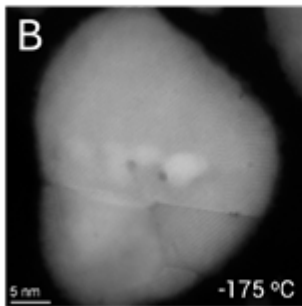
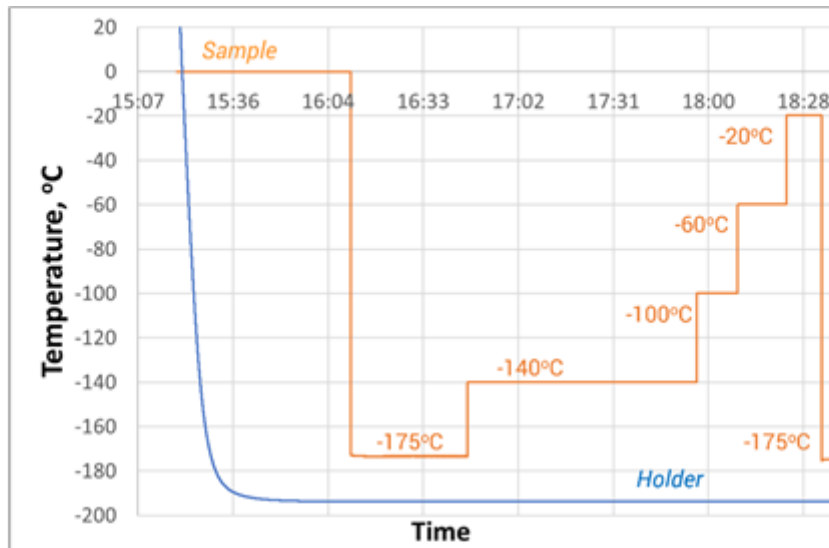
<sup>1</sup>DENSsolutions, Delft, The Netherlands, <sup>2</sup>TU Darmstadt, Darmstadt, Germany, <sup>3</sup>GFZ German Research Center for Geosciences, Potsdam, Germany, <sup>4</sup>Imperial College London, London, United Kingdom

PS-08 (2), Lecture Theater 2, August 27, 2024, 14:00 - 16:00

Cryo scanning transmission electron microscopy (STEM) is becoming an indispensable tool for studying phase transitions in a vast range of applications in the field of quantum materials [1], magnetic materials and nanostructures, ferroelectrics [2], topological insulators, etc. at the atomic scale. A detailed characterization of a sample's structural and electronic properties across phase transitions necessitates a sample holder with double tilt capability and a continuous temperature control of the specimen while maintaining a sample stability that enables atomic resolution imaging.

In this contribution, we will share our latest developments of a combined in situ cooling, biasing, and heating holder able to achieve atomic resolution imaging in a wide temperature range [3]. The holder, cooled by liquid nitrogen, allows to set any user-defined temperature (Figure 1). The temperature control is achieved using microelectromechanical systems (MEMS)-based heating and biasing chips [4, 5] in combination with a dedicated cryo TEM sample holder. Due to the low power consumption of the microheater, it is possible to sweep the temperature of the sample from -175°C to +800°C, while maintaining the holder at liquid nitrogen temperatures. It was found that atomic resolution imaging can be attained while continuously varying the temperature over a thousand degrees with marginal focus and image shift.

We will present several application examples applied to ferroelectrics that include thermal and electrical cycling including cooling conditions.



**Keywords:**

In Situ, cooling, phase transitions

**Reference:**

1. B. H. Goodge, et al., *Microscopy and Microanalysis* 27 (2020) 346.
2. N. Schnitzer, et al., *Microscopy and Microanalysis* 26 (2020) 2034.
3. Y. Pivak, et al., Development of a Stable Cryogenic In Situ Biasing System for Atomic Resolution (S)TEM, *Microscopy and Microanalysis*, Volume 29, Issue Supplement\_1, 1 August 2023
4. H. Perez Garza, et al., 19th International Conference on Solid-State Sensors, Actuators and Microsystems (TRANSDUCERS) (2017) 2155. L. Molina-Luna, et al., *Nat. Com.* 9 (2018) 4445.

780

## Platform for the in-situ measurement of magnetic transport properties in the transmission electron microscope

Sebastian Schneider<sup>1,2</sup>, Steven Waddy<sup>1</sup>, Takanori Sato<sup>1</sup>, Vijay Bhatia<sup>1</sup>, Yevheniy Pivak<sup>3</sup>, David J. Reilly<sup>1</sup>, Bernd Rellinghaus<sup>2</sup>, Julie M. Cairney<sup>1</sup>, Magnus Garbrecht<sup>1</sup>

<sup>1</sup>The University Of Sydney, Sydney Microscopy And Microanalysis, Sydney, Australia, <sup>2</sup>Dresden Center for Nanoanalysis (DCN), TU Dresden, Dresden, Germany, <sup>3</sup>DENSsolutions, , Netherlands

PS-08 (2), Lecture Theater 2, august 27, 2024, 14:00 - 16:00

### Background incl. aims

In order to unveil the magneto-resistive fingerprint of Skyrmions, it is necessary to measure the material's magnetic field dependence of the Hall resistance while acquiring Lorentz TEM (L-TEM) images at the same time [1, 2]. We demonstrate a measurement platform allowing for in-situ magnetic transport measurements in a TEM [3] by utilizing a DENSsolutions biasing holder and a Hall sensor for quantification of the objective lens' magnetic field. We aim to correlate the Hall effect in skyrmionic materials with the magnetic field dependent occurrence of topologically protected magnetic phases such as the helical phase and Skyrmions [4].

### Methods

In-situ L-TEM investigations were conducted using a FEI Themis-Z double-corrected microscope (300 kV, X-FEG) equipped with a fast Ceta-M camera. A DENSsolutions Lightning holder with spring contacts connected to electrical feedthroughs was used to measure the Hall voltage.

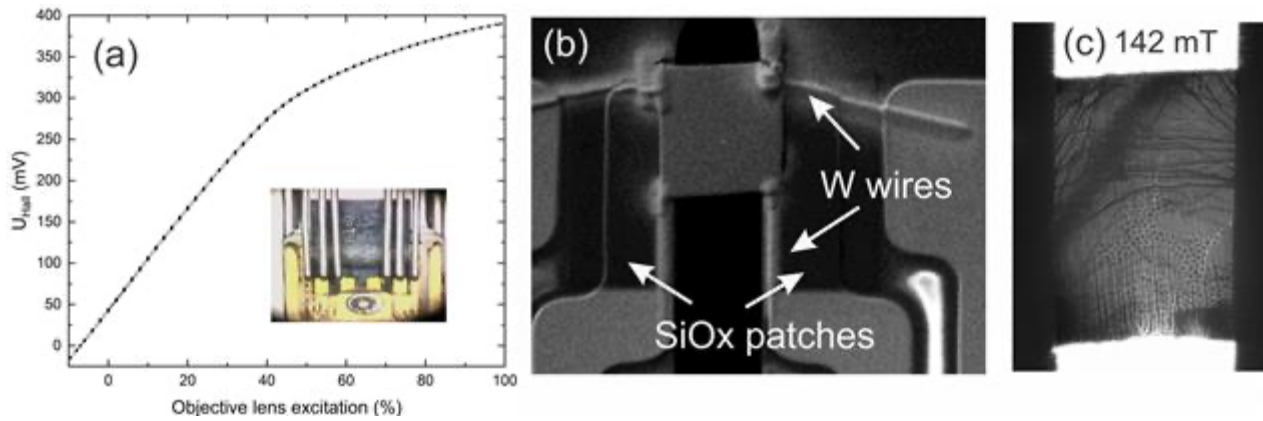
In Lorentz mode, the objective lens of the microscope was used to apply an external magnetic field perpendicular to the sample plane. The magnetic field of the objective lens was calibrated with an Asensor Technology analog Hall sensor fitted into the in-situ biasing holder, see Fig. 1 (a). A Co<sub>8</sub>Zn<sub>9</sub>Mn<sub>3</sub> TEM lamella was cut using a Thermofisher G4 Hydra Plasma FIB. Subsequently, the lamella was positioned on a commercial chip and soldered to the underlying substrate by Pt deposition in the FIB. The DENSsolutions nano-chip was then further modified for the Hall measurements: In order to realise a four-point measurement geometry, insulating SiO<sub>x</sub> patches were deposited on top of the inner tracks. By writing W tracks over the SiO<sub>x</sub>, the conductive paths were bridged (cf. Fig. 1 (b)).

### Results & Conclusions

The demonstrated in-situ setup allows for the simultaneous acquisition of L-TEM images and the measurement of the Hall voltage as function of the out-of-plane magnetic field, which we can control precisely by tuning the objective lens excitation. Fig. 1 (c) shows the Skyrmion phase in Co<sub>8</sub>Zn<sub>9</sub>Mn<sub>3</sub> at 142 mT. Although the lamella is hosting Skyrmions, no signature of topological solitons is observable in the Hall voltage. The observed Skyrmions do not exhibit any distinctive characteristics in the magnetic transport measurements.

### Graphic caption

Figure 1 (a) Magnetic field of the objective lens of a FEI Themis-Z double-corrected TEM as measured with an analog Hall sensor fitted into a DENSsolutions Lightning holder (inset). (b) SEM image of the modified MEMS chip with a Co<sub>8</sub>Zn<sub>9</sub>Mn<sub>3</sub> TEM lamella, showing the FIB deposited W tracks and SiO<sub>x</sub> rectangles. (c) L-TEM image of the Skyrmion phase in Co<sub>8</sub>Zn<sub>9</sub>Mn<sub>3</sub> at 142 mT.



**Keywords:**

In-situ, magnetic transport, Lorentz TEM

**Reference:**

1. M. J. Stolt, S. Schneider et al., *Adv. Func. Mater.* 29 (2019) 1805418.
2. D. Wolf, S. Schneider et al., *Nat. Nanotechnol.* 17 (2021) 250.
3. D. Pohl, S. Schneider et al., *Sci. Rep.* 13 (2023) 14871.
4. S. Schneider et al., in preparation (2024).
5. S. Schneider gratefully acknowledges financial support through the Walter Benjamin Programme of the German Research Foundation (DFG) within project 458685885.



871

## STEM-EELS and Image simulations of inelastic spin-scattering of magnons in confined geometries

Julio Do Nascimento<sup>1,2</sup>, Dr. Demie Kepaptsoglou<sup>1,4</sup>, Prof. Quentin Ramasse<sup>2,4</sup>, Prof. Vlado Lazarov<sup>1,2</sup>

<sup>1</sup>School of Physics, Engineering and Technology, University of York, York, United Kingdom, <sup>2</sup>York-JEOL Nanocentre, University of York, York, United Kingdom, <sup>3</sup>SuperSTEM Laboratory, SciTech Daresbury, Daresbury, United Kingdom, <sup>4</sup>School of Chemical and Process Engineering & School of Physics and Astronomy, University of Leeds, Leeds, United Kingdom

PS-08 (2), Lecture Theater 2, august 27, 2024, 14:00 - 16:00

### Background incl. aims

Application of magnons requires generation, manipulation, and their characterisation in high resolution in both energy and spatial scales. Magnons are commonly studied by inelastic neutron scattering techniques, time-resolved Kerr microscopy, and Brillouin light scattering. While these techniques probe the energy-momentum dispersion of magnons with high energy resolution, their spatial resolution is fundamentally limited to hundreds of nanometres.

Progress in electron beam monochromators in scanning transmission electron microscopy (STEM) has enabled the use of electron beams to study magnons with nanometer and sub-nanometer spatial resolution. Previous studies have successfully collected signals of scattered electrons through electron energy loss spectroscopy (EELS), demonstrating the detection of collective excitations like phonons [1]. The energy range of phonon modes, extending up to a few hundred meV in solid-state materials, aligns qualitatively with magnons, hence efforts aiming to detect magnons using STEM-EELS are ongoing.

Although the interaction strength between magnons and electrons is known to be three or four orders of magnitude weaker compared to the Coulomb interaction, experimental evidence has shown that magnetic ordering can be detected through Bragg reflections of electrons [2].

Furthermore, recent theoretical predictions suggest an EELS signal from thermal magnons in bulk specimens [2, 3], supporting the potential use of STEM-EELS for measuring magnons in confined geometries, including interfaces and surfaces.

### Methods

In this study, we employ the second quantization of the Heisenberg Hamiltonian to calculate the dynamics of magnon modes in finite systems, allowing the inclusion of thin films, interfaces, and heterostructures between ferromagnetic (FM) and antiferromagnetic (AFM) layers, with different relative orientations between the electron beam and the Curie/Neel vector. We then employ the general formalism by van Hove [4] to calculate the double cross-section accounting for the spin-spin interaction of the electron probe with the system, as well as the effect of the system's vector potential on the charged probe's canonical momentum. In addition, by using the multislice method, we simulate high resolution STEM images due to the electron-magnon interaction.

### Results

We present our result on simulations using Fe, NiO and YIG as prototypical examples of the effects captured by the method, Figure 1. By quantifying separately, the spin-based and charge-based interactions in STEM-EELS, we reveal distinct behaviours: charge-based interaction shows a linear dependence on beam momentum, while spin-based interaction follows an inverse relationship akin to phonons, suggesting potential magnon-related peak enhancement compared to phonon peaks at higher acceleration voltages. Additionally, charge-based interaction exhibits an inverse square dependence with a scattering vector. Furthermore, the image simulations show a dependence with the magnetic moment's orientation relative to the electron beam.

### Conclusion

Overall, our study advances our understanding of electron-matter interactions in EELS, offering insights for designing and interpreting experiments probing the magnetic properties of nanomaterials. The magnon EELS calculations suggest that these interactions would be dominant for higher beam acceleration and within the first Brillouin zone, while the image simulations point to the possibility of probing the local magnetic moment's orientations.

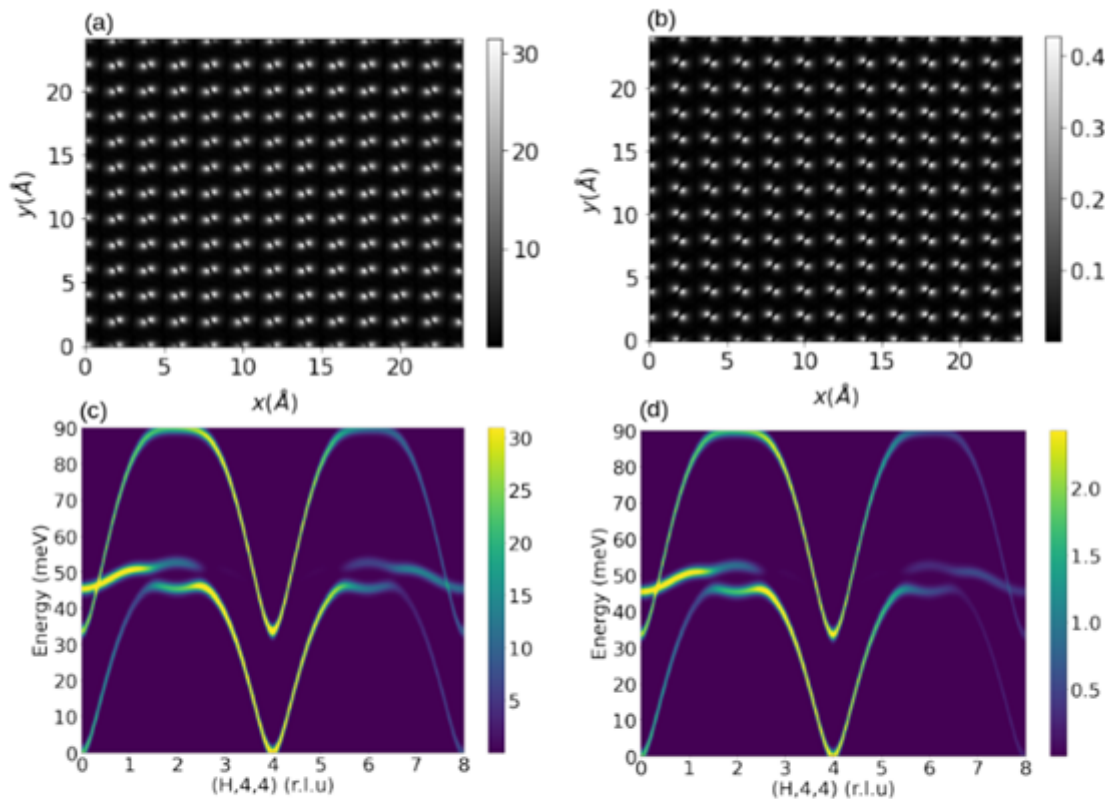


Figure 1. a) and b) NiO TEM simulation for two different magnetic moment orientations, showing the orientation dependence of the image seen as a rotation of the dumbbells formed in the image. c) Momentum resolved STEM-EELS simulation for YIG regarding the spin-based interaction and d) the charge-based interaction.

### Keywords:

magnons, EELS, image simulations, STEM

### Reference:

- [1] Ondrej L. Krivanek, et.al., Vibrational spectroscopy in the electron microscope. Nature, 514(7521):209–212, Oct 2014.
- [2] J. C. Loudon. Antiferromagnetism in NiO observed by transmission electron diffraction. Phys. Rev. Lett., 109:267204, Dec 2012.
- [3] Keenan Lyon, et. al., Theory of magnon diffuse scattering in scanning transmission electron microscopy. Phys. Rev. B, 104:214418, Dec 2021.
- [4] L. Van Hove, Phys. Rev. 95, 249 (1954).

1094

## Quantitative EMCD analysis of Fe thin films on MgOx substrates

Mr. Sharath Kumar Manjeshwar Sathyanath<sup>1</sup>, Dr Anna L. Ravensburg<sup>2</sup>, Professor Vassilios Kapaklis<sup>2</sup>, Professor Björgvin Hjörvarsson<sup>2</sup>, Professor Klaus Leifer<sup>1</sup>

<sup>1</sup>Department of Materials Science and Engineering, Uppsala University, Uppsala, Sweden,

<sup>2</sup>Department of Physics and Astronomy, Uppsala University, Uppsala, Sweden

PS-08 (2), Lecture Theater 2, august 27, 2024, 14:00 - 16:00

### Background

The structure and electronic structure of interfaces determine their magnetic properties in many modern materials. Yet, X-ray and neutron-based analysis techniques, albeit their fantastic contributions to the field, cannot give the real space image of magnetization. And among the TEM techniques, the close-to-atomic scale analysis of magnetic interfaces remains a challenge. All three magnetic analysis techniques in the TEM, electron holography, Lorentz microscopy, and electron energy loss magnetic circular dichroism (EMCD) have now established the first results demonstrating that with TEM techniques, we can obtain magnetic information at this length scale [1-4]. In the EMCD technique, magnetic information originates from the interference of electrons inelastically scattered into different beams. This interference giving rise to the EMCD signal is appearing at well-defined and conjugated  $q$ -vectors called C+ and C- positions. It bears an intensity that can be interpreted as resulting from the orbital and spin magnetic moments of the involved magnetic atoms. The technique can address both ferro- and antiferromagnetic materials.

Here, we present EMCD measurement on thin Fe films on MgOx substrate and show how accurate alignment and experimental parameters like convergence and collection angles modify the EMCD signal and interpret this change in magnetic signal to obtain magnetization and orbital/spin magnetic moment ratio in the Fe and at the Fe/MgO interface.

### Methods

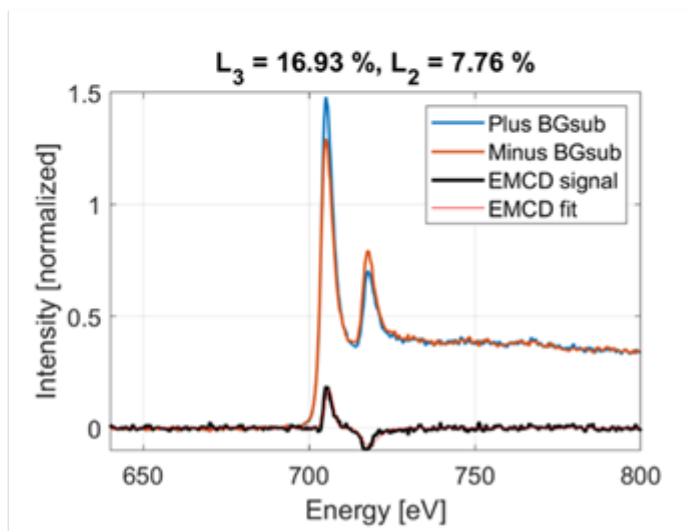
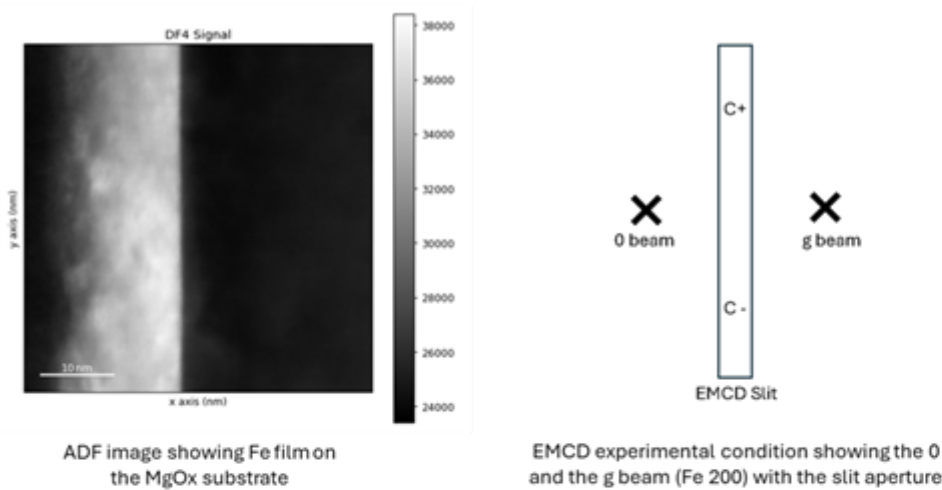
Fe films were grown on MgOx (001) substrate by sputter deposition. The cross-sectional and plan view samples were analysed using the EMCD technique in STEM mode. Spectra of the L3 and L2 edge of Fe corresponding to the C+ and C- positions were acquired at 2 beam condition using a Titan/Themis probe corrected TEM at an acceleration voltage of 200 - 300 kV with Gatan energy filter and a CEFID energy filter equipped with a direct electron camera ELA. The  $q$ -selection of the EELS spectra was carried out by using a custom-made script to shift the diffraction pattern and by placing a slit aperture into the EELS entrance aperture holder, see schematic Figure below. Each acquisition contains between 2000-10000 spectra which enables the treatment of individual spectra or sum spectra as well as the use of statistical methods in data analysis.

### Results

Refinements of both, EELS analysis conditions as well as the sample quality enables us to improve the EMCD signal strength from the original paper of around 4 % to 17 % as shown in the figure below, which was taken at small convergence angle and using the conventional circular EELS entrance aperture. Though, aiming to approach atomic resolution in magnetic measurements, high convergence angles in the EMCD analysis are needed, which will be typically larger than 5 mrad. The other limit of such EMCD analysis is beam damage. We analysed the EMCD signal as a function of convergence angle and optimized acquisition conditions in view of limiting beam damage. With those conditions, we analyse EMCD signals at the Fe/MgOx interface with down to 2Å resolution [4,5].

### Conclusion

In summary, we have optimized and analysed signals in EMCD measurements on Fe/MgOx . An excellent EMCD difference signal as well as improvement in the signal-to-noise ratio is evident due to the crystalline quality. We have obtained interfacial profiles of EMCD signals with down to 2Å resolution.



Background subtracted and normalized C+ and C-spectra with the EMCD difference signal

### Keywords:

EMCD, HRSTEM, Magnetic measurement.

### Reference:

1. Hébert, C., and P. Schattschneider. "A Proposal for Dichroic Experiments in the Electron Microscope". *Ultramicroscopy* 96, no. 3–4
2. Schattschneider, P., S. Rubino, C. Hébert, J. Ruzs, J. Kuneš, P. Novák, E. Carlino, M. Fabrizioli, G. Panaccione, and G. Rossi. "Detection of Magnetic Circular Dichroism Using a Transmission Electron Microscope." *Nature* 441, no. 7092
3. Thersleff, T., Ruzs, J., Rubino, S. et al. Quantitative analysis of magnetic spin and orbital moments from an oxidized iron (1 1 0) surface using electron magnetic circular dichroism. *Sci Rep* 5, 13012
4. Hasan Ali, Jan Ruzs, Tobias Warnatz, Björgvin Hjörvarsson & Klaus Leifer. " Simultaneous mapping of EMCD signals and crystal orientations in a transmission electron microscope". *Scientific Reports* (2021)
5. Ravensburg, Anna L., Gunnar K. Pálsson, Merlin Pohlit, Björgvin Hjörvarsson, and Vassilios Kapaklis. "Influence of Misfit Strain on the Physical Properties of Fe Thin Films." *Thin Solid Films* 761 (November 1, 2022)

1143

## Imaging Chiral Spin Textures with Electron Interferometry and Polarimetry

Professor Benjamin McMorran<sup>1</sup>, Dr. Sergio Montoya<sup>2</sup>, Prof. Eric E. Fullerton<sup>2</sup>

<sup>1</sup>University of Oregon, Eugene, USA, <sup>2</sup>Center for Memory and Recording Research, University of California, San Diego, USA

PS-08 (2), Lecture Theater 2, August 27, 2024, 14:00 - 16:00

### Background incl. aims

Magnetism and spintronics play increasingly significant roles in modern technologies such as data storage and logic devices, sensors, quantum computing, and transportation and electricity generation. The three-dimensional nanoscale spin texture within magnetic materials plays a large role in the behavior of these technologies, and also provides a rich area of fundamental study. Electron, x-ray, and scanning probe microscopies can be used to image 2-D projections of spin textures, yet each technique has strengths and limitations. Lorentz TEM, for example, projects images of the average magnetic field inside a specimen while exposing it to an external field or temperature, but it is insensitive to the field component along the beam path. We aim to combine these techniques with new ones to obtain the 3-D structure of magnetic spin textures.

### Methods

Here we discuss the use of specialized electron microscopies, STEM holography and scanning electron microscopy with polarization analysis (SEMPA), to understand the 3D structure of nanomagnetic spin textures such as skyrmions. STEM holography [1,2] is an interferometric 4D-STEM technique where electrons in the beam are coherently divided into a superposition of two or more separate probes and then scanned over the specimen. If one probe passes through vacuum while the other transmits through the specimen, the resulting phase shift can be measured by recording the interference pattern formed in the far-field at the detector. That is, the bright field discs of the two probes overlap at the detector, forming interference fringes (Fig. 1). Unlike defocus- and deflection-based magnetic imaging techniques such as Lorentz TEM or DPC which are sensitive to phase gradients within the specimen, STEM holography is directly sensitive to the phase relative to the reference beam. With this, STEM holography can be used to directly measure the component of the magnetic vector potential parallel to the beam.

SEM with polarization analysis (SEMPA) [3] is a surface-sensitive technique that can image all three vector components of the surface magnetization. Special detectors can measure the average spin polarization of secondary electrons. Each detector returns information about two components of the magnetization vector; one returns in-plane ( $M_x$  and  $M_y$ ) and the other returns one in-plane ( $M_x$ ) and the out-of-plane component ( $M_z$ ). Therefore, two consecutive scans provides complete, quantitative imaging of the in-plane and out-of-plane magnetic nanostructure as well as normal SE contrast.

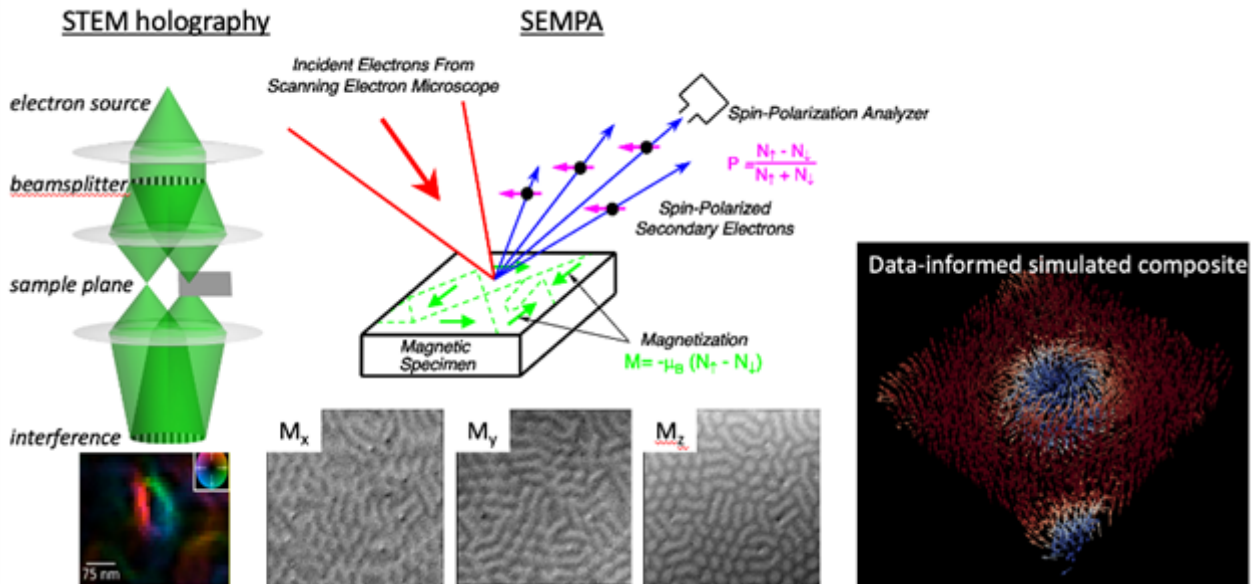
### Results

STEM holography and Lorentz TEM were used to provide images of the skyrmion magnetic field projected through the thickness of the specimen, and SEMPA was provided images of the magnetization at the surface. We find that whereas crystalline specimens can host magnetic skyrmions with whorl-like magnetic fields that extend uniformly through the thickness of the material, here we observe a more intricate magnetic structure. TEM indicates that in the bulk of the material, the magnetic flux wraps around the core like a vortex, yet SEMPA indicates that near the surface the magnetic flux points radially [4], such that the 3D structure is akin to that of a vortex ring.

### Conclusion



We used SEMPA, STEM holography, and Lorentz TEM on the same Fe/Gd multilayer materials to understand the 3D structure of magnetic skyrmions, observing knotted vortex ring-like structures. This illustrates that multimodal magnetic electron microscopy can be used to provide 3D information about magnetic skyrmions that cannot be observed with a single technique alone.



### Keywords:

Skyrmions, magnetic microscopy, electron holography

### Reference:

- [1] F. S. Yasin, T. R. Harvey, J. J. Chess, J. S. Pierce, C. Ophus, P. Ercius, and B. J. McMorran, *Nano Lett.* 18, 7118 (2018).
- [2] T. R. Harvey et al., *Phys. Rev. Appl.* 10, 061001 (2018).
- [3] M. R. Scheinfein, J. Unguris, M. H. Kelley, D. T. Pierce, and R. J. Celotta, *Rev. Sci. Instrum.* 61, 2501 (1990).
- [4] R. Moraski, I. Gilbert, S. A. Montoya, E. E. Fullerton, and B. J. McMorran, *Microsc. Microanal.* 28, 1688 (2022).
- [5] The author gratefully acknowledges the work of John Unguris (NIST) and PhD students Jordan Chess, Alice Greenberg, Tyler Harvey, Rich Moraski, Will Parker, Jacques Reddinger, and Fehmi Yasin. This work is supported by National Science Foundation Grants 2012191 and 2105400.

## Chemical and structural investigations of epitaxial Fe-Cr-O thin films

Dr Benedicte Warot-Fonrose<sup>1</sup>, Dr Pamela Vasconcelos Borges Pinho<sup>2</sup>, Dr Alain Chartier<sup>2</sup>, Dr Antoine Barbier<sup>3</sup>, Dr Denis Menut<sup>4</sup>, Dr Myrtille Hunault<sup>4</sup>, Dr Cecile Marcelot<sup>1</sup>, Dr Frederic Miserque<sup>2</sup>, Dr Jean-Baptiste Moussy<sup>3</sup>

<sup>1</sup>CEMES-CNRS, Toulouse, France, <sup>2</sup>Université Paris-Saclay, CEA, Service de recherche en Corrosion et Comportement des Matériaux, Saclay, France, <sup>3</sup>Université Paris-Saclay, CEA, CNRS, SPEC, Saclay, France, <sup>4</sup>Synchrotron SOLEIL, Gif sur Yvette, France

Poster Group 1

The Fe-Cr-O ternary system has been studied extensively since the mid-20th century due to its applications in various fields, such as geology, metallurgy, corrosion, and (more recently) spintronics. In this system, solid oxide phases may appear in three different crystallographic structures: the halite, the corundum and the spinel phases. The spinel structure ( $\text{Fe}_3\text{-xCr}_x\text{O}_4$ ) is a mix of divalent and trivalent cations in the cubic  $\text{MgAl}_2\text{O}_4$ -type structure. Multivalence cations are organized in a geometrically frustrated network of octahedral and tetrahedral sites, termed here Oh-sites and Td-sites respectively. The complexity of the spinel structure opens the way for tailoring the functional properties of these materials (magnetization, Curie temperature, electronic transport by incorporating different metal cations into the host matrix. For instance, substitution of Fe cations for Cr in magnetite converts the half-metal host ferrimagnet into either a semiconductor or an insulator, depending on the x values.

Most previous works on the  $\text{Fe}_3\text{-xCr}_x\text{O}_4$  series are based on bulk-like samples, while thin films have received limited consideration. Numerous studies have shown that physical and chemical properties of thin films strongly deviate from the bulk, depending on the growth method, film thickness, and surface and interface effects.

This work presents a comprehensive study of the influence of composition and structural properties of epitaxial Fe-Cr-O thin films.

Thin films were deposited by oxygen-plasma-assisted molecular beam epitaxy (O-MBE) on single crystalline  $\alpha\text{-Al}_2\text{O}_3(0001)$  substrates. This method was chosen as it enables the synthesis with a perfect control of the chromium content (x) by using individual Knudsen effusion cells under a reactive atomic oxygen plasma. During deposition, reflection high-energy electron diffraction (RHEED) patterns were acquired in real time to control the crystalline structure of the oxide formed. Epitaxial growth of 15nm thick  $\text{Fe}_3\text{-xCr}_x\text{O}_4(1\ 1\ 1)$  thin films of high crystalline quality has been obtained.

Following growth, several characterization techniques were used to obtain chemical and structural information from the thin films. The stoichiometry of the  $\text{Fe}_3\text{-xCr}_x\text{O}_4$  films were verified ex situ by X-ray photoemission spectroscopy (XPS) measurements. The film microstructure was investigated via high-resolution transmission electron microscopy (HRTEM) and complementary quantitative elemental analyses were performed by electron energy loss spectroscopy (EELS) and energy-dispersive X-ray spectroscopy (EDX). X-ray absorption near-edge structure (XANES) and extended X-ray absorption fine structure (EXAFS) measurements were carried out on MARS Beamline of synchrotron SOLEIL to resolve the oxidation state and the first cation-neighbors bond distances. Magnetic hysteresis loops and in-plane electrical measurements were conducted. The Cr and Fe cation site distribution was determined by exploring the L<sub>2,3</sub>-edge X-ray absorption (XAS) and circular dichroism (XMCD) measurements performed on DEIMOS Beamline of synchrotron SOLEIL. Multiplet calculations were used to interpret the dichroism signal.

Stoichiometric series of epitaxial  $\text{Fe}_3\text{-xCr}_x\text{O}_4(111)$  thin films were prepared with x varying from 0 to 1.7. The film stoichiometry was first evaluated ex situ by XPS measurements. Since XPS probes only

the surface, complementary chemical analyses were performed by STEM-EELS and STEM-EDX. Those analytical techniques presented similar trends with minimal fluctuations in the Fe and Cr signals throughout the layers and no composition gradient.

For  $x < 1.4$ , RHEED patterns exhibit sharp streaks and no spots, indicating a bidimensional growth mode and layers of high crystalline quality without secondary phases. However, for  $x > 1.4$ , RHEED images are blurred and the streaks are almost indistinguishable. The layer-substrate interface and structural defects were evaluated by cross-sectional transmission electron microscopy (TEM) images. Figure 1 (left) depicts TEM images of a representative  $\text{Fe}_{2.8}\text{Cr}_{0.2}\text{O}_4$  film studied along the  $[1210]$  direction. Low magnification TEM image shows that the film is homogeneous and has a constant thickness of about 15 nm. A perfectly flat and abrupt  $\text{Fe}_{2.8}\text{Cr}_{0.2}\text{O}_4/\text{Al}_2\text{O}_3$  interface is observed with no noticeable parasite phases at atomic scale. Misfit dislocations, which takes part on the relaxation mechanism of these films, are observed, as already mentioned for other ferrites grown on sapphire substrate by O-MBE (e.g.  $\text{NiFe}_2\text{O}_4$  and  $\text{MnFe}_2\text{O}_4$ ). When comparing HRTEM images of  $\text{Fe}_{2.8}\text{Cr}_{0.2}\text{O}_4$  and  $\text{Fe}_{2.3}\text{Cr}_{0.7}\text{O}_4$  films, the increasing Cr content seems to induce disorder in the crystalline structure of the film and many stacking defects (e.g., APBs and dislocations) are observed. To investigate further this issue, HRTEM images were acquired for  $\text{Fe}_{1.6}\text{Cr}_{1.4}\text{O}_4$  (figure 1 right) and buffer- $\text{Fe}_{1.3}\text{Cr}_{1.7}\text{O}_4$ . The increase in the amount of the crystalline nanodomains is unmistakable for both of these layers compared to the first two compositions. These results corroborate well with the decrease in quality of RHEED images. The influence of Cr content on the crystalline quality of the films can be associated to either changes in the cation distribution among tetrahedral and octahedral sublattices or modifications in the growth conditions as the deposition rate is different. For  $x < 0.5$  the replacement of  $\text{Fe}^{3+}$  by slightly smaller  $\text{Cr}^{3+}$  in Oh-sites does not modify drastically the structure, whereas for  $0.6 < x < 1.3$  the displacement of larger  $\text{Fe}^{2+}$  into Td-sites has a huge influence. Indeed, orbitally active  $\text{Fe}^{2+}$  cations in Td-sites lead to tetragonal distortions due to cooperative Jahn-Teller effects. For compositions with  $x > 1.4$ , films are assumed to have the normal type of spinel structure,  $\text{Fe}^{3+}$  cations are replaced by smaller  $\text{Cr}^{3+}$  in Oh-sites.

In addition to changing the structural quality, cation disorder has a major impact on the physical properties of the films. The total magnetization and the magnetic anisotropy of  $\text{Fe}_{3-x}\text{Cr}_x\text{O}_4$  thin films decrease as the  $x$  values increase. But unlike bulk materials, thin films with high Cr content ( $x \geq 1.2$ ) still show magnetization at room temperature, i.e., near (or above) the Curie temperature of bulk samples. These features were interpreted in the light of the cationic site distribution. For both bulk and thin films, the inversion parameter steadily evolves with composition, ranging from an inverse arrangement ( $\text{Fe}_3\text{O}_4$ ) to normal ordering ( $\text{FeCr}_2\text{O}_4$ ). Because Cr-rich thin films are still intermediate spinels, while bulk samples are normal spinels, the Curie temperature of these films were increased as they present stronger Td-Oh antiferromagnetic interactions. These results confirm that doping magnetite thin films with Cr is very effective to control the magnetic behavior of this material.

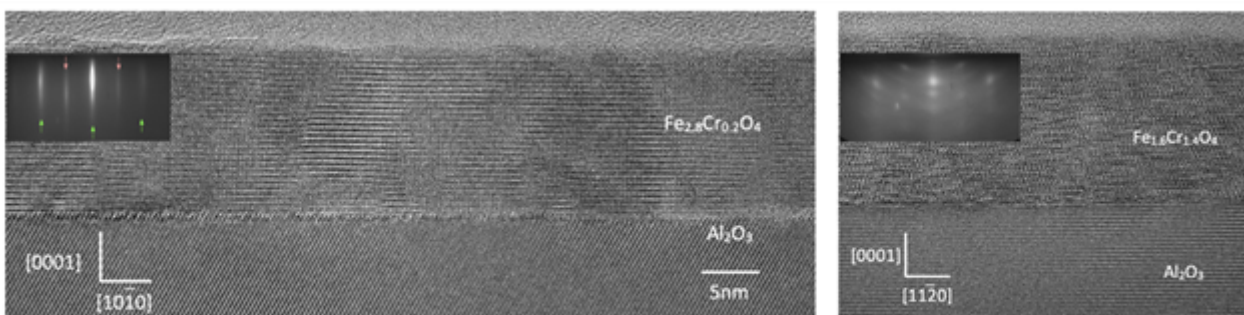


Figure : High resolution TEM image and associated RHEED patterns of  $\text{Fe}_{2.8}\text{Cr}_{0.2}\text{O}_4$  films (left), and  $\text{Fe}_{1.6}\text{Cr}_{1.4}\text{O}_4$  films (left)

#### Keywords:

Magnetic materials, EELS, EDS, HRTEM

#### Reference:

P.V.B. Pinho et al. "Stoichiometry Driven Tuning of Physical Properties in Epitaxial Fe<sub>3-x</sub>Cr<sub>x</sub>O<sub>4</sub> Thin Films," Applied Surface Science 615 (2023) 156354

## Manipulating topological magnetic structures by in-situ Lorentz microscopy

Dongsheng Song<sup>1</sup>

<sup>1</sup>Institutes of Physical Science and Information Technology, Anhui University, Hefei 230601, China, Hefei, China

Poster Group 1

Topological magnetic structures, i.e., skyrmions, have been considered as promising carriers in future magnetic storages or logical devices since their discovery in chiral magnets from 2009, owing to their nanometer-sized dimension, high stability and low critical current density of manipulation. The topologically protected spin textures are fundamental to these excellent performance metrics over the conventional magnetic domain walls or nanoparticles. Here, we have utilized the state-of-the-art magnetic imaging techniques, i.e., Lorentz microscopy and off-axis electron holography, to visualize the magnetization or emergent field of topological magnetic objects, in order to clarify the underlying mechanism of stability and evolution. Moreover, in-situ electrical Lorentz microscopy is employed to investigate the current-driven dynamics of skyrmions in nanostructures under the nanosecond current pulses. The skyrmion velocity and skyrmion Hall angle are measured with respect to the current density. Our results prove the possibility of coding the skyrmions in prototypical devices and have immediate significance towards the skyrmion-based memory or logic devices.

### Keywords:

Lorentz microscopy, electron holography, skyrmion

### Reference:

- [1] Z. He, D. Song\*, et al., *Advanced Functional Materials* 32, 2112661 (2022).
- [2] W. Wang, D. Song\*, et al., *Nat Commun* 13, 1 (2022).
- [3] D. Song et al., *Phys. Rev. Lett.* 120, 167204 (2018).
- [4] L. Li, D. Song\*, et al., *Advanced Materials* 35, 2209798 (2023).



## Characterisation of Skyrmion Spin Textures in CoB/CoFeB Multilayers

Colin Kirkbride<sup>1</sup>, Dr Razan Aboljadayel<sup>2</sup>, Dr Kayla Fallon<sup>1</sup>, Ms Sara Villa<sup>1</sup>, Dr Trevor Almeida<sup>1</sup>, Prof. Marrows CH<sup>2</sup>, Prof. Stephen McVitie<sup>1</sup>

<sup>1</sup>University of Glasgow, Glasgow, United Kingdom, <sup>2</sup>University of Leeds, Leeds, United Kingdom

Poster Group 1

### Background incl. aims

Developing energy efficient data storage requires the discovery of novel materials which can host a variety of high density and controllable magnetic textures. In recent years this has led to an interest in materials capable of supporting magnetic skyrmions owing to their variability in size from several nanometres to microns [1]. In addition, their discrete nature makes them attractive candidates for forming magnetic logic gates, advanced signal multiplexing and neuromorphic computing applications [2]. In this work, we analyse the field dependence of skyrmion spin textures formed in magnetic multilayers of [Ru(7)Pt(X)CoB(4.3)Ru(7)Pt(X)CoFeB(5.3)]<sub>15</sub> (all in Å) where X is 8.5Å (S1) or 10.5Å (S2) (Fig.1a). The overall aim is to highlight the importance of Pt thickness on the established spin textures and to motivate these materials as candidates for field controllable skyrmion applications.

### Methods

Throughout this work, we utilise a range of microscopic analysis techniques with a strong emphasis on Lorentz transmission electron microscopy (LTEM). All images were acquired using a JEOL JEM-ARM200cF microscope operating in either LTEM or STEM mode equipped with a CEOS probe corrector. Qualitative Fresnel images were captured within a field range of  $\pm 130$  mT. Single image transport of intensity (sTIE) reconstructions were used as a method of semi-quantitative magnetic characterisation and supported with more robust differential phase contrast mapping of the integrated magnetic induction at a range of key fields. Topographical and phase characterisation is provided through tapping zero-field MFM and bulk magnetic measurements are analysed with SQUID-VSM. Elemental mappings of multilayer cross-sections are measured using electron energy loss spectroscopy (EELS) and provide layer thickness measurements which aid magnetic volume characterisation.

### Results

By comparing the magnetic states of S1 and S2 at a range of fields, we analyse the effects of interlayer coupling within the multilayer. Reducing the applied field from the saturated state above 130 mT, S1 first stabilises a ferromagnetic (FM) skyrmion lattice (SkL) phase which expands into FM domains before forming a second SkL at zero field (Fig.1b). The SkL contrast is then slowly removed as S1 enters a field stabilised synthetic antiferromagnetic phase around -40 mT before the magnetisation switches into a FM domain phase and saturates at high field. We correlate this behaviour with strong coupling between the CoB and CoFeB layers. For S2 the behaviour is markedly different on the reduction of field from saturation. We first form sparsely distributed skyrmions with weak contrast which expand into a FM domain state covering the film. We next form a mixed-phase FM state (Fig.1c) with strong and weak contrast which reduces to a purely strong contrast FM domain state at zero field. Upon field reversal, these FM domains contract to form skyrmions with strong and weak contrast below -100 mT, before proceeding towards saturation. We propose that the varying levels of contrast in S2 are caused by the thicker Pt layer forcing an effective decoupling between the CoB and CoFeB layers allowing each to act independently in response to applied field. The formation of chiral textures is then driven by the different strengths of interfacial Dzyaloshinskii-Moriya interaction at the CoB/Pt and CoFeB/Pt interfaces [3].

## Conclusion

Using Lorentz microscopy, we show that the separation between magnetic layers in CoB/CoFeB multilayers can have a significant impact on the observed magnetic textures. This has important consequences for applications, for example, if one desires a high density skyrmion state at low field (eg: for reservoir computing), then strongly coupled systems, similar to S1, would be useful. In contrast, if sparse skyrmion states are required (eg: for racetrack memories), then decoupled systems such as S2 may be more appropriate. Overall, the work serves as motivation for careful, application specific tuning of layer thicknesses during material growth, and highlights the valuable information that nanoscale magnetic imaging can provide for skyrmion stabilising systems.

## Graphic

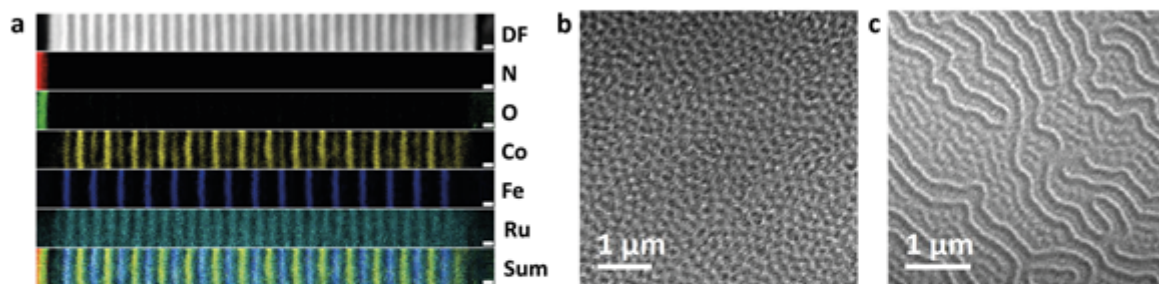


**Fig.1:** a Cross-sectional analysis of S2 with dark-field (DF) image of STEM-EELS mapping regions of N, O, Co, Fe and Ru; with the bottom panel indicating a sum of the mappings (scale-bar is 2 nm). Fresnel images of b 0 mT SkL state of S1; and c mixed-phase state of S2 at 48 mT highlighting strong contrast FM domains and weak contrast skyrmions/domains. Both images were captured using a 200 kV accelerating voltage, a sample tilt of 25° and respective defocuses of 5.2 mm and 2.2 mm.

## Keywords:

Lorentz TEM, DPC, Magnetism, Skyrmions

## Reference:

- [1] Wang, X.S., et. al., A theory on skyrmion size. *Commun.Phys.* 1, 31 (2018)
- [2] Song, K.M., et al. Skyrmion-based artificial synapses for neuromorphic computing. *Nat.Electron* 3, 148–155 (2020)
- [3] Alshammari, et. al. Scaling of Dzyaloshinskii-Moriya interaction with magnetization in Pt/Co(Fe)B/Ir multilayers. *Phys.Rev.B* 104, 224402 (2021)

147

## Deformation mapping in Lorentz transmission electron microscopy images of magnetic skyrmion lattices

Dr. Thibaud Denneulin<sup>1</sup>, Dr. András Kovács<sup>1</sup>, Pr. Rafal E. Dunin-Borkowski<sup>1</sup>

<sup>1</sup>Ernst Ruska-Centre for Microscopy and Spectroscopy with Electrons and Peter Grünberg Institute, Forschungszentrum Jülich, Jülich, Germany

Poster Group 1

### Background

Magnetic skyrmions are quasi-particles with a swirling spin texture. In chiral magnets, skyrmions are stabilized by the balance between the exchange interaction and the Dzyaloshinskii-Moriya interaction. They have raised interest because of their potential applications in the field of spintronics, for instance in racetrack memories where they are treated as information carriers [1]. Axially symmetric chiral skyrmions usually form 2D hexagonal close-packed lattices [2]. Similarly to atomic lattices, skyrmion lattices can exhibit local deformations and crystalline defects such as dislocations and grain boundaries depending on the geometric constraints and the external magnetic fields [3]. Measuring deformations in skyrmion lattices is important to understand the interplay between the lattice structure and external influences.

In previous studies, skyrmion lattice deformations were investigated using real-space methods applied to Lorentz transmission electron microscopy (LTEM) images, which involves detecting intensity maxima or minima, finding nearest neighbors and calculating inter-skyrmion distances [3,4]. Here, we investigate the applicability of geometric phase analysis (GPA) [5]. GPA is a lattice deformation analysis technique based on Fourier transforms primarily used in high resolution TEM images. Compared to real-space methods, GPA is straightforward computationally because there is no need to detect individual maxima and perform any pixel-to-pixel operation. A Fourier transform of the image is first calculated and numerical apertures are applied to a pair of Bragg spots with non-colinear reciprocal lattice  $g$ -vectors. After inverse Fourier transform, the geometric phase term  $\varphi(r) = -2\pi g \cdot u(r)$  associated to each  $g$ -vector is retrieved, where  $u$  is the displacement vector. The deformation fields are then obtained using differentiation of the displacement fields.

### Methods

Experiments were carried out using a TFS Titan TEM equipped with a Schottky field emission gun operated at 300 kV, a CEOS image aberration corrector and a 4k\*4k Gatan K2-IS direct electron detector. The microscope was operated in Lorentz mode by using the first transfer lens of the aberration corrector as the main imaging lens. The objective lens was used to apply magnetic fields perpendicular to the sample which were precalibrated using a Hall probe. A liquid-nitrogen-cooled specimen holder (Gatan model 636) was used to vary the sample temperature. The Digital Micrograph software and a GPA plugin were used to calculate deformation maps. A TEM lamella of FeGe was prepared from a bulk crystal using focused Ga<sup>+</sup> ion beam sputtering in a scanning electron microscope (FIB-SEM) FEI Helios dual-beam platform.

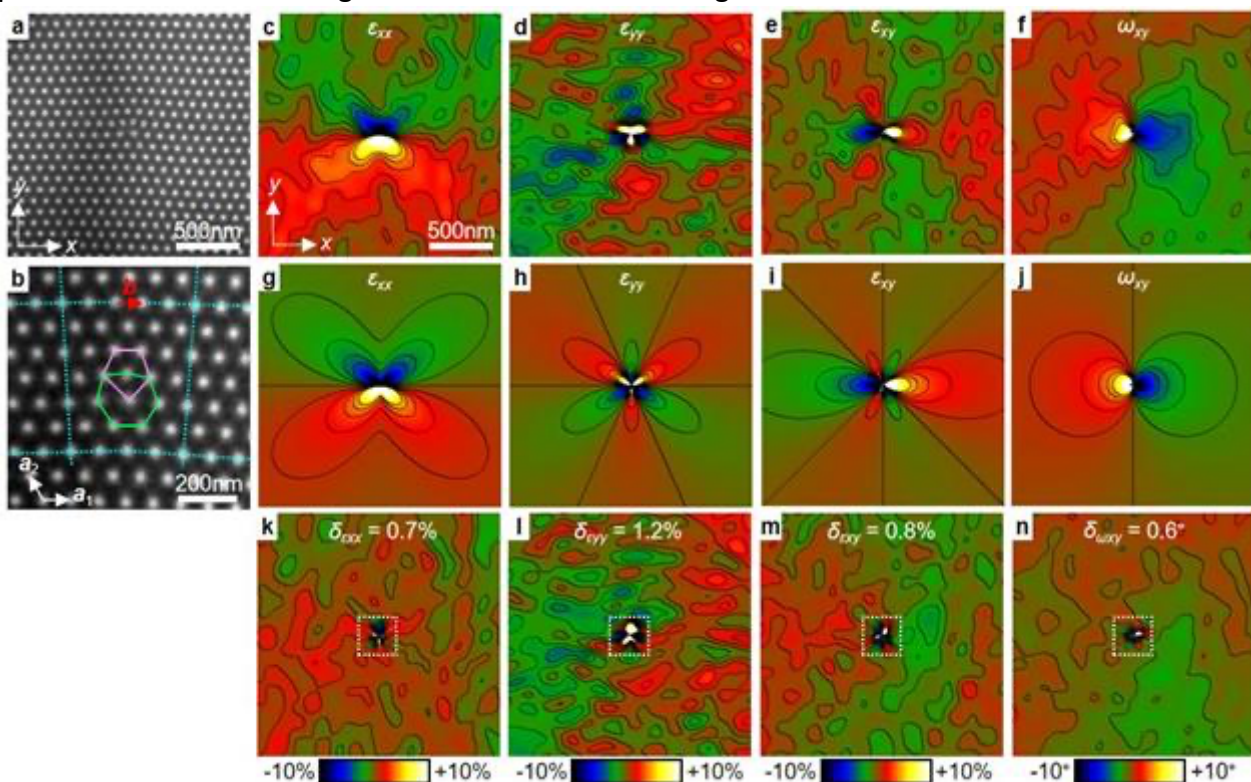
### Results

Figure (a) shows an example of Lorentz TEM image of a skyrmion lattice in a 150 nm thick FeGe lamella recorded at 230 K with a defocus of 800  $\mu\text{m}$  and in the presence of an external magnetic field of 145 mT. Normally, each skyrmion has 6 neighbors in a hexagonal lattice. However, it is common to observe dislocations formed by pairs of 5 and 7-coordinated skyrmions. Such a dislocation is present in the middle of the image and it is magnified in Fig. (b) where the heptagon and the pentagon have been drawn. A Burgers circuit has also been traced to show the Burgers vector  $b$ . Figure (c-f) shows the experimental deformation fields calculated using GPA and Fig. (g-j) shows the corresponding

theoretical deformation fields calculated from linear elastic theory. The horizontal deformation  $\epsilon_{xx}$ , along the direction parallel to the Burgers vector, shows a butterfly shape with negative (compressive) deformation in the top part of the image and positive (tensile) deformation in the bottom part. The vertical deformation  $\epsilon_{yy}$  shows a three-fold symmetry with alternating negative and positive deformations around the dislocation core. The shear deformation  $\epsilon_{xy}$  and the rigid-body rotation  $\omega_{xy}$  show primarily loops oriented along the horizontal direction, parallel to the Burgers vector. Visually, the shape of the experimental and theoretical deformation fields is in good agreement even though the experimental images show some random fluctuations. To provide a quantitative comparison, Fig. (k-n) shows the difference between the experimental and theoretical deformation fields. The standard deviation  $\delta$  was calculated and is indicated on each image. The region in the vicinity of the core (approximately 150 nm around the core, as indicated by the dotted square) was excluded from the measurement. The small values of  $\delta \approx 1\%$  or  $1^\circ$  indicate a good quantitative agreement.

### Conclusions

We have studied deformations in skyrmion lattices in a sample of FeGe by applying GPA to Lorentz TEM images. Deformation fields measured around a single dislocation were found to be in good agreement with deformation fields calculated from linear elastic theory. In the conference presentation, we will also show rotation fields measured at the boundaries between crystal grains and compare them with angles calculated from the density of dislocations. We will also discuss the evolution of deformation fields in applied magnetic fields series of LTEM images and explain how to calculate an orientational order parameter to study the evolution of the disorder. The influence of potential artifacts such as geometric distortions and large defoci will also be discussed.



### Keywords:

skyrmions, Fresnel, deformations, lattice, GPA

### Reference:

- [1] Fert, A. et al., Nat. Rev. Mater. 2 (2017)
- [2] Mühlbauer, S. et al., Science 323, 915–919 (2009)
- [3] Pöllath, S. et al., Phys. Rev. Lett. 118, 207205 (2017)

[4] Schönenberger, T. et al., *Nanoscale Res. Lett.* 17 (2022)

[5] Hÿtch, M. J. et al., *Ultramicroscopy* 74, 131–146 (1998)



## Quantitative Analysis of Magnetic Spin Textures in $\text{Fe}_{3-x}\text{Co}_x\text{GeTe}_2$ Compositions using 4D-STEM

Mr. Aidan Horne<sup>1</sup>, Dr. Daniel Mayoh<sup>1</sup>, Dr. Damien McGrouther<sup>2</sup>, Prof. Geetha Balakrishnan<sup>1</sup>, Dr. Peng Wang<sup>1</sup>

<sup>1</sup>Department of Physics, University of Warwick, Coventry, United Kingdom, <sup>2</sup>JEOL (UK) Ltd., Welwyn Garden City, United Kingdom

Poster Group 1

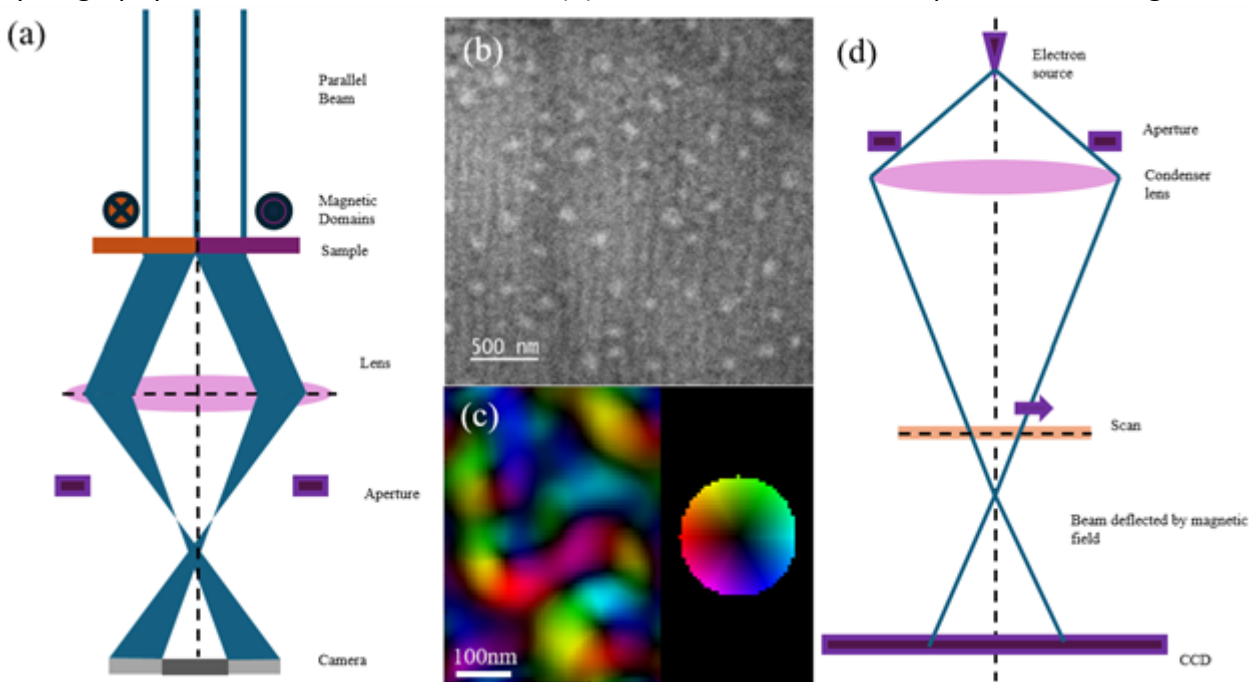
Magnetic spin textures are becoming increasingly important in the field of spintronics due to their potential uses in devices such as racetrack memory. The discovery of skyrmions in  $\text{Fe}_3\text{GeTe}_2$  (FGT), has triggered a great interest in studying spin textures in 2D-van der Waals (2D-vdW) magnets. These textures arise from the interplay between the Dzyaloshinskii-Moriya interaction (DMI), exchange interaction and the Zeeman interaction in the presence of an external magnetic field [1]. Controlling these textures can further be achieved through factors such as thickness of the material, the temperature and structural defects [2]. Recently, it has been reported that the level of substitution of the Fe within the material by Co can change the ordering temperature and thus the behaviour of the material  $\text{Fe}_{3-x}\text{Co}_x\text{GeTe}_2$  or (FCGT) [3]. Understanding how these factors affect the behaviour of the skyrmions including the size, mobility and stability is crucial, as these features will be important when considering the materials used in potential spintronic devices such as racetrack memory or in probabilistic computing applications [4]. Here we use transmission electron microscopy (TEM) as well as four-dimensional scanning transmission electron microscopy (4D-STEM) to quantify the behaviour of FCGT as the composition of the material changes. Additionally, we simulate the textures using micromagnetic simulation software mumax3 [5].

In this work we utilize Fresnel imaging in Lorentz TEM (LTEM), a technique where the objective lens of the microscope is turned off to reduce the magnetic field so that the sample is not uniformly magnetized by the magnetic lenses. The beam is then defocused to the order of 0.1 mm so that Fresnel fringes appear caused by the magnetic potential of the sample revealing the spin textures in the sample as seen in Figure 1(a-b). These images can then be reconstructed using transport-of-intensity (TIE) equations to obtain the magnetic field information of the sample, an example of which is demonstrated in Figure 1(c). Chemical vapour transport and standard focused ion beam lift-out procedure were used to prepare the sample. During TEM imaging, the samples were cooled to liquid nitrogen temperatures and then heated to the appropriate temperature desired. The residual magnetic field within the TEM was calibrated using a custom-built in-situ Hall probe holder. The composition mapping was studied using energy dispersive x-ray (EDX) methods. Additional investigations into the material's bulk magnetic properties were carried out using magnetic force microscopy (MFM).

Using the methods described we have studied a range of stoichiometries of FCGT by varying out-of-plane (OOP) magnetic fields and temperatures and have demonstrated how the domain structure and temperatures at which these domains occur vary depending on the composition of the material. We have also confirmed the level of cobalt doping in FGT using EDX methods to quantify how this doping affects the behaviour of the materials, as well as investigated whether the elements are uniformly distributed throughout the material and how this affects the spintronic behaviour. Using the techniques described and through controlling the temperature and OOP magnetic field we have investigated the spin texture the material occupies at any given phase. Micromagnetic simulations were done to estimate the behaviour of the materials at different thicknesses to verify results as well as to improve the speed of workflow when working on time intensive processes such as MFM and LTEM where the sample has to be cooled before imaging.

We have observed magnetic spin textures in a range of compositions of FCGT, showing that the behaviour of the materials depends directly on the levels of iron and tellurium as well as on any cobalt doping. Work has begun to further quantify the behaviour of these systems more accurately using 4DSTEM methods such as centre of mass measurements (COM) and ptychography, the methodology of which is shown in Figure 1(d).

Figure 1: Experimental setup of Fresnel TEM and 4D-STEM data acquisition. (a) Schematic of Fresnel TEM set up in overfocused condition. (b) Fresnel TEM image of FGT showing skyrmions. (c) Reconstruction magnetic data. Here showing TIE reconstruction but other methods such as COM or ptychography would obtain a similar result. (d) Schematic of 4D-STEM experimental configuration.



### Keywords:

Skyrmion, Ptychography, 4D-STEM, Fe<sub>3</sub>GeTe<sub>2</sub>, LTEM

### Reference:

- [1] I. Dzyaloshinskii Phys. Chem. Solids 4 241–55 (1958).
- [2] H. Zhang et al. Sci. Adv. 8, eabm7103 (2022).
- [3] D. Mayoh et al. Cryst. Growth Des. 21 6786-6792 (2021).
- [4] F. Giovanni et al. J. Phys. D: Appl. Phys. 49 423001 (2016).
- [5] A. Vansteenkiste et al. AIP Adv. 4, 107133 (2014).

## Fine structure tuning for strongly correlated functionalities in high entropy oxides

Dr. Di Wang<sup>1,2</sup>, Mr. Abhishek Sarkar<sup>1,3</sup>, Mr. Gleb Iankevich<sup>1,4</sup>, Mr. Zhibo Zhao<sup>1</sup>, Mr. Horst Hahn<sup>1,3,4</sup>, Mr. Robert Kruk<sup>1</sup>, Mr. Christian Kuebel<sup>1,2</sup>

<sup>1</sup>Karlsruhe Institute of Technology, Institute of Nanotechnology, Karlsruhe, Germany, <sup>2</sup>Karlsruhe Institute of Technology, Karlsruhe Nano Micro Facility (KNMFi), Karlsruhe, Germany, <sup>3</sup>KIT-TUD Joint Research Laboratory Nanomaterials – Technical University of Darmstadt, Darmstadt, Germany, <sup>4</sup>Karlsruhe Institute of Technology, Institute for Quantum Materials and Technologies, Karlsruhe, Germany

Poster Group 1

### Background incl. aims

Strongly-correlated phenomena, such as, colossal magnetoresistance (CMR) and metal-insulator transitions (MIT), exhibited by perovskite manganites are accompanied and reinforced by coexistence of competing magneto-electronic phases [1]. Such magneto-electronic inhomogeneity is governed by the intrinsic lattice-charge-spin-orbital correlations, which are conventionally tailored via chemical substitution, charge doping or strain engineering. Alternately, the recently discovered high entropy oxides (HEOs), owing to the presence of multiple-principal cations on a given sub-lattice, exhibit indications of an inherent magneto-electronic phase separation encapsulated in single crystallographic phase. In this abstract we present the structure characterization at atomic resolution for a series of single-phase orthorhombic HE-manganites,  $(\text{Gd}_{0.25}\text{La}_{0.25}\text{Nd}_{0.25}\text{Sm}_{0.25})_{1-x}\text{Sr}_x\text{MnO}_3$  ( $x = 0 - 0.5$ ), which combines high entropy (HE) concept with standard property control by  $\text{Sr}^{2+}$  (hole) doping, with the aim to extend the HE based approach to design strongly-correlated systems. High resolution scanning transmission electron microscopy (HR-STEM) and integrated differential phase contrast (iDPC) imaging have been used to determine the crystal structure variations in HEO introduced by different Sr concentrations. Electron energy-loss spectroscopy (EELS) has used to reveal the Mn valence change with Sr doping levels. We aim to correlate the atomically resolved geometric and electronic structures to the finely tuned electromagnetic properties of the series of Sr doped HEOs.

### Methods

The powder samples were synthesized using nebulized spray pyrolysis (NSP) technique. The details of the synthesis procedure can be found elsewhere [2]. A double aberration corrected transmission electron microscope Themis Z (Thermo Fisher) equipped with a Super-X energy dispersive X-Ray detector and Gatan GIF Continuum 970 HR + K3 IS camera (operated at 300 kV) were used to examine the specimens.

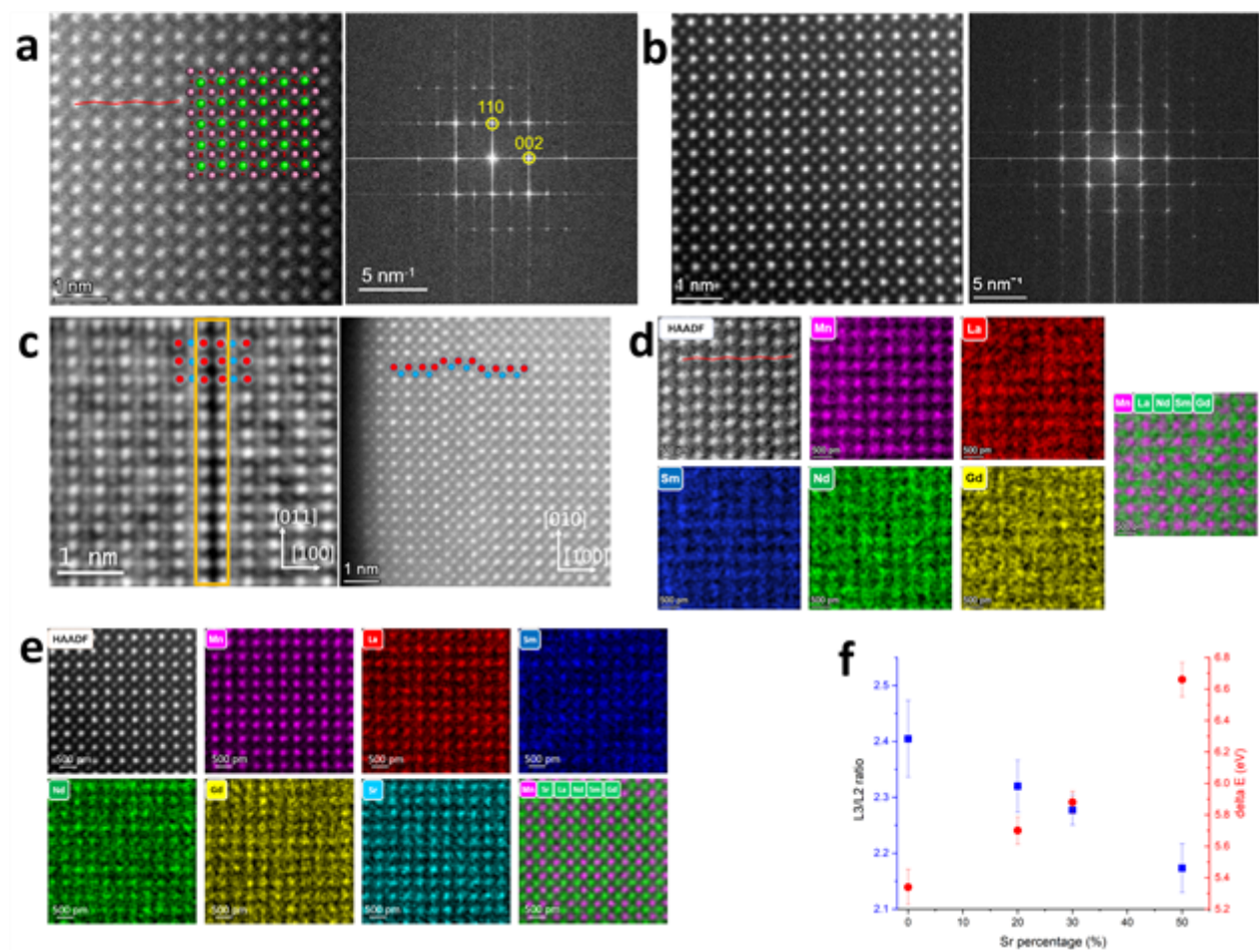
### Results

From the high-angle annular dark-field (HAADF) STEM images, the strong orthorhombic distortion can be identified for  $x = 0$  (Figure 1a). The distortion becomes weak with increasing the Sr concentration. For  $x = 0.5$  system (Figure 1b), the crystal structure is very close to pseudo-cubic. However, the higher symmetric phase shows noticeably higher density of different types of lattice defect, including twin boundaries and Ruddlesden-Popper faults, as revealed by iDPC and HAADF images in Figure 1c along  $[01-1]$  and  $[001]$  zone axis, respectively. Figure 1d and 1e present the HAADF STEM image and the corresponding atomically resolved elemental distribution maps for  $x = 0$  and  $x = 0.5$ . A homogenous distribution of the rare-earth cation (and Sr for  $x = 0.5$ ) on the A-site (RE) sub-lattice along with presence of Mn on the B-site sub-lattice, without any observable segregation at the atomic length scales, can be confirmed. The change in the oxidation state of Mn can be evaluated from the integrated area ratio of the Mn L3 to L2 edges (L3/L2 ratio) and the energy difference ( $\Delta E$ ) for the O K-edge features between the Mn 3d feature ( $\sim 530$  eV) and the RE 5d/Sr 4d

feature ( $\sim 536$  eV). The changes in the Mn L3/L2 ratio and  $\Delta E$  as a function of Sr<sup>2+</sup> doping (Figure 1f) unambiguously confirms that increasing amount of Sr<sup>2+</sup> doping results in change of Mn valence state from  $\sim 3.1+$  for 0%Sr to  $\sim 3.6+$  for 50% Sr. The quantitative EELS analysis indicates that the separation of the antiferromagnetic ferromagnetic phases mainly depends on the ratio of the Mn<sup>3+</sup> and Mn<sup>4+</sup>. More Mn<sup>4+</sup> enhances the double-exchange interaction between Mn<sup>3+</sup> – O – Mn<sup>4+</sup>, which increases the ferromagnetic component.

### Conclusion

This initial study signals excellent potential to achieve complex magneto-electronic phase diagram with unique temperature dependencies that stem from competing magneto-electronic interactions. The unique subtle properties can be tuned by the merger of the high entropy-based design approach with the strongly correlated electron systems. The tunable electromagnetic properties are attributed to the structure changes by the high-resolution imaging and EELS analyses showing an increase in the amount of Mn<sup>4+</sup> and a corresponding decrease in Jahn–Teller effect and the degree of orthorhombic distortion upon increasing amount of Sr<sup>2+</sup> doping [3].



### Keywords:

high entropy oxide, STEM, EELS

### Reference:

- [1] E. Dagotto, *Science*. 2005, 309, 257
- [2] A. Sarkar et al., *J. Eur. Ceram. Soc.* 2017, 37, 747.
- [3] A. Sarkar et al., *Adv. Mater.* 2023, 35, 2207436.



## Vacancy-driven electron spin engineering to promote Li-S redox reactions

PhD JING YU<sup>1,2</sup>, Mr. Andreu Cabot<sup>2</sup>, Mr. Jordi Arbiol<sup>1</sup>

<sup>1</sup>Catalan Institute of Nanoscience and Nanotechnology (ICN2), Bellaterra, 08193, Spain, <sup>2</sup>Catalonia Institute for Energy Research (IREC), Sant Adrià de Besòs, 08930, Spain

Poster Group 1

### Background

Lithium-sulfur batteries (LSBs) are promising energy storage devices due to their high theoretical energy density (2600 Wh kg<sup>-1</sup>), large specific capacity (1675 mAh g<sup>-1</sup>), potential cost-effectiveness, and environmental friendliness.[1] However, the commercialization of LSBs is limited by factors such as polysulfide migration, sluggish kinetics of the sulfur redox reaction (SRR), and poor electronic and ionic cathode conductivities.[2] The use of defect-engineered catalysts, with tunable surface chemistry and electronic properties, as cathode additives in LSBs is a promising strategy to accelerate the Li-S redox reactions and thus promote LSB performance. In contrast to earlier research that predominantly concentrated on how defects influence the electronic density of states, the present work explores the impact of defects in modulating electronic spins and how these changes in spin configuration influence the macroscopic adsorption properties and activity of the catalytic additive.

### Methods

In this study, a defect engineering strategy was used to tune the electron spin state of an SRR electrocatalyst. This strategy was showcased by introducing controlled amounts of cation vacancies within ultrathin CoSe nanosheets through plasma etching. Atomic resolution aberration-corrected high-angle annular dark-field scanning transmission electron microscopy (AC-HAADF-STEM) was used to gain in-depth insights into the spatial distribution of Co vacancies. 3D atomic models were obtained by using Rhodius and the corresponding AC-HAADF-STEM image simulations obtained by using STEM-CELL software.[3-4] XRD, EXAFS, XPS, Raman spectroscopy, XMCD, DFT calculations, EPR, in situ XRD combined with electrochemical test were conducted.

### Results

Vacancies were also indirectly evidenced by an increase of disorder and reduced lattice spacing, Co-Se bond length, and Se coordination number using XRD, HRTEM, EXAFS, XPS, and Raman spectroscopy. XANES and XPS spectroscopy further showed an increase in the average oxidation state of cobalt with the introduction of vacancies and EELS pointed to a higher occupation of Co 3d states in v-CoSe. Beyond modifying the structural parameters and electronic state occupation, the presence of vacancies resulted in a polarization of the 3d electron spins as evidenced by an increase in the intensity of the satellite peak in the Co 2p XPS spectra, a strong Co dichroism signal obtained by XMCD and magnetic measurements that confirmed a large moment per Co ion of 2.8  $\mu_B$  in v-CoSe. EPR spectroscopy further confirmed the generation of additional electrons with unpaired spins by the introduction of Co vacancies.

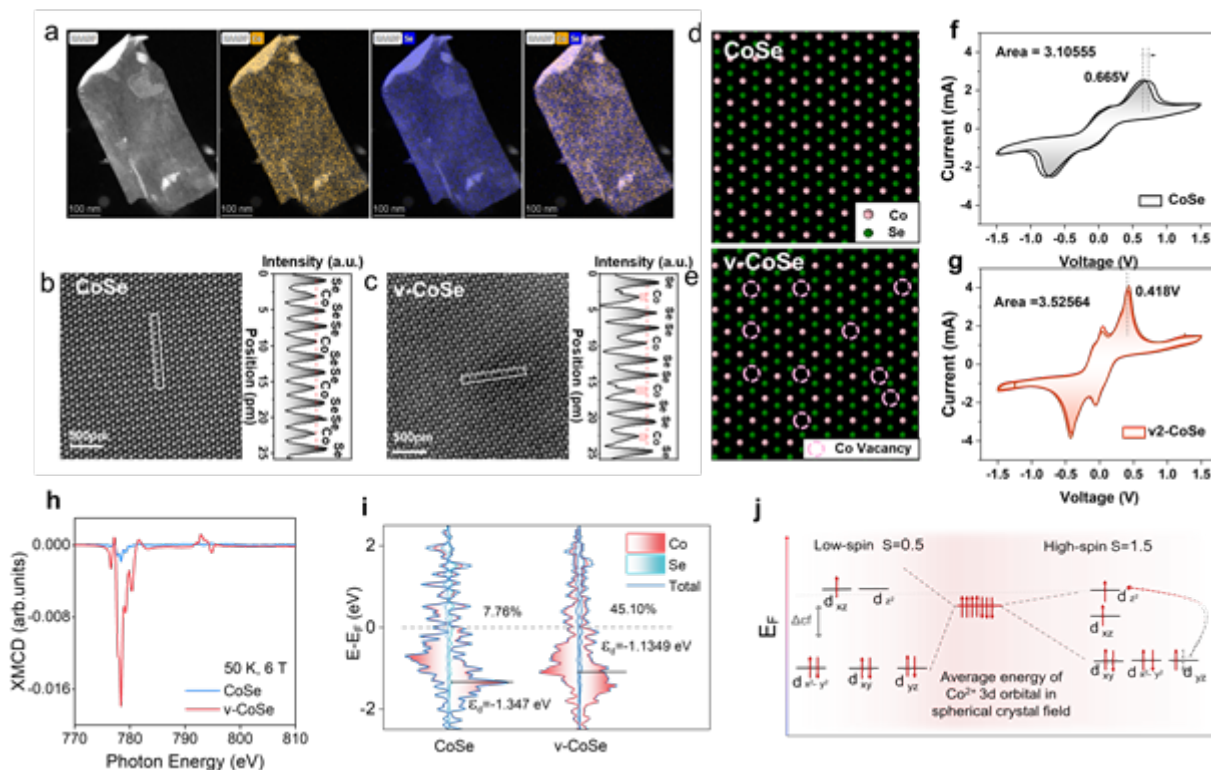
DFT calculations showed these spin-polarized unpaired electrons to be easily transferred from v-CoSe to polysulfide. Computational results showed that the d band center shifts toward the Fermi level with the introduction of vacancies, which involves that electrons are more prone to disperse in the high-spin configuration. The altered spin configuration results in a swift transferability of additional unpaired electrons to the polysulfide. DFT calculations also showed v-CoSe to have significantly higher lithium polysulfide adsorption energies and to decrease the polysulfide stability upon adsorption, thus enhancing both polysulfide adsorption and conversion activity. Besides, computational results showed the modified spin configuration to result in a more favorable thermodynamic reduction process, particularly for the transition from soluble polysulfide to solid Li<sub>2</sub>S that showed a lower nucleation energy barrier.

Experimental measurements confirmed an enhanced adsorption of the lithium polysulfide on the v-CoSe surface. Symmetric cells showed v-CoSe to provide a low polarization voltage and sharper and more intense redox peaks. In situ XRD showed a very rapid and complete transformation of S8 and a high lithium polysulfide redox activity in v-CoSe. EIS analyses showed v-CoSe to be characterized by a low SRR activation energy, particularly for the liquid-solid conversion stage. Besides, the presence of vacancies resulted in promoted Li2S nucleation, reduced LSB polarization voltages, and higher Q2/Q1 ratios. v-CoSe cathodes not only demonstrated excellent electrocatalytic properties but also outstanding LSB electrochemical performance in terms of specific capacity, rate performance, and cycling stability, even at high sulfur loadings.

As a result, more uniform nucleation and growth of Li2S and an accelerated liquid-solid conversion in LSB cathodes are obtained. These translate into CoSe-based LSB cathodes exhibiting capacities up to 1089 mAh g<sup>-1</sup> at 1C with 0.039% average capacity loss for 1500 cycles, and up to 5.2 mAh cm<sup>-2</sup>, with 0.16% decay per cycle after 200 cycles in high sulfur loading cells.

### Conclusion

Overall, this study demonstrates the need for considering the electronic spin configuration in the design of electrocatalysts, particularly for developing robust LSBs. Thus, the spin engineering approach showcased here paves the way to the rational design of new generations of LSB cathodes based on defect-engineered SRR electrocatalysts, toward the development of a cost-effective LSB technology with market-ready potential.



### Keywords:

battery, cationic vacancy, spin polarization

### Reference:

- [1] A. Manthiram, et al., *Advanced Materials* 2015, 27, 1980.
- [2] Z. Liang, et al., *Advanced Energy Materials* 2021, 11, 2003507.
- [3] J. Arbiol et al., *Appl. Phys. Lett.* 2002, 80, 2.
- [4] S. Bernal, et al., *Ultramicroscopy* 1998, 72, 135-164.



248

## Investigating multiferroic phase change dynamics using in-situ electron counted spectrum imaging with synchronized holder control

Liam Spillane<sup>1</sup>, Dr Michele Conroy<sup>2</sup>

<sup>1</sup>Gatan Inc., Pleasanton, USA, <sup>2</sup>Department of Materials, London Centre of Nanotechnology, Henry Royce Institute, Imperial College London, London, UK

Poster Group 1

Improper ferroelectrics have strong potential for use in low power domain wall nano-electronic devices, as the formation and motion of conducting domain walls in such materials is governed by strain as opposed to their electric polarization [1,2]. Multimodal STEM spectrum imaging performed in the (scanning) transmission electron microscope (S)TEM is ideal for characterization of the ferroelectric domain dynamics in improper ferroelectrics, as the technique enables correlation of local chemistry and bonding information, with crystallographic and strain information determined from identical specimen regions at micro to (near) atomic scale.

The ferroic phase changes of the improper ferroelectric: Co-Cl, Cu-Cl and Fe-I based boracites ( $M_3B_7O_{13}X$ ) are complex, with the materials undergoing multiple phase transitions from low temperature up to  $T_c$ . For example, Co-Cl boracite undergoes a trigonal to monoclinic transition at 296 K, monoclinic to orthorhombic transition at 500 K and orthorhombic to cubic transition at 673 K. No memory effect is apparent through the paraelectric to ferroelectric transition though memory effect from trigonal to monoclinic phases are observed [3].

MEMS based heating-biasing and cooling-biasing holders can be used to investigate phase change dynamics in these materials as a function of applied temperature and bias, though manual holder control becomes impractical if high stimuli resolution is required, due to the large number of temperature steps required for meaningful analysis in combination with the large number of individual biasing steps required at each temperature.

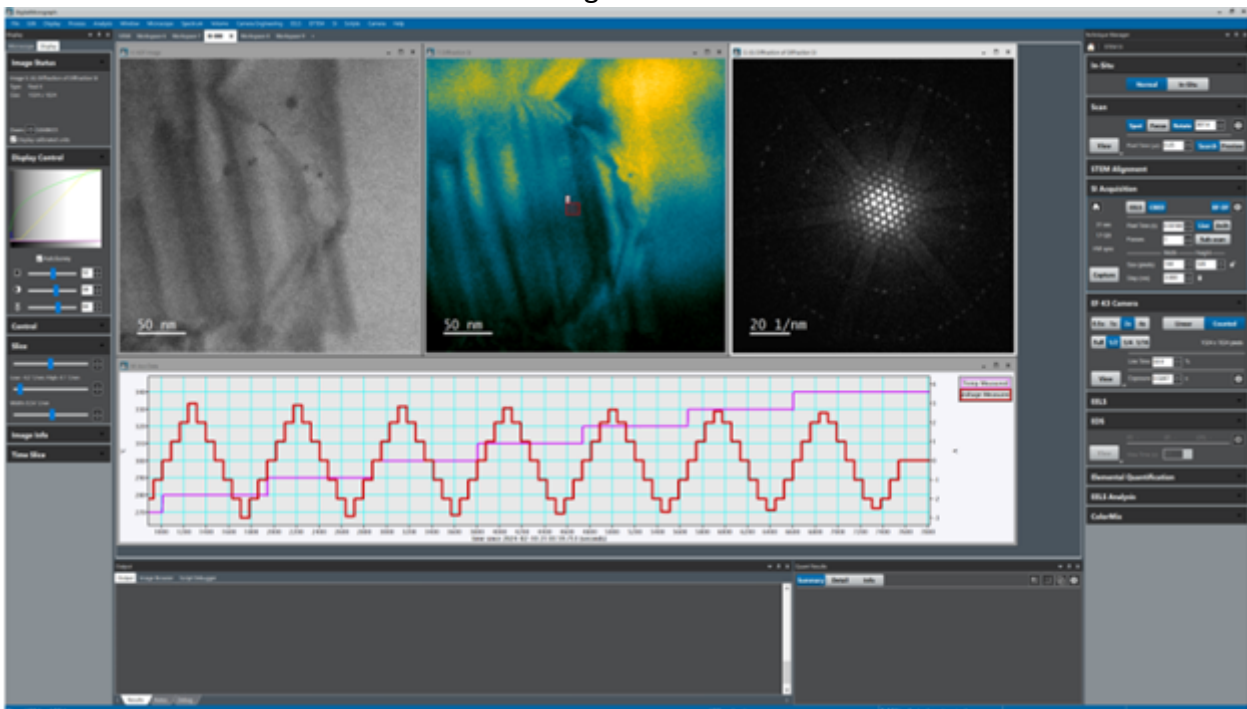
Here we present a holder automation strategy that takes advantage of the high-level communication Python library, ZMQ, to generalize external stimulus control within the DigitalMicrograph Python scripting framework. Control commands from the embedded in-situ SI data acquisition routine are sent via a generalized modular framework, enabling synchronized control of any external device supporting Python and ZMQ.

In-situ spectrum imaging was performed on Co-Cl, Cu-Cl and Fe-I based boracites ( $M_3B_7O_{13}X$ ) with a 50-80 pA probe at 300 kV, using a counted mode EELS / energy filter system (GIF Continuum K3, Gatan) and flexible scan control system (Digiscan3). Domain wall dynamics were investigated as a function of applied bias at variable temperature using MEMS based in-situ heating-biasing, and cryogenic cooling-biasing holders (Lightning & Lightning-Arctic, DENSSolutions). Holder control and synchronization to data capture was performed using Python scripting in the DigitalMicrograph and DENSSolutions Impulse software packages. This scripting allowed multiple pass in-situ spectrum image (SI) data acquisition with all SI passes acquired at fixed holder stimuli conditions. Full voltage sweeps were applied at each temperature step in a temperature series. All data acquisition and holder control was fully automated. Data processing was performed using a combination of DigitalMicrograph (EELS, 4D STEM) and the Py4DSTEM (4D STEM) software packages.

Gatan's eaSI platform and DigitalMicrograph 3.60, allowed multipass single electron counted SI data capture with zero dead time between passes, at SI pixel rates of up to 3000 pix/s with continuous

drift tracking in real time. A software screenshot showing the results of an in-situ energy-filtered 4D STEM data acquisition from Co-Cl boracite is shown in figure 1. Heating was applied in 10 °C steps from 270 °C – 340 °C. Biassing was applied at each temperature step in increments of 1 V from 0 V to  $V_{max} = + 3.0$  V and  $V_{min} = -3.0$  V and back to 0 V. The in-situ dataset comprises three primary data objects. An ADF image time series, a simultaneously acquired energy-filtered (EF) 4D STEM time series, and a holder auxiliary data plot. Measured temperature is shown in the auxiliary plot in pink. Voltage (holder bias) is shown in red. Both profiles are stepped, indicating SI passes are acquired at fixed holder stimuli conditions. A summed EF-CBED image from the highlighted region is also shown. In spite of the low probe current, the SNR of this image is high due to the high sensitivity of the counting detector. Two HOLZ rings are clearly visible.

Python scripting was successfully utilized to customize in-situ spectrum image capture, allowing synchronized control of a remote application using the ZMQ Python library. and a client-server design pattern. This design strategy was found to be a powerful means of leveraging the strengths of the native software application such as zero dead time multipass scanning, sub-pixel scanning, continuous drift tracking, etc. while also enabling holder control options not yet natively supported. In the case of Co-Cl, Cu-Cl and Fe-I based boracites ( $M_3B_7O_{13}X$ ), this allows the setup of complex heating and biasing conditions at high temperature and bias resolution that would be unachievable if a manual approach was adopted. Such setups allow exploration of the FE memory affect at specific phase transitions in addition to complex analyses such as the correlation of strain mapping with local chemical and coordination environment changes at micro and macro domain walls in these materials.



### Keywords:

ELNES, 4DSTEM, InSitu, Ferroelectric

### Reference:

- [1] Anisotropic conductance at improper ferroelectric domain walls. Nature materials (2012)
- [2] Anomalous Motion of Charged Domain Walls and Associated Negative Capacitance in Copper-Chlorine Boracite, Advanced Materials (2021)
- [3] Iliev, M., et al., Acta Physica Polonica A, 116, 2009 p.19-24.
- [4] M.C. acknowledges funding from Royal Society Tata University Research Fellowship (URF\R1\201318), EPSRC NAME Programme Grant EP/V001914/1&Royal Society Enhancement Award.

265

## Ex situ observation of ferroelectric domain evolution in wurtzite-type AlScN thin films

Dr. Niklas Wolff<sup>1</sup>, Tim Grieb<sup>2</sup>, Georg Schönweger<sup>3</sup>, Md. Redwanul Islam<sup>1</sup>, Florian F. Krause<sup>2</sup>, Andreas Rosenauer<sup>2</sup>, Stefano Leone<sup>5</sup>, Isabel Streicher<sup>5</sup>, Simon Fichtner<sup>1,4</sup>, Lorenz Kienle<sup>1</sup>

<sup>1</sup>Department of Material Science, Kiel University, Kiel, Germany, <sup>2</sup>Department for Solid State Physics, Bremen University, Bremen, Germany, <sup>3</sup>Department of Electrical and Information Engineering, Kiel University, Kiel, Germany, <sup>4</sup>Fraunhofer Institute for Silicon Technology (ISIT), Itzehoe, Germany, <sup>5</sup>Fraunhofer Institute for Applied Solid State Physics, Freiburg, Germany

Poster Group 1

### Background

Since the discovery of ferroelectricity in solid solutions of  $\text{Al}_x\text{Sc}_{1-x}\text{N}$  in 2019, the new class wurtzite-(W)-type ferroelectrics have raised huge expectations for the introduction of ferroelectric functionality into novel transistor structures, e.g., with integrated memory. Although most of the challenges targeting the materials integrability, e.g., temperature stability, thickness scaling and epitaxy with GaN have been overcome through the past years, a fundamental understanding of the switching mechanisms has been mainly approached by theoretical studies describing the local atomic origins for switching, the switching kinetics and possible pathways. However, while visualizing local polarization switching with the scanning transmission electron microscope (STEM) seems impressive,[1] an overview onto the established polar domain structures within w-type ferroelectric thin films in support of the theoretical models remains elusive; a fact which is strongly coupled to the crystalline quality of sputtered films, whereas the accessibility of monocrystalline films grown by MBE remains limited.

### Methods

We exploit annular-bright field STEM, differential phase contrast (DPC) and 4D-STEM methods to visualize the local atomic structure, polarization direction and large-scale distribution and strain of polar nano-domains.

### Results

Recently, we reported on the analog switching capabilities achieved in sub-5 nm thin films and demonstrated for the first time the realization of a multiple domain state within a single grain of AlScN linked to the presence of horizontal polarization discontinuities.[2] Moreover, here we report on the first large scale observation of ferroelectric domain patterns in monocrystalline-like epitaxial AlScN films enabled by the realization of 250 nm thin ferroelectric AlScN films grown on GaN/Sapphire templates by metal organic chemical vapor deposition.[3] The analyses reveal cone-like shaped pinned interfacial domains of opposite polarization present for the “fully” polarized states even after wake-up and 400 x cycling and their spiking extension into the bulk after further biasing. The lateral dimensions of pinned and spiking domains suggest that lateral growth is complicated by the vertical grain boundaries.

### Conclusions

The results will be discussed with respect to the proposed domain propagation models for w-type ferroelectrics. The existence of pinned domains with opposite polarization serve as nucleation sites which mainly reduce the overall required energy to domain wall motion rather than the formation of new nucleation sites. These results provide the next step in understanding of the ferroelectric switching mechanisms of epitaxially grown wurtzite-type ferroelectrics driving research on ferroelectric memory, power electronics and innovative computing applications.

**Keywords:**

STEM, ferroelectric, AlScN, thin films

**Reference:**

- [1] S. Calderon, et al. Science 2023, 380, 1034.
- [2] G. Schönweger, et al. Advanced Science 2023, 10, 2302296.
- [3] N. Wolff, et al. Advanced Physics Research n.d., n/a, 2300113.

## L-TEM characterization of controlled skyrmion nucleation in synthetic antiferromagnetic multilayers

Sara Villa<sup>1</sup>, Dr Christopher Barker<sup>2</sup>, Dr Kayla Fallon<sup>1</sup>, Mr Colin Kirkbride<sup>1</sup>, Dr Trevor Almeida<sup>1</sup>, Prof. Christopher Marrows<sup>3</sup>, Prof. Stephen McVitie<sup>1</sup>

<sup>1</sup>School of Physics and Astronomy, University of Glasgow, Glasgow, United Kingdom, <sup>2</sup>National Physics Laboratory (NPL), Teddington, United Kingdom, <sup>3</sup>School of Physics and Astronomy, University of Leeds, Leeds, United Kingdom

Poster Group 1

### Background incl. aims

Skyrmions are circular magnetic textures whose topologically protected nature makes them great candidates for the development of novel information storage devices which are both power efficient and non-volatile [1]. Effective control of the skyrmion nucleation process is required for the development of such devices. Previous research has demonstrated how a focused ion beam (FIB) microscope can be used to engineer skyrmion nucleation sites in ferromagnetic multilayers by creating artificial point-like defects [2]. Such defects induce intermixing at the interfaces between the layers, which results in local modifications of the magnetic properties in this kind of samples where the strength of exchange interactions is highly correlated with the sharpness of the interfaces. The present work builds on this research by applying this technique to a synthetic antiferromagnetic (SAF) multilayer sample. SAF multilayers are characterized by the presence of the RKKY interaction, which creates antiferromagnetic coupling between individual ferromagnetic layers. SAF skyrmions, which have been found to arise in such systems under specific field regimes, are characterised by minimal dipolar fields and are not susceptible to the skyrmion Hall effect. These properties make them more stable and better suited for spintronic applications than ferromagnetic skyrmions [3].

### Methods

In this project, an array of point-like defects was irradiated on a SAF multilayer using the 10 nm probe (FWHM) of a Ga<sup>+</sup> FIB. Defects were induced by a range of Ga<sup>+</sup> ion doses, spanning from 10<sup>13</sup> ions/cm<sup>2</sup> to 10<sup>18</sup> ions/cm<sup>2</sup>. The magnetic behaviour of the sample within the irradiated region was observed under Lorentz transmission electron microscopy (L-TEM) in the Fresnel mode, which allows for the direct visualization of magnetic textures. This led to the in-situ observation of the skyrmion nucleation and pinning behaviour in the presence of an external magnetic field. The magnetic behaviour of the sample outside of the skyrmion phase was also recorded.

### Results

Nucleation and pinning of skyrmions were observed at the location of the defects. This behaviour was observed in the ferromagnetic regime of both sides of the hysteresis loop (Fig.1). We note that, in the non-irradiated state, skyrmion nucleation is only observed when starting from a saturated state, and only after the field had passed through zero.

### Conclusion

The behaviour recorded in the irradiated areas of this SAF system differs from the behaviour recorded prior to irradiation. The field regime at which we observe skyrmion nucleation and pinning at the location of the artificial defects indicates that these skyrmions are likely to be ferromagnetic in nature in this initial study. The effects of FIB irradiation on the SAF phase of the sample are currently under investigation.

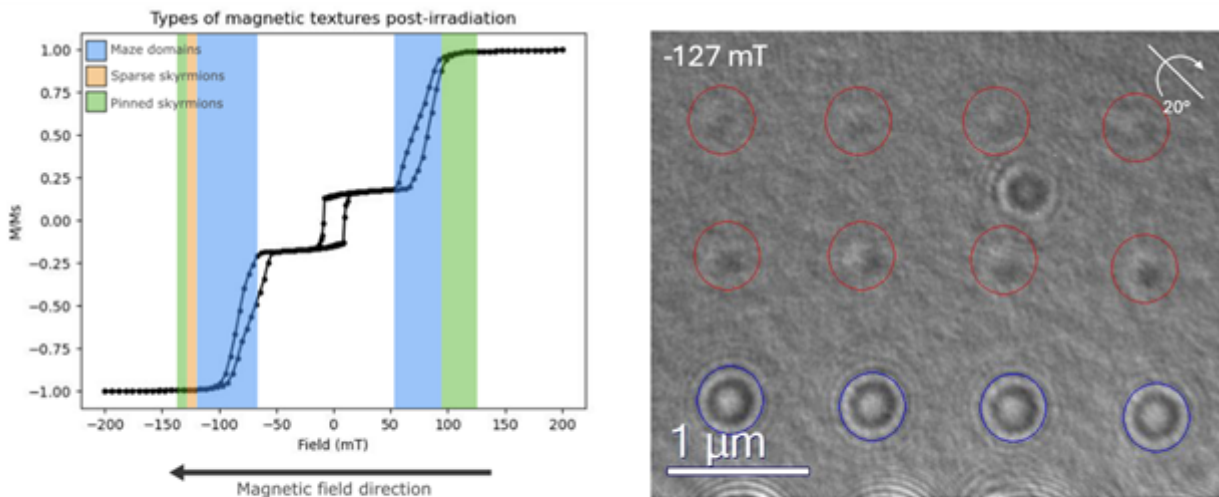


**Figure 1** Left: hysteresis loop showing the magnetic behavior of the SAF sample, highlighting the location of the three main magnetic textures observed in this study. Right: L-TEM image showing skyrmions pinned at the location of the artificial defects (circled in red). Some electrostatic contrast (circled in blue) can also be seen coming from a row of defects whose irradiation dose was high enough to cause surface damage.

### Keywords:

Magnetism, Skyrmions, L-TEM, Synthetic Antiferromagnets

### Reference:

- [1] Fert, A. et al. «Magnetic skyrmions: advances in physics and potential applications,» *Nature Reviews Materials*, 2017, 2(7), 1-15.
- [2] Fallon, K. et al. «Controlled individual skyrmion nucleation at artificial defects formed by ion irradiation,» *Small*, 2020, 16(13), 1907450.
- [3] Legrand, W. et al. «Room-temperature stabilization of antiferromagnetic skyrmions in synthetic antiferromagnets,» *Nature materials*, 2020, 19(1), 34-42.



355

## Observation of novel ferroelectric domain configurations in PbTiO<sub>3</sub>/DyScO<sub>3</sub> epitaxial films

Pau Torruella-Besa<sup>1</sup>, Chih-Ying Hsu<sup>1,2</sup>, Ludovica Tovaglieri<sup>2</sup>, Iaroslav Gaponenko<sup>2</sup>, Cécile Hébert<sup>1</sup>, Jean-Marc Triscone<sup>2</sup>, Céline Lichtensteiger<sup>2</sup>, Duncan T. L. Alexander<sup>1</sup>

<sup>1</sup>Electron Spectrometry and Microscopy Laboratory (LSME), Institute of Physics (IPHYS), Ecole Polytechnique Fédérale de Lausanne (EPFL), Lausanne, Switzerland, <sup>2</sup>Department of Quantum Matter Physics, University of Geneva, Geneva, Switzerland

Poster Group 1

PbTiO<sub>3</sub> is a ferroelectric material with the perovskite structure that exhibits polarization below a T<sub>c</sub> of 765 K. PbTiO<sub>3</sub> thin films are known to have complex domain configuration as a function of deposition temperature, epitaxial strain, film thickness and electrostatic boundary conditions. In this work, atomic resolution scanning transmission electron microscopy (STEM) characterization is used to investigate the ferroelectric polarization configuration in PbTiO<sub>3</sub> films grown under 0.2% biaxial compressive strain on a (110)<sub>o</sub>-oriented DyScO<sub>3</sub> substrate, separated by a SrRuO<sub>3</sub> bottom electrode.

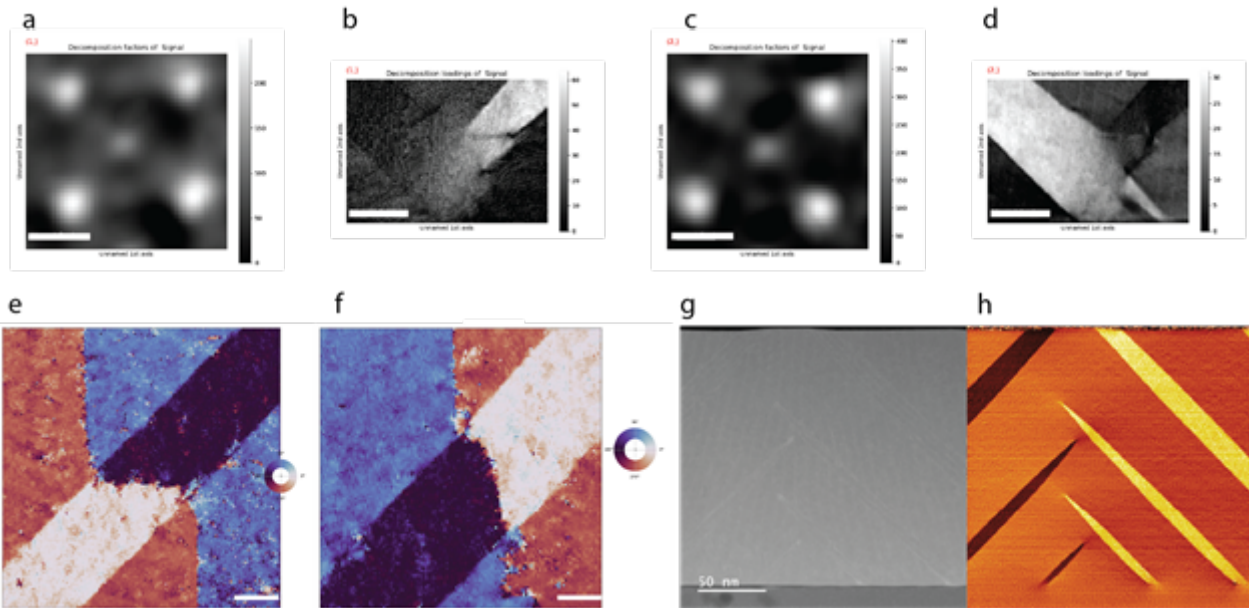
Ferroelectric polarization in PbTiO<sub>3</sub> is commonly mapped by carefully monitoring small displacements of the Ti atomic columns relative to neighboring Pb columns in aberration-corrected high angle annular dark-field (HAADF) STEM images. However, the thickness of our film of interest is around 240nm, with domains of similar size. Following this approach therefore implies tracking the position of tens of thousands of atomic columns over many tens of nanometers with picometer precision, over large images having high enough pixel density that each atomic column is separated by  $\geq 40$  pixels. To this end, we acquire 8k x 8k pixel images at relatively low magnifications, while aiming to keep the associated scan distortions to a minimum and maintaining a probe with atomic resolution.

Even when the acquisition of these large experimental images is successful, the challenge of analyzing them remains. In this work, we innovate an approach where each large-scale image is split into sub-images, each containing just one perovskite unit cell. Compared to whole-image analysis, we find that tracking the positions of atomic columns in these sub-images is greatly facilitated. It further yields a dataset that is suitable for multivariate analysis (figure 1a-d); an approach analogous to that shown by Ziatdinov et al.<sup>1,2</sup>.

The results are large-scale polarization maps that reveal novel a/c domain configurations in the form of needles, stacked a-domains (figure 1 g-h), as well as strongly and weakly charged 180° domain walls (figure 1 e-f). Interestingly, a potentially new type of line defect is observed, that may play a role in stabilizing the observed domain walls that we hypothesize to be of high energy.

In conclusion, we present ongoing analyses of novel domain configurations in strained films of ferroelectric PbTiO<sub>3</sub>, where we combine large-scale atomic resolution STEM imaging with machine-learning analyses to identify and understand domain boundary and structural defects.

Figure 1 . a-d) Non-negative matrix factorization results on unit-cell subimages revealing the complex structure of a-c configuration with both 90° and 180° domain walls. Scale bars correspond to 2 Å for panels a,c and 15 nm for panels b,d. e-f) Polarization angle of maps of different observed 180° domain walls across a and c domains. Polarization up, down, right and left directions correspond to blue, red, black and white colors respectively. Scale bars correspond to 20 nm. g-h) Stacked needles configuration of a-c domains revealed by geometrical phase analysis.



**Keywords:**

Ferroelectric, PTO, STEM-HAADF, atomic resolution

**Reference:**

1. Ziatdinov, M., Nelson, C., Vasudevan, R. K., Chen, D. Y. & Kalinin, S. V. Building ferroelectric from the bottom up: The machine learning analysis of the atomic-scale ferroelectric distortions. *Appl. Phys. Lett.* 115, 52902 (2019).
2. Ziatdinov, M., Ghosh, A., Wong, C. Y. & Kalinin, S. V. AtomAI framework for deep learning analysis of image and spectroscopy data in electron and scanning probe microscopy. *Nat. Mach. Intell.* 2022 412 4, 1101–1112 (2022)

401

## Magnetic behavior of steel studied by in-situ Lorentz microscopy, magnetic force microscopy and micromagnetic simulations

Mari Honkanen<sup>1</sup>, Suvi Santa-aho<sup>2</sup>, Sami Kaappa<sup>3</sup>, Lucio Azzari<sup>1</sup>, Henri Lukinmaa<sup>4,5</sup>, Jaakko Kajan<sup>4</sup>, Samuli Savolainen<sup>4</sup>, Mikko Palosaari<sup>4</sup>, Lasse Laurson<sup>3</sup>, Minnamari Vippola<sup>1,2</sup>

<sup>1</sup>Tampere Microscopy Center / Tampere University, Tampere, Finland, <sup>2</sup>Materials Science and Environmental Engineering / Tampere University, Tampere, Finland, <sup>3</sup>Computational Physics Laboratory / Tampere University, Tampere, Finland, <sup>4</sup>Stresstech Oy, Jyväskylä, Finland, <sup>5</sup>Verity, Zurich, Switzerland

Poster Group 1

Many industrially relevant steels are ferromagnetic such as ferritic-pearlitic steel characterized in this study. Ferritic-pearlitic steels are commonly used, for example, in automotive components. Microstructural features of ferromagnetic materials influence their mechanical and micromagnetic properties. Traditionally, the microstructure, for example, cementite ( $\text{Fe}_3\text{C}$ ) content, has been studied with destructive methods. To save time and money, destructive methods should be replaced with non-destructive testing (NDT) techniques. One of the potential NDT methods is magnetic Barkhausen noise (MBN) testing. It is used in industry to detect for example localized microstructure and stress variations. MBN testing is based on the motion of magnetic domain walls in ferromagnetic materials exposed to a time-varying external magnetic field. The motion of domain walls is hindered by the microstructural pinning sites such as carbides, grain boundaries, and dislocations. In the varying magnetic field, domain walls stop and finally jump over the pinning features, causing discontinuous and abrupt changes in the magnetization of the workpiece. These changes result in electromagnetic burst-like signal, i.e., Barkhausen noise, measured with an inductive coil. However, the applicability of the Barkhausen noise method is currently limited due to the stochastic nature of the phenomenon itself. Thus, more scientific knowledge is needed. Recently, we mimicked and visualized the Barkhausen noise measurement by in-situ Lorentz microscopy. This study gives general information about the behavior of domain walls in ferromagnetic steel. In addition, we have utilized magnetic force microscopy and micromagnetic simulations to deepen our knowledge on the magnetic behavior of steels.

In this study, we used multi-instrumental and computational approach. Traditional microstructural characterization of ferritic-pearlitic steel was carried out by SEM-EBSD-TKD and (S)TEM-EDS. The magnetic structure of the thin sample was studied by Lorentz microscopy (Fresnel mode), while the bulk sample was studied by magnetic force microscopy (MFM). The dynamics of domain walls were studied by in-situ Lorentz microscopy. A varying, external magnetic field was generated by a normal objective lens of TEM, and the images were collected in LOW MAG mode using objective mini lens. The recorded frames of each sample were jointly post-processed as a single video using video denoising and frame alignment procedures. To measure a single point magnetic flux density generated with different excitation values of the normal objective lens inside the TEM, we used a custom-made holder equipped with a Hall-effect sensor. We also run micromagnetic simulations to verify domain wall dynamics in certain magnitudes of magnetic fields.

Our multi-instrumental characterization, dynamical in-situ Lorentz microscopy studies, and micromagnetic simulations with the complex ferritic-pearlitic structure revealed the interaction of different domain walls and pinning sites. Thus, we could visualize and verify hypotheses related to the origin of Barkhausen noise signal. Comparing Lorentz microscopy and MFM results, we indicated that thin and bulk samples studied have similar magnetic structure. So, TEM studies are also relevant from the industrial point of view, although usually bulk samples are used in industrial applications. To

measure the magnetic field strength generated by the normal objective lens of TEM in dynamical in-situ studies, we built a custom-made Hall-effect sensor holder. It measures the flux density at the same location as the TEM sample. Based on the measurements, the objective lens of our TEM has almost linear response to the magnetic field strength, and when the objective lens is switched off, the magnetic field in the sample area is close to 0 mT.

Based on our studies, the carbides are very strong pinning sites for domain walls. In addition, larger globular and thicker lamellar carbides can have their own magnetic structure. In the increasing magnetic field, domain walls in the ferritic matrix perpendicular to the lamellar cementite carbides begin to move first. Then, the domain walls inside the carbides start to disappear. Finally, domain walls parallel to the lamellar carbides move. However, some of them are very strongly pinned by carbides. When the magnetic field is decreased back to 0 mT, the domain walls appear in the opposite order. We simulated the magnetization dynamics where microstructural information is extracted from the SEM-TKD and (S)TEM results. To explain the domain wall behavior in certain magnitudes of the magnetic field as observed using in-situ Lorentz microscopy, we ran dynamical micromagnetic simulations to reproduce the domain wall disappearance in the globular carbide. In general, the simulations supported very well the interpretation of the experimental findings, although the re-appearance of the domain walls with decreasing field could not be reproduced. In the next step, our multi-instrumental and computational approach will be extended by transport of intensity equation (TIE) method and off-axis electron holography. These results will be reported in the near future.

Imaging methods and micromagnetic simulations have their own limitations. Despite using multi-imaging techniques, it is probable that not all magnetic features can be visualized by microscopes and on the other hand, simulations cannot always reproduce all events observed experimentally. However, our combined multi-instrumental and computational approach gives novel knowledge on how iron-based carbides affect magnetic domain wall dynamics in ferromagnetic steel.

**Keywords:**

Ferromagnetism, Lorentz microscopy, Micromagnetic simulations

**Reference:**

Honkanen et al., *Acta Materialia* 221 (2021) 117378.

Santa-aho et al., *Materials & Design* 234 (2023) 112308.

Honkanen et al., Abstract in Scandem 2023 conference, Uppsala, Sweden, 2023.

Honkanen et al., manuscript submitted to *Ultramicroscopy* (2024).

458

## Nanoscale Chemical Segregation to Twin Interfaces in $\tau$ -MnAl-C and Resulting Effects on the Magnetic Properties

Mr. Panpan Zhao<sup>1</sup>, Markus Gusenbauer<sup>3</sup>, Harald Oezelt<sup>3</sup>, Daniel Wolf<sup>1</sup>, Thomas Gemming<sup>1</sup>, Thomas Schrefl<sup>3</sup>, Kornelius Nielsch<sup>1,2</sup>, Thomas George Woodcock<sup>1</sup>

<sup>1</sup>Leibniz IFW Dresden, Dresden, Germany, <sup>2</sup>TU Dresden, Dresden, Germany, <sup>3</sup>Department for Integrated Sensor Systems, Danube University Krems, Krems an der Donau, Austria

Poster Group 1

### Background incl. aims

Among various candidates for the rare-earth free permanent magnets, the ferromagnetic  $\tau$ -MnAl-C (L10, P4/mmm) shows great potential to replace ferrites and bonded Nd-Fe-B magnets for its attractive magnetic properties and the non-critical nature of the raw elements [1, 2]. Further magnetic properties enhancement will depend on understanding of the effect of various crystallographic defects in the magnet, e.g. twin boundaries, and on developing novel processing routes for microstructure optimization.

Twin boundaries are frequently observed in both the as-transformed and hot deformed  $\tau$ -MnAl-C magnets [3]. Three different types of twin boundaries have been discovered in the  $\tau$ -MnAl-C magnet and they are described as true twins, order twins and pseudo twins [4]. Considering the tetragonal structure of the chemically ordered  $\tau$ -MnAl-C magnet, it is reasonable to assume that a different atomistic structure exists at these three types of twins, as well as its local magnetic properties.

### Methods

In this study, aberration-corrected scanning transmission electron microscopy coupled with electron energy-loss spectroscopy (STEM-EELS) was used to investigate the atomistic structure and chemical composition at various twin boundaries in  $\tau$ -MnAl-C [5].

### Results

The results show differing levels of structural disorder at the various types of twin boundaries and EELS data reveal the presence of a Mn-enriched layer at the twin boundary surrounded by Al-enriched layers. The thickness of these layers and the magnitude of the chemical segregation vary with the level of structural disorder. Micromagnetic simulations based closely on the experimental results showed that the coercivity tends to increase with increasing structural and chemical disorder at the twin interface.

### Conclusions

These results suggest that targeted doping of interfaces in  $\tau$ -MnAl may be a promising strategy to increase the coercivity of the material for applications.

### Keywords:

Twin boundaries

STEM-EELS

Elemental segregation

### Reference:

- [1] L. Feng, J. Freudenberger, T. Mix, K. Nielsch, T.G. Woodcock, *Acta Mater*, 2020, 199, 155-168.
- [2] T. Ohtani, N. Kato, S. Kojima, K. Kojima, Y. Sakamoto, I. Konno, M. Tsukahara, T. Kubo, *IEEE Trans. Magn*, 1977, 13, 1328-1330.
- [3] P. Zhao, L. Feng, K. Nielsch, T.G. Woodcock, *J. Alloys Compd*, 2021, 852, 156998.
- [4] F. Bittner, L. Schultz, T.G. Woodcock, *Acta Mater*, 2015, 101, 48-54.
- [5] P. Zhao, M. Gusenbauer, H. Oezelt, D. Wolf, T. Gemming, T. Schrefl, K. Nielsch, T.G. Woodcock, *J. Mater. Sci. Technol*, 2023, 134, 22-32.

468

## Twinning in HfO<sub>2</sub> nanocrystals

Hongchu Du<sup>1</sup>, Prof. Dr. Joachim Mayer<sup>1,2,3</sup>

<sup>1</sup>Forschungszentrum Jülich GmbH, Jülich, Germany, <sup>2</sup>RWTH Aachen University, Aachen, Germany,

<sup>3</sup>Jülich Aachen Research Alliance, Jülich, Germany

Poster Group 1

### Background

Twinning, a phenomenon observed in a variety of crystalline solids, often arises during growth, deformation, and phase transformations [1]. The symmetry connecting adjacent crystal twins differs from the point group symmetries of the parent crystal. These additional symmetry operations, known as twin operations, typically include rotation, reflection, and inversion [1].

Materials with polar point group symmetries exhibit spontaneous polarization. An emergent polarization from twinning is anticipated when the additional symmetry coincides with a polar point group's symmetry. Nonetheless, the complex interplay between twinning and polarization has been scantily addressed in the literature.

The twinning associated with the tetragonal to monoclinic phase transformation in ZrO<sub>2</sub> and HfO<sub>2</sub> has undergone extensive study. Twin planes are commonly observed on the (100) plane and potentially on others, such as (001) and {110} [2]. A thorough understanding of twinning necessitates resolving both the heavier metal and lighter oxygen atoms.

The negative spherical aberration (Cs) imaging (NCSI) technique provides optimal negative phase contrast under conditions of negative Cs and overfocus in conventional transmission electron microscopy (TEM) mode [3]. Comparative studies have demonstrated the superiority of NCSI over positive Cs imaging in terms of image contrast, signal intensity, and noise robustness. Notably, NCSI excels in visualizing all atoms, including oxygen, in metal oxides.

This work aims to elucidate the atomic structure of twin boundaries in HfO<sub>2</sub> nanocrystals using the NCSI technique [3].

### Methods

In this study, NCSI TEM images were captured at 200 kV with a Gatan OneView phosphor-CMOS camera on an FEI Titan 50-300 PICO electron microscope, featuring a Schottky field emission electron gun and a CEOS Cc/Cs corrector. Additional NCSI images were obtained at 300 kV using a Thermo Fisher Scientific Spectra 300 microscope equipped with a high-brightness X-FEG source, a piezo-enhanced CompuStage, a CEOS CETCOR Cs corrector for the S-TWIN objective lens, and a fast Ceta CMOS camera. The monoclinic HfO<sub>2</sub> nanocrystals under study were synthesized via a sol-gel method [5].

### Results

Using the NCSI TEM technique, we resolved both hafnium and oxygen atoms within individual HfO<sub>2</sub> nanocrystals (Fig. 1). The NCSI findings disclosed both individual and unit-cell-wise multiple consecutive twinning on the (200) plane of colloidal HfO<sub>2</sub> nanocrystals. Each twinning event involves two-fold screw symmetry, leading to a unit-cell scale polar orthorhombic phase with a Pbc2<sub>1</sub> space group at the twin boundary. The unit-cell-wise multiple consecutive twinning gives rise to a novel antipolar phase with the Pbca space group. These interpretations were corroborated through an iterative two-step optimization process for image matching between experimental and simulated images.

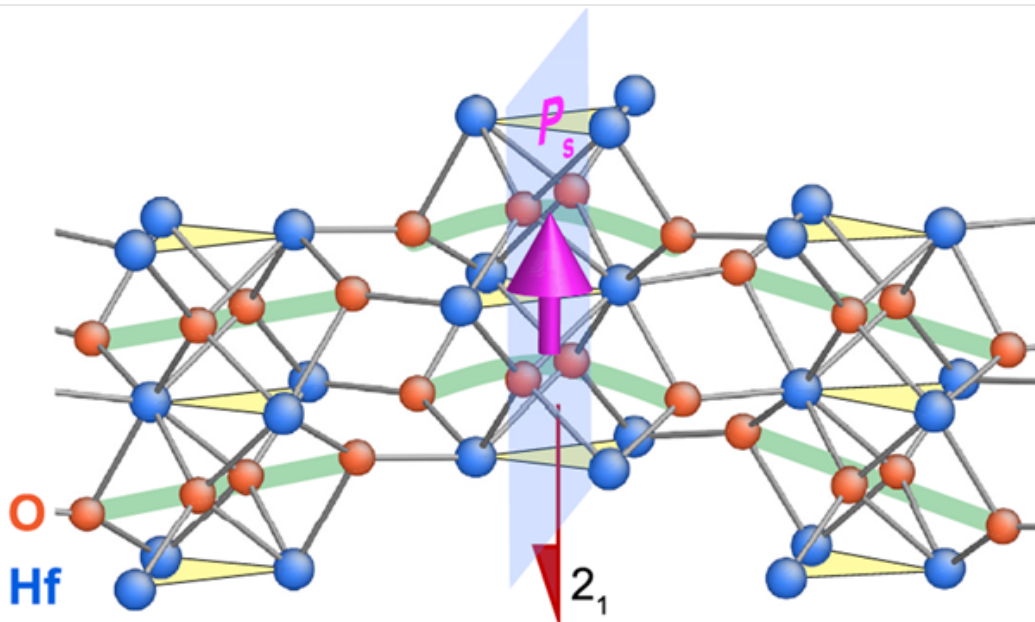
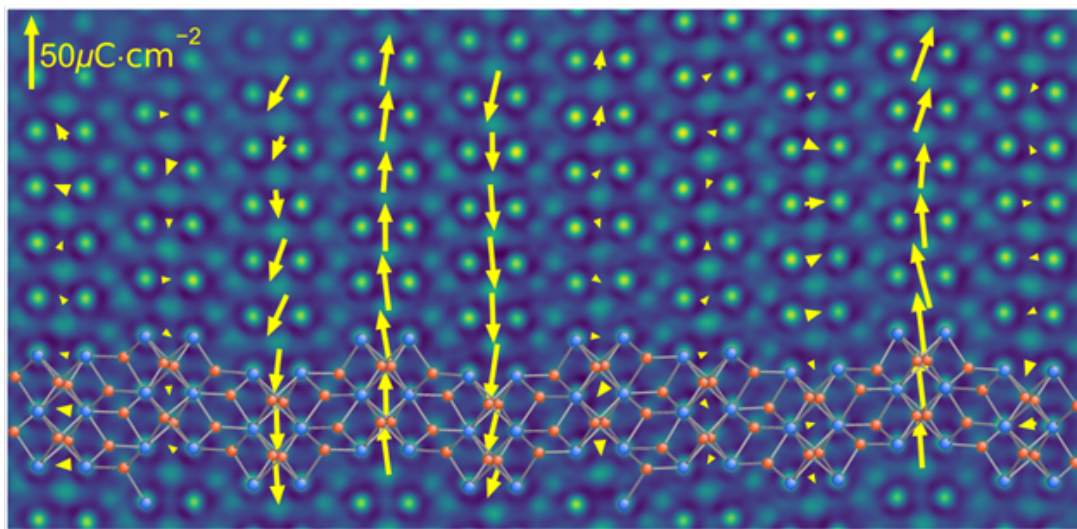
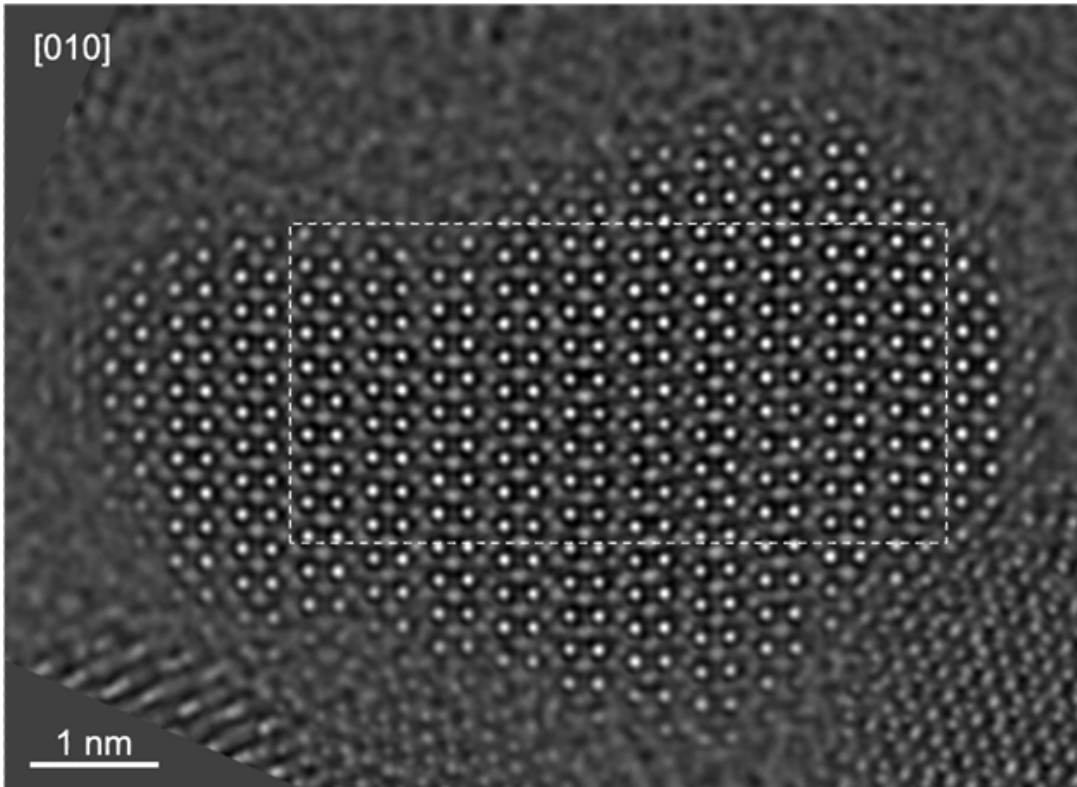
Figure 1 Top: Atomic resolution TEM image of an HfO<sub>2</sub> nanocrystals recorded using the negative spherical aberration (Cs) imaging (NCSI) technique. Middle: Map of polarization vectors and structure



model (blue: Hf, orange: O, grey: bond) superimposed on the NCSI image of the region marked in the top. Bottom: Structural illustration of polarization resulting from twinning.

### Conclusions

We have revealed the correlation between twinning and polarization in HfO<sub>2</sub> colloidal nanocrystals via the NCSI technique [3]. The polarization induced by twinning correlates with sub-nanometer ferroelectric and antiferroelectric phases. The discovery of twinning-induced polarization may offer a new avenue for identifying novel ferroelectric phases in ionic compounds beyond oxides.



**Keywords:**

NCSI, Twinning, Polarization, HfO<sub>2</sub>

**Reference:**

- [1] W. D. Nesse, *Introduction to Mineralogy*, 2017, Oxford University Press, New York.
- [2] J. E. Bailey, *Proc. R. Soc. Lond. A*, 1964, 279, 395.
- [3] H. Du, C. Groh, C.-L. Jia, T. Ohlerth, R. E. Dunin-Borkowski, U. Simon, J. Mayer, *Matter*, 2021, 4, 986.
- [4] C.L. Jia, L. Houben, A. Thust, J. Barthel, *Ultramicroscopy*, 2010, 110, 500.
- [5] T. Ohlerth, H. Du, T. Hammor, J. Mayer, U. Simon, *Small Science*, 2024, 2300209.

## Atomically Sharp Domain Walls in an Antiferromagnet

Jan Michalička<sup>1</sup>, Filip Křížek<sup>2</sup>, Sonka Reimers<sup>3</sup>, Zdenek Kašpar<sup>2</sup>, Ondrej Man<sup>1</sup>, Jan Ruzs<sup>4</sup>, Juan Carlos Idrobo<sup>5</sup>, Peter Wadley<sup>3</sup>, Tomas Jungwirth<sup>1,3</sup>

<sup>1</sup>CEITEC - Brno University of Technology, Brno, Czech Republic, <sup>2</sup>Institute of Physics of CAS, Prague, Czech Republic, <sup>3</sup>School of Physics and Astronomy, University of Nottingham, Nottingham, United Kingdom, <sup>4</sup>Department of Physics and Astronomy, Uppsala University, Uppsala, Sweden, <sup>5</sup>Center for Nanophase Materials Sciences, ORNL, Oak Ridge, USA

Poster Group 1

### Introduction

Efficient manipulation of antiferromagnetic (AF) domains and domain walls has opened up new avenues of research towards ultrafast, high-density spintronic devices [1,2]. AF domain structures are known to be sensitive to magnetoelastic effects, but the microscopic interplay of crystalline defects, strain and magnetic ordering remained largely unknown. Recently, we have explored antiferromagnetic CuMnAs thin films in which imaging by x-ray photoemission electron microscopy (XPEEM) revealed that its AF domain structure is dominated by nanoscale crystalline defects [3]. However, even smaller magnetic objects were indirectly observed in the material, but they remained below the detection limit of the used established XPEEM methods.

### Materials and Methods

Scanning transmission electron microscopy (STEM), differential phase-contrast (DPC) and 4D-STEM techniques are utilized CuMnAs epilayers grown by molecular beam epitaxy.

### Results

Here, we achieve atomic resolution imaging of abrupt AF magnetic domain walls in CuMnAs epilayers [4]. The identification of the magnetic domain DPC signal is based on the specific symmetry of the CuMnAs crystal, where the opposite magnetic Mn sublattices occupy crystallographically distinct noncentrosymmetric sites, Fig. 1A. With focus on small field-of-view high-resolution imaging, we could associate the DPC-STEM signals with two types of abrupt Néel vector reversals, schematically illustrated in Fig. 1C and D: The first type occurs at a crystallographic antiphase boundary defect (Fig. 1C), while the second type forms in a part of the epilayer with no crystallographic perturbation detectable by STEM (Fig. 1D).

### Conclusions

The results emphasized the crucial role of these defects in determining the AF domains and domain walls, and provided a route to optimizing device performance in term of scaling limits for the data density in the bulk of the antiferromagnet.

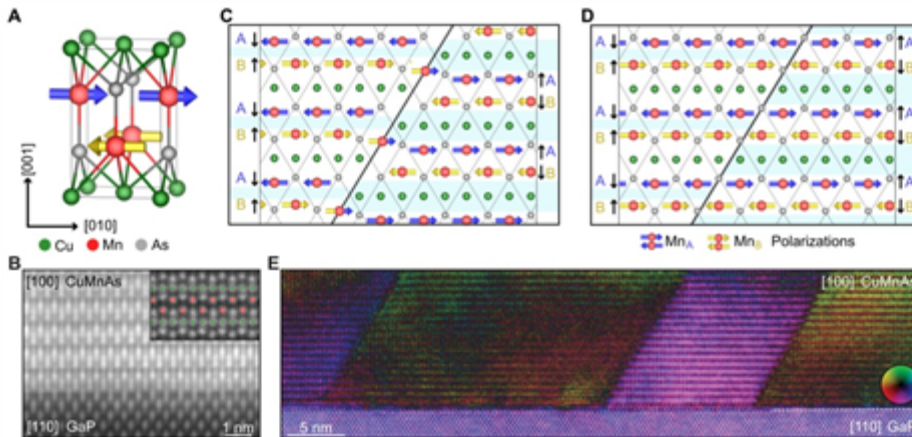


Fig. 1: (A) CuMnAs unit cell. (B) HAADF-STEM of [100] CuMnAs epilayer on GaP. (C, D) Atomically sharp domain walls at antiphase boundary defect and in unperturbed area of the CuMnAs single crystal, respectively. Black arrows represent Lorentz force direction at individual sublattices. (E) DPC-STEM overview of atomically sharp domain walls in CuMnAs.

### Keywords:

DPC, 4D-STEM, Antiferromagnets

### Reference:

- [1] Jungwirth, T. et al. Antiferromagnetic spintronics. *Nature Nanotechnology*, 11(3), pp. 231–241 (2016)
- [2] Wadley, P. et al. Electrical switching of an antiferromagnet. *Science*, 351(6273), pp. 587–590 (2016)
- [3] Reimers, S. et al. Defect-driven antiferromagnetic domain walls in CuMnAs films. *Nature Communications*, 13(1), pp. 724 (2022)
- [4] Křížek, F. et al. Atomically sharp domain walls in an antiferromagnet. *Science Advances*, 8(13), pp. 3535 (2022)

478

## Observing Magnetic Skyrmions in Pt/Co/Cu Multilayers using in-situ Lorentz Transmission Microscopy

Nuria Bagues<sup>1,2,3</sup>, Binbin Wang<sup>1,2,4</sup>, Shuyu Cheng<sup>5</sup>, Shekhar Das Das<sup>5</sup>, Ziling Li<sup>5</sup>, Jacob Freyermuth<sup>5</sup>, Camelia Selcu<sup>5</sup>, Denis V. Pelekhov<sup>5</sup>, Chris Hammel<sup>5</sup>, Mohit Randeria<sup>5</sup>, Roland Kawakami<sup>5</sup>, David W McComb<sup>1,2</sup>

<sup>1</sup>Center for Electron Microscopy and Analysis, The Ohio State University, Columbus , US, <sup>2</sup>Department of Material Science and Engineering, The Ohio State University, Columbus , US, <sup>3</sup>Present address: Alba Synchrotron Light Facility, CELLS, Cerdanyola del Vallès, Spain , <sup>4</sup>Present address: Intel Corporation, Hillsboro, US, <sup>5</sup>Department of Physics, The Ohio State University, Columbus , US

Poster Group 1

Magnetic multilayer systems hosting skyrmions at room temperature have attracted considerable interest for their potential application in the forthcoming generation of magnetic data storage devices. Pt/Co/X multilayer systems, where X represents a metallic element, stand out as a prospective candidate due to their versatile adjustability of magnetic properties. Recent theoretical predictions indicate that the size of skyrmions within this multilayer architecture can be finely tuned by varying the repetition of stack layers, the thickness of individual metallic layers and the element X [1]. A pivotal milestone towards employing these multilayer systems in data storage devices lies in the capacity to both stabilize skyrmions and manipulate their movement across the material. In this work, in situ in Lorentz transmission electron microscopy (LTEM) is used to investigate nucleation, stability, and mobility of magnetic phases in [Pt/Co/Cu]<sub>x5</sub> multilayer specimens.

[Pt/Co/Cu]<sub>x5</sub> multilayer specimens were grown on Pt buffer layer grown on an insulator substrate (Al<sub>2</sub>O<sub>3</sub> [111]) using molecular beam epitaxy (MBE) [2]. Cu was chosen as a X mainly for two reasons: 1) its close lattice parameter to Co and Pt favors an epitaxial grown of the layers, and 2) there isn't a magnetic dead layer in this system [3,4]. Cross-section and plan-view specimens were prepared using dual focused ion beam (FIB) instrument. High angle annular dark field (HAADF) STEM imaging and energy-dispersive X-ray (EDX) mapping analysis in cross-section specimens was performed to characterize the layered structure of specimens. L-TEM in Fresnel mode with variable applied magnetic field was used to investigate magnetic domain structure and skyrmions in plan-view specimens. As a further step, biasing experiments applying current (DC and pulses) using an in-situ TEM holder (DENS Wildfire-Lightning) connected to a pulse generator were performed to explore the stability of magnetic phases and its dynamics.

Room temperature magnetic phases as a function of applied magnetic field (from 0mT to 300mT) are identified by LTEM imaging, showing "labyrinth" texture at 0mT that evolves into magnetic stripes domains followed by a transition to isolated bubbles-like skyrmions around 135mT [2,5]. The contrast in the LTEM images, suggest coexistence of multitype bubbles-like skyrmions, Bloch-type and Néel-type. This observation is quite surprising since a Néel-type configuration is expected for such interfacial Dzyaloshinskii–Moriya interactions (DMI) system. As a result of our biasing experiments, it was observed that skyrmion's type, stability and density can be modulated by the thermal effect caused by current pulses or DC current. Ultimately, the correlation between current density and applied magnetic field for this system is summarized in a magnetic phase diagram.

Our findings reveal a broad range of magnetic conditions enabling the manipulation and control of skyrmions by varying biasing current parameters and could be considered within similar systems.



**Keywords:**

Magnetic multilayer, LTEM, Skyrmions

**Reference:**

- [1] H. Jia, et al., Material systems for FM-/AFM-coupled skyrmions in Co/Pt-based multilayer, *Phys. Rev. Materials* 4, 094407 (2020). DOI: 10.1103/PhysRevMaterials.4.094407
- [2] S. Cheng, et al., Room-temperature magnetic skyrmions in Pt/Co/Cu multilayers, *Phys. Rev. B* 108, 174433 (2023) DOI: 10.1103/PhysRevB.108.174433
- [3] L. Sun, et al., Magnetic stripe domains of [Pt/Co/Cu]<sub>10</sub> multilayer near spin reorientation transition, *AIP Adv.* 6, 056109 (2016). DOI: 10.1063/1.4943360
- [4] M. Belmeguenai, et al., Influence of the capping layer material on the interfacial Dzyaloshinskii-Moriya interaction in Pt/Co/capping layer structures probed by Brillouin light scattering, *J. Phys. D* 52, 125002 (2019). DOI: 10.1088/1361-6463/aafdf5
- [5] B. Wang, et al., Insights into the Origin of Skyrmion Pinning in [Pt/Co/Cu] Magnetic Multilayers, *Microscopy and Microanalysis*, 28 (S1), 2328-2330 (2022) DOI:10.1017/S1431927622008947

538

## Polar textures in multiferroic BiFeO<sub>3</sub>-based superlattices

Dr. Razvan Burcea<sup>1</sup>, Oana Condurache<sup>1</sup>, Mouna Khiari<sup>2</sup>, Maxime Vallet<sup>1</sup>, Stephane Roux<sup>3</sup>, Pascal Ruello<sup>4</sup>, Brahim Dkhil<sup>1</sup>, Houssny Bouyanfif<sup>2</sup>

<sup>1</sup>Université de Paris-Saclay, CentraleSupélec, SPMS, Gif-sur-Yvette, France, <sup>2</sup>LPMC EA2081, Université de Picardie Jules Verne, Amiens, France, <sup>3</sup>Université de Paris-Saclay, ENS Paris-Saclay, LMPS, Gif-sur-Yvette, France, <sup>4</sup>IMMN, Le Mans Université, , France

Poster Group 1

### Background incl. aims

Over the last few decades, the properties of ferroelectrics and their polar arrangements have been extensively studied in thin films or bulk systems. However, it is only recently that ferroelectric-based superlattices (SLs), i.e. an alternation of two layers with a chemical period  $\Lambda$ , have emerged and led to the discovery of exotic polar textures such as skyrmionic states or vortices in PbTiO<sub>3</sub>/SrTiO<sub>3</sub> SLs. [1,2] Thus, SLs offer a unique and promising new platform to study these novel polar states which result mainly from the effects of strain, confinement, and competing interactions between the degrees of freedom (polar displacements, oxygen tilts) of these perovskite layers. BiFeO<sub>3</sub>/LaFeO<sub>3</sub> (BFO/LFO) SLs, have also showed interesting features in recent work.[3] BFO is, in essence, the model multiferroic material which exhibits in its bulk form ferroelectric polar states coexisting with a complex magnetic state. However, when it's incorporated in such SLs, an unusual antiferroelectric like-state is observed. Here, the aim of our study is to understand, through scanning transmission electron microscopy (STEM) characterization, how the buffer (LaFeO<sub>3</sub> or NdFeO<sub>3</sub>) layers influence the polar states of BFO.

### Methods

BFO/LFO (or NFO) SLs were grown on cubic single crystal (001) STO substrate by pulsed laser deposition (MECA 2000 chamber) using a KrF laser (248 nm). BFO and LFO (or NFO) layers were grown at the same conditions under 0.5 mbar of oxygen pressure (PO<sub>2</sub>) at 740°C at 6 Hz repetition rate. Cross-section transmission electron microscopy (TEM) samples were prepared on an FEI ThermoFisher Helios Nanolab 660 by using the standard lift-out technique. The annular bright field (ABF) and high angle annular dark field (HAADF) STEM images were acquired by a FEI Titan3 G2 80-300 microscope, operated at 300 kV and equipped with a Cs probe corrector. The analysis of atomic displacements has been performed by the Python open-source library Atomap and Temul-Toolkit library for visualization.[4,5] In complement, STEM images were also analyzed by a "render-and-compare" (RAC) method based on Principle Component Analysis (PCA).

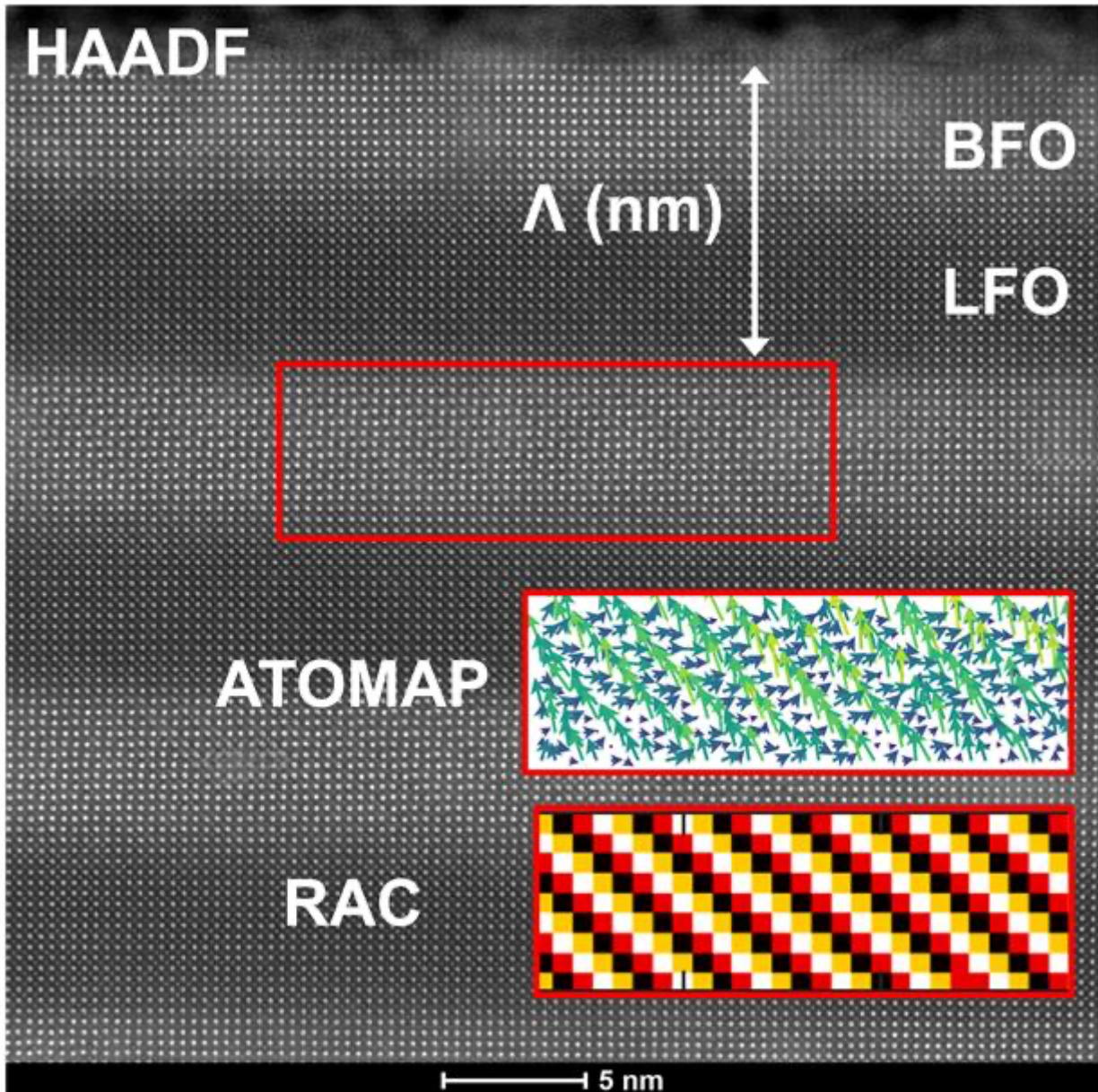
### Results

We analyzed several BFO/LFO and BFO/NFO SLs, with various periods  $\Lambda$  (3, 6, 12 and 20 nm) and same BFO/LFO (or NFO) thickness ratio, deposited on STO substrates. We were able to reveal various polar textures within the BFO layers by analyzing the relative atomic displacements as well as the Fourier components with Atomap and RAC respectively. Among them, we unexpectedly observed in-plane and  $\sim 45^\circ$  ferroelectric displacements, but also step-like polar arrangements resulting in a quadrupling of the unit cell confirmed by fast Fourier transform (FFT) images. While Atomap indicates an (up-up-right-right)-like shifts (see Figure), RAC rather suggests a more complex polar distribution with 4 different types of displacements. Moreover, some polar singularities showing hedgehog-like, i.e. skyrmionic textures, were also observed revealing the wild variety of the polarization in BFO.

### Conclusions

STEM analysis shows that introducing BFO in SLs systems induces drastic changes of its polar textures, mainly by strain and confinement effects, thus showing the high potential for modulating its

polarization. Besides, the comparison of data analysis methods shows that Atomap and RAC are complementary into revealing the nature of the observed displacements.



**Keywords:**

HR-STEM, ferroelectricity, polarization, data analysis

**Reference:**

- [1] Das, S., Tang, Y.L., Hong, Z. et al. Observation of room-temperature polar skyrmions. *Nature* 568, 368–372 (2019).
- [2] Yadav, A., Nelson, C., Hsu, S. et al. Observation of polar vortices in oxide superlattices. *Nature* 530, 198–201 (2016).
- [3] B. Carcan, H. Bouyanfif, et al. Interlayer strain effects on the structural behavior of BiFeO<sub>3</sub>/LaFeO<sub>3</sub> superlattices. *J. Appl. Phys.* 124(4), 044105 (2018).
- [4] Nord, M., Vullum, P.E., MacLaren, I. et al. Atomap: a new software tool for the automated analysis of atomic resolution images using two-dimensional Gaussian fitting. *Adv Struct Chem Imag* 3, 9 (2017).
- [5] E. O’Connell, M. Hennessy, and E. Moynihan, “PinkShnack/TEMUL: Version 0.1.3,” (2021) 10.5281/zenodo.4543963.

606

## Atomic-resolution STEM analysis of polar states in Sr<sub>1-x</sub>Ba<sub>x</sub>MnO<sub>3</sub> thin films

Dr César Magén<sup>1,2</sup>, Mr Panagiotis Koutsogiannis<sup>1,2</sup>, Prof. PA Algarabel<sup>1,2</sup>, Ms. MP Morales<sup>1</sup>, Dr. JA Pardo<sup>3</sup>

<sup>1</sup>Instituto de Nanociencia y Materiales de Aragón (INMA), Universidad de Zaragoza-CSIC, Zaragoza, Spain, <sup>2</sup>Departamento de Física de la Materia Condensada, Universidad de Zaragoza, Zaragoza, Spain, <sup>3</sup>Departamento de Ciencia y Tecnología de Materiales y Fluidos, Universidad de Zaragoza, Zaragoza, Spain

Poster Group 1

### Background incl. aims

Subtle changes in stoichiometry and crystal symmetry govern the fundamental physics of perovskite oxides. Particularly in thin films, the interplay between chemistry and structure can be altered by fine-tuning the conditions for epitaxial growth. A good example is the family of multiferroics AMnO<sub>3</sub> (A = Ca, Sr, Ba) perovskite antiferromagnets in which ferroelectricity driven by the off centering of the magnetic cation Mn<sup>4+</sup> can emerge through selective crystal distortions [1]. In this talk we will explore how the polar states of the family of epitaxial Sr<sub>1-x</sub>Ba<sub>x</sub>MnO<sub>3-δ</sub> (SBMO), thin films [2] can be controlled by careful selection of the substrate, growth conditions and post-deposition annealing parameters.

### Methods

Epitaxial Sr<sub>1-x</sub>Ba<sub>x</sub>MnO<sub>3-δ</sub> (0 ≤ x ≤ 0.5) thin films with thickness in the range 7–18 nm were grown by pulsed laser deposition (PLD) using a KrF excimer laser, a fluence of 1 J/cm<sup>2</sup>, and a pulse repetition rate of 10 Hz on single-crystalline (001)-oriented (LaAlO<sub>3</sub>)<sub>0.3</sub>(Sr<sub>2</sub>TaAlO<sub>6</sub>)<sub>0.7</sub> (LSAT) substrates. The crystal structure and thickness of the films were studied by X-ray diffraction (XRD) and X-ray reflectivity (XRR), while atomic-level analysis of the SBMO films was performed by scanning transmission electron microscopy (STEM). The atomic displacements were measured from the annular bright field (ABF) and high-angle annular dark field (HAADF) images by determining the displacement of the Mn and O sublattices with respect to the centrosymmetric positions defined by the Sr/Ba sublattice, from which the film polarization was evaluated. Electron energy loss spectroscopy (EELS) was performed to assess the oxygen content of the films. The fine structure of the background-subtracted O–K edge was fitted to a double Gaussian to quantify the Mn valence following the procedure described by Varela et al. [3]

### Results

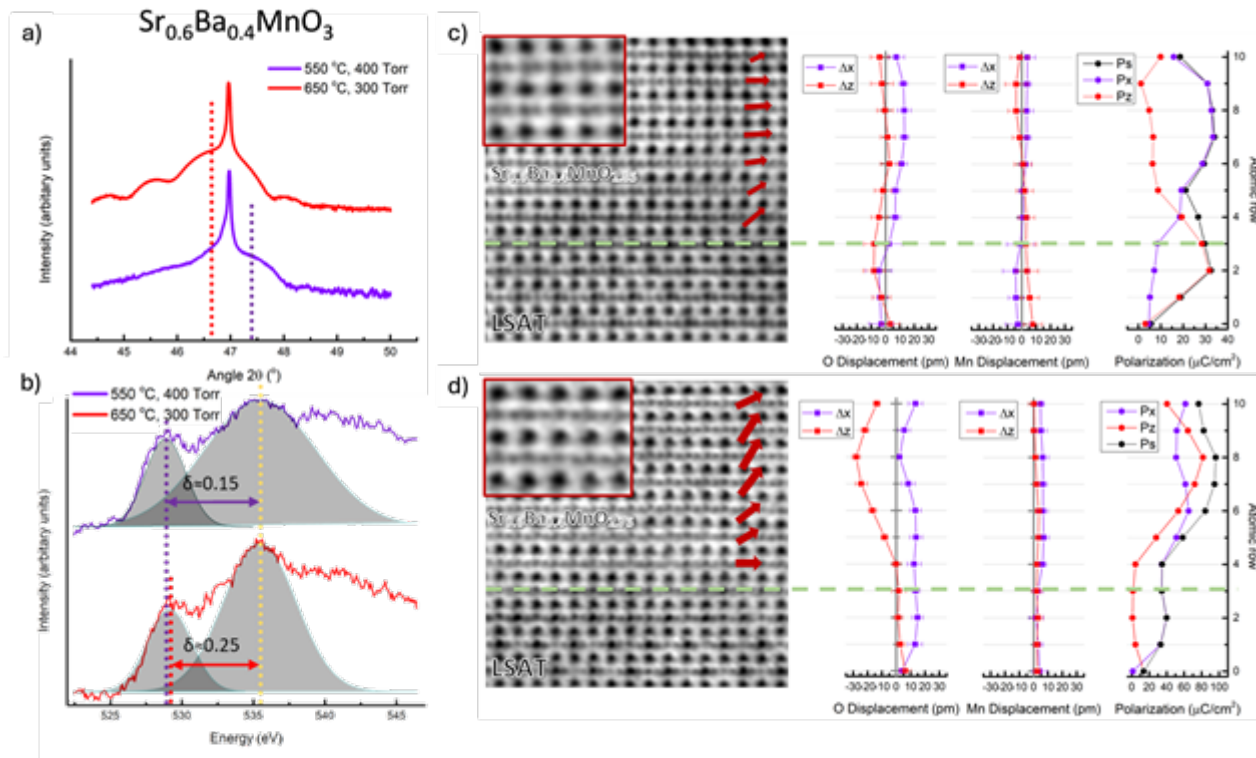
A combination of macroscopic XRD characterization and atomic scale STEM of the SBMO films has evidenced that the polar displacements are extremely dependent on the oxygen stoichiometry, Ba content and epitaxial strain. The parent compound SrMnO<sub>3</sub> grown on LSAT upon tensile strain is known to present in-plane polar displacements along the pseudocubic <110> directions [4]. On the other hand, this scenario can be altered by tuning both the Ba doping and oxygen stoichiometry. As an example, in the case of x = 0.4, the epitaxial strain shifts from tensile to compressive when the annealing conditions change from 550 °C at 400 Torr O<sub>2</sub> to 650 °C at 350 Torr O<sub>2</sub> (see Fig. 1a). The EELS fine structure of the O–K edge shows that this phenomenon is accompanied by a remarkable variation of the oxygen content (from δ=0.15 to 0.25), and therefore of the nominal valence of the Mn cation (Fig.1b). Atomic resolution ABF enables to resolve the Mn and O sublattices, revealing that structural and chemical variations induce a drastic change in the axis of polar displacements of Mn and O. While highly oxygenated SBMO (x = 0.4) presents in-plane atomic displacements with an estimated value of in-plane polarization of approximately 30 μC/cm<sup>2</sup> (Fig. 1c), the more oxygen



deficient and compressively strained film with the same Ba content, shows a predominantly out-of-plane polarization with a deduced polarization as high as  $95 \mu\text{C}/\text{cm}^2$  (Fig. 1d) [5].

### Conclusion

Polarization is intimately linked to the sign and magnitude of epitaxial strain, film thickness and oxygen stoichiometry. It can be tuned either in-plane or out-of-plane with respect to the substrate plane by the adequate choice of the substrate-induced strain, Ba doping and O content –induced by controlled annealing. This chemistry-mediated engineering of the polarization orientation and magnitude of oxide thin films opens new venues for the design of functional multiferroic architectures and the exploration of novel physics and applications of ferroelectric textures with exotic topological properties.



### Keywords:

Oxides, multiferroics, STEM, films, polarization

### Reference:

- [1] H Sakai et al., Phys. Rev. Lett. 107 (2011), p. 137601
- [2] A Edström and C Ederer, Phys. Rev. Materials 2 (2018), p. 104409
- [3] M Varela et al., Phys. Rev. B, 79 (2009), p. 085117
- [4] C Becher et al., Nature Nanotechnology 10 (2015), p. 661-665
- [5] P Koutsogiannis et al., APL Materials 12, (2024), p. 011113



614

## Investigation of Ferroelectricity using Advanced Microscopy

Xinxin Hu<sup>1</sup>, Felip Sandiumenge<sup>2</sup>, Umair Saeed<sup>1</sup>, Rohini Kumara Cordero Eduards<sup>1</sup>, Gustau Catalan<sup>1,3</sup>, Jordi Arbiol<sup>1,3</sup>

<sup>1</sup>Catalan Institute of Nanoscience and Nanotechnology(ICN2), CSIC and The Barcelona Institute of Science and Technology(BIST), Barcelona, Spain, <sup>2</sup>Institute of Materials Science of Barcelona (ICMAB-CSIC), Barcelona, Spain, <sup>3</sup>ICREA, Barcelona, Spain

Poster Group 1

### Backgrounds:

Ferroelectric materials, characterized by their ability to exhibit spontaneous electric polarization switchable under applied electric fields, manifest intricate interactions among electrical, thermal, and mechanical properties. These materials, pivotal in various applications such as spintronics, computing, communications, memories, actuators, motors, and sensors, undergo changes in behavior and properties in response to factors like temperature, electric field, pressure, and strain. To explore ferroelectricity, some basic techniques, such as single-crystal X-ray diffraction, second harmonic generation measurement and dielectric measurement, were used to investigate the crystal structure, symmetry and dielectric anomaly. However, it is difficult to accurately determine whether the crystal structure is centrosymmetric or non-centrosymmetric down to nanoscale level by virtue of these basic measurement. This has hindered the progress of investigating the ferroelectricity related properties in the past.

### Methods:

Advanced microscopies including Piezoresponse Force Microscopy (PFM) and Scanning Transmission Electron Microscopy (STEM), have been regarded as powerful approaches for evaluating the physical properties of materials down to nano, or even atomic scale. PFM has already been an essential method to investigate materials with piezoelectric properties. Especially, PFM shows its superiority in the studies of local non-destructive visualization of ferroelectric domain structures. In addition, Scanning Transmission Electron Microscopy (STEM), a fundamental tool in nanoscience, facilitates the acquisition of atomic-scale images and spectra. These images and spectra provide information on the structural and chemical properties of the studied nanostructures. As a result, STEM aids in a comprehensive understanding of the physical properties of functional materials at the atomic level. Consequently, combining advanced microscopies such as PFM and STEM has been shown as a powerful approach for evaluating the ferroelectric properties down to nanoscale even atomic level.

### Results:

This study delves into a comprehensive examination of several ferroelectrics including organic-inorganic hybrid perovskites and traditional inorganic ferroelectrics utilizing advanced microscopies including PFM and STEM. These approaches enable a profound understanding of the intricate relationship between domain structure, electric polarization, lattice structure, and electronic states, thereby offering control over the nuanced mechanisms of ferroelectrics. Leveraging advanced microscopy including PFM and high-resolution STEM, we precisely investigated ferroelectric domain structures, the atomic and electronic structures of ferroelectric materials, shedding light on the impacts of domain properties, atomic displacements, and electronic configurations on ferroelectrics.

### Conclusions:

The findings of this research hold significant implications for deepening the understanding on the ferroelectric properties, including changes in the ferroelectric domain structure and atomic level displacements, potentially paving the way for the creation of more efficient and reliable memory

storage, sensors, and energy converters. We anticipate that our research will establish a robust foundation for the examination of ferroelectricity and other complex functional materials down to atomic level.

**Keywords:**

Ferroelectrics, thin Films, Advanced Microscopy

625

## Revealing atomic structure and composition in ultrahigh energy storage density ferroelectric thin-films

Prof Shery Chang<sup>1,2</sup>, Dr Daniel Stroppa<sup>3</sup>, Dr Richard Webster<sup>1</sup>, Prof Danyang Wang<sup>2</sup>

<sup>1</sup>Electron Microscope Unit, Mark Wainwright Analytical Centre, University of New South Wales, Sydney, Australia, <sup>2</sup>School of Materials Science and Engineering, University of New South Wales, Sydney, Australia, <sup>3</sup>Dectris Ltd, Baden-Daetteil, Switzerland

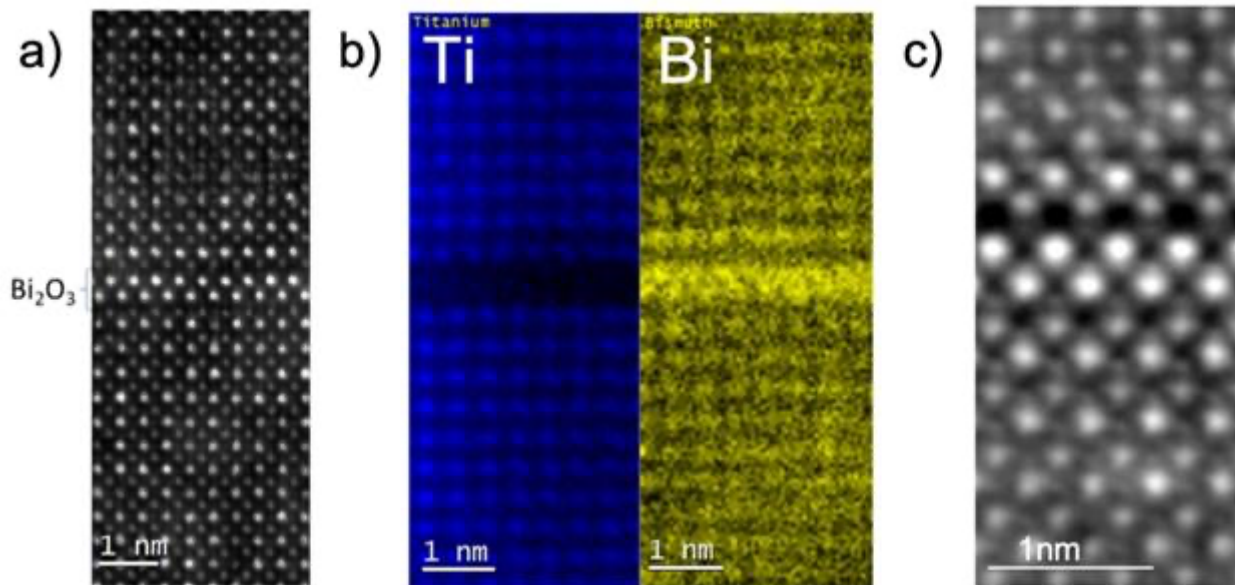
Poster Group 1

Ferroelectric thin film material is positioned to be a strong candidate for nano/microelectronics component with ultra-high energy storage density with low electric field [1]. One of the key strategies to achieve such high energy storage density is by creating a secondary phase nanostructure around the morphotropic phase boundary.

Here we show detailed characterisation of (Bi, Na)TiO<sub>3</sub> (BNBT) thin films grown on SrTiO<sub>3</sub> single crystal substrate. The nanostructures in the thin films as well as their electronic structures and composition variations were characterised using 4D STEM. Due to the presence of Na, it has been found that the BNBT structure can change under the electron beam, causing by the migration of Na. The ultra-fast ARINA detector allows acquisition of 4D STEM data with only few pA current, and short dwell time to avoid the electron beam damage to the BNBT film. Moreover, electron energy loss spectroscopy (EELS) was acquired using the K3 detector, to probe the composition and the electronic structure across the nanostructured domains.

We found that there is Bi segregation forming strips of half unit cell wide Bi<sub>2</sub>O<sub>3</sub> layers. Such composition is confirmed by the atomic resolution EELS maps, showing no presence of Ti within the Bi<sub>2</sub>O<sub>3</sub> bright strips. The effect of the Bi<sub>2</sub>O<sub>3</sub> layers is to laterally displace the lattice above the defect by half a unit cell, resulting a morphotropic anti-phase domain boundary. In addition, the Bi<sub>2</sub>O<sub>3</sub> segregation layer gives about 22% longer c-axis for the 3 unit cell around the defect. Such large expansion of c-axis is attributed to the presence of the super-tetragonal phase (super-T) [2-3]. The electronic structures of Ti and O sites adjacent to the Bi<sub>2</sub>O<sub>3</sub>, measured using EELS Ti L edge and O K edge, is consistent with the lattice distortions. Density functional theory calculations were carried out to probe that the origin of the super-T structure is likely due to the oxygen vacancies around the Bi<sub>2</sub>O<sub>3</sub> strips.

Such complex nanostructures with multiple structure phases co-existent forming nanodomains is found to be the key for the ultra-high performance of such ferroelectric thin films.



**Keywords:**

4D-STEM, EELS, ferroelectric

**Reference:**

[1] Pan, H.; Lan, S.; Xu, S.; Zhang, Q.; Yao, H.; Liu, Y.; Meng, F.; Guo, E.-J.; Gu, L.; Yi, D. (2021) *Science* 2021, 374 (6563), 100-104.

[2] Sun, Y., Zhang, L., Huang, Q., Jin, L., Chang, S. L. Y., Wang, Y., Zhang, P., Liao, X., Li, S., Zhang, S., Wnag, D. (2022) *Adv. Sci.*, 2203926.

648

## Magnetic layers reversal in new MRAM devices measured with operando Electron Holography

Augustin Nogier<sup>1</sup>, Bernard Dieny<sup>1</sup>, Ricardo Sousa<sup>1</sup>, Christophe Gatel<sup>2</sup>, Eric Gautier<sup>1</sup>, Aurélien Masseboeuf<sup>1</sup>, Kévin Garello<sup>1</sup>

<sup>1</sup>SPINTEC, Grenoble, France, <sup>2</sup>CEMES, Toulouse, France

Poster Group 1

### Background incl. aims

Recent improvements in spintronics led to new types of non-volatile Magnetoresistive Random-Access Memories (MRAM) with low power consumption and short switching times, such as the current-induced Spin-Orbit Torque (SOT). So far, studies of such devices mostly rely on the measurement of their electrical and magnetic characteristics using external electrical methods [1]. However, their optimization ultimately requires a deeper understanding of the internal processes through direct observation. Given the usual dimensions of these components (<60 nm lateral, <1nm in thickness), observing magnetization textures and reversal during their activation requires the use of large-scale instruments [2].

In particular, Transmission Electron Microscopy (TEM) is a tool of choice for this matter, offering the combination of nm-scale spatial resolution and magnetic sensitivity. Indeed, Electron Holography (EH) gives access to 2D projected electric field and magnetic induction maps with a sensitivity in the nm.T range [3], which can lead to information about various electrical properties of the sample. This work aims for a better understanding of the switching processes taking place inside these devices upon writing and reading data by performing an operando analysis (e.g the quantitative dynamic imaging of their inner magnetic structure) on electrically biased samples using EH [4]. We will present here the study of the free layer reversal process inside Magnetic Tunnel Junctions (MTJ) in both isolated and array-like SOT devices. Given that the zone of interest is a ferromagnetic layer less than 1nm-thick with weak internal fields close to the detection limit, we also chose to study the reversal process in a wider in-plane MTJ as preliminary results less sensitive to the measurement quality.

### Methods

Most of the EH measurements presented here use Phase Shifting (PS) by combining several holograms recorded with different beam tilting angles as a mean to enhance both spatial resolution and magnetic sensitivity. While this method gives an exact analytical solution to the PS matrix equation, it comes at the expense of limiting ourselves to study the reversal processes in a pseudo-static regime.

In any case, separating the electric and magnetic components of the electron wave phase requires two holograms to begin with. We perform all image alignments using points with strong Mean Inner Potential (MIP) gradient and theoretical zero magnetic field in an iterative correction process. In order to ensure the best measurement quality regardless, the device under observation must be sufficiently thinned down below 100 nm to limit the electron beam absorption through heavy materials, while remaining intact regarding its electrical behavior. Additionally, the injection of an external electrical bias on the sample inside the microscope chamber remains a technological challenge [5]; these conditions for accurate measurements require a highly controlled preparation process that will be presented.

### Results

We first performed PS electron holography on a 8nm-wide in-plane double MTJ without any electrical bias, where a controlled external magnetic field acted as the trigger for the free layers



switching. In this experiment, we were able to witness the reversal on phase maps approaching the pixel resolution for an external field of around 9mT [Fig.1]

We also conducted experimentations leading to a complete preparation process for the electrical connections of SOT samples inside the TEM chamber in order to perform PS on them, this time with a voltage bias for triggering the layer switching. Although the MTJ in SOT are typically smaller than that of our previous experiment, they still exceed the 0.12 nm spatial resolution limit of our image pixel size.

## Conclusions

These first results on unbiased samples show that a pixel-precision magnetic induction map is obtainable through the PS method with some image realignments and additional precautions. Given our advancement on the SOT preparation, we thus expect to be able to measure the free layer switching in these particular devices with a similar spatial resolution, keeping in mind the study of domain wall motion as the next step towards a deeper understanding of the SOT mechanisms.

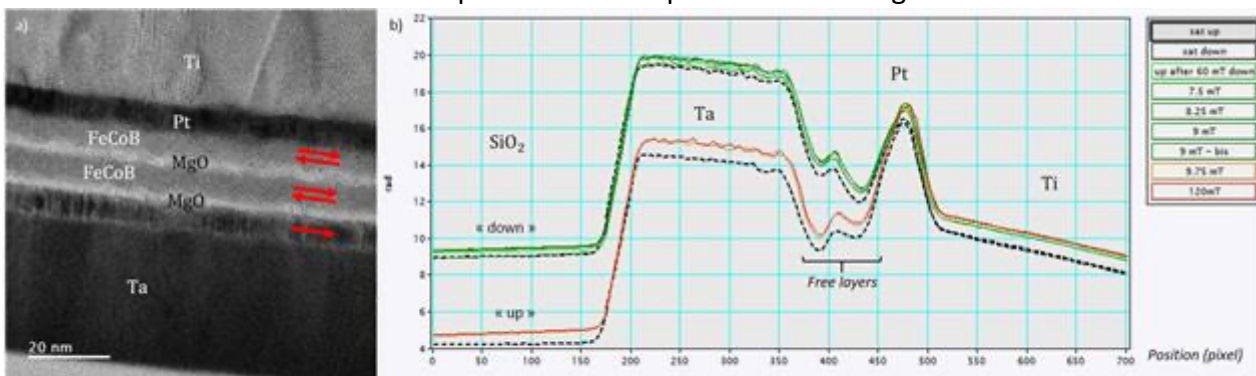


Fig 1: Electron Holography measurements on the wide MTJ: a) TEM view of the structure. Red arrows show the switching magnetization direction - b) Total phase profiles for gradual external in-plane field values. The phase gradient switching in the free layers occurs between 9 and 9,75 mT.

## Keywords:

Phase-Shifting Holography, operando, MTJ, SOT

## Reference:

- [1] Cheng Song, Ruiqi Zhang, Liyang Liao, et al. Spin-orbit torques: Materials, mechanisms, performances, and potential applications. *Progress in Materials Science* 118, 100761 (2021).
- [2] Manuel Baumgartner, Kevin Garello, Johannes Mendil, et al. Spatially and time-resolved magnetization dynamics driven by spin-orbit torques. *Nature Nanotechnology* 12, 980–986 (2017).
- [3] E. Javon, C. Gatel, A. Masseboeuf, and E. Snoeck. Electron holography study of the local magnetic switching process in magnetic tunnel junctions. *Journal of Applied Physics* 107, 09D310 (2010).
- [4] Maria Brodovoi, Kilian Gruel, Aurélien Masseboeuf, et al. Mapping electric fields in real nanodevices by operando electron holography. *Applied Physics Letters* 120, 233501 (2022).
- [5] M. Mecklenburg, M. Brodie, W. Hubbard, et al. Fabrication of a Lift-Out Grid with Electrical Contacts for Focused Ion Beam Preparation of Lamella for In Situ Transmission Electron Microscopy. *Microscopy and Microanalysis* 19, 458–459 (2013).

659

## Domain structures in ferroelectric epitaxial WO<sub>3</sub> thin films

Ewout Van Der Veer<sup>1</sup>, Stijn Feringa<sup>1</sup>, Jack Eckstein<sup>2</sup>, Bart Kooi<sup>1</sup>, Beatriz Noheda<sup>1</sup>

<sup>1</sup>University of Groningen, Groningen, The Netherlands, <sup>2</sup>Cambridge University, Cambridge, United Kingdom

Poster Group 1

### Background incl. aims

Tungsten oxides (WO<sub>3</sub>- $\delta$ ) have in the past received attention for their gas sensing, catalytic and electrochromic properties. Recently, ferro- and piezoelectric properties<sup>1,2,3</sup> coupled to local mechanical strain and even superconductivity<sup>4,5</sup> have been reported in tungsten (tri)oxide as well, inspiring interest in the electronic properties of these materials. However, this behavior is not yet fully understood and investigations of epitaxial films of tungsten oxides are particularly scarce. In this work, we aim to provide some insight into the nature and formation of ferroelectric domains and domain walls and their structural and electronic properties.

### Methods

Epitaxial films of tungsten (tri)oxide were grown by pulsed laser deposition at different thicknesses on a number of different substrates to reveal the effects of (epitaxial) strain. The substrates used are yttrium aluminate, lanthanum aluminate and strontium titanate. Atomic force microscopy and piezoresponse force microscopy were used to visualize the surface topography of the resulting films and to image the ferroelectric domain structures, respectively. In addition, conducting atomic force microscopy was utilized to show local electrical conductivity. The nanoscale structure of the films was probed using aberration-corrected scanning transmission electron microscopy (STEM). Differential phase contrast imaging enables the imaging of the lighter oxygen anions. Real-space analysis of the STEM images using an in-house developed software tool provides a sensitive means for visualizing local strain gradients and polarization.

### Results

Our results suggest an intricate coupling between the epitaxial strain imposed by the substrate, film thickness and the ferroelectric domain structure in the film. Low-strain films grown on yttrium aluminate show a fairly traditional domain structure consisting of a combination of purely polar, non-ferroelastic and ferroelastic domain walls, distinct from the type of domain structure reported for thicker films on the same substrate<sup>1</sup> in which the polar nature of the film is localized to the domain walls, as well as those reported for bulk tungsten trioxide based on theory<sup>2</sup>. Electrical conductivity is found to be enhanced in the vicinity of the domain walls. In contrast, a higher degree of epitaxial tensile strain suppresses the formation of domains altogether, favoring strain accommodation through an extended planar defect.

### Conclusion

We provide some new insights into the formation of polar domain walls and strain accommodation in epitaxial thin films of tungsten trioxide under different conditions of epitaxial strain and show that there is potential for the functionalization of domain walls therein.

### Keywords:

ferroelectrics, strain, STEM, PFM, epitaxy

**Reference:**

1. Dong et al. A review on WO<sub>3</sub> based gas sensors: Morphology control and enhanced sensing properties J. Alloys Compd. 820 153194 (2020)
2. Dong et al. WO<sub>3</sub>-based photocatalysts: morphology control, activity enhancement and multifunctional applications Environ. Sci. Nano 4(3) p. 539 (2017)
3. Niklasson and Granqvist Electrochromics for smart windows: thin films of tungsten oxide and nickel oxide, and devices based on these J. Mater. Chem. 17(2) p. 127 (2007)
4. Yun et al. Flexopiezoelectricity at ferroelastic domain walls in WO<sub>3</sub> films Nature Communications 11(1) 4898 (2020)
5. Eckstein et al. Symmetry and strain analysis of combined electronic and structural instabilities in tungsten trioxide, WO<sub>3</sub> J. Appl. Phys. 131(21) 215101 (2022)

711

## Unveiling moiré-induced topological polar structures in freestanding ferroelectric membranes

Dr Gabriel Sanchez Santolino<sup>1</sup>, Victor Rouco<sup>1</sup>, Sergio Puebla<sup>2</sup>, Hugo Aramberri<sup>3</sup>, Victor Zamora<sup>1</sup>, Fabian Cuellar<sup>1</sup>, Carmen Munuera<sup>2,4</sup>, Federico Monpean<sup>2,4</sup>, Mar García-Hernandez<sup>2,4</sup>, Andrés Castellanos-Gomez<sup>2,4</sup>, Jorge Íñiguez<sup>3,5</sup>, Carlos León<sup>1,4</sup>, Jacobo Santamaría<sup>1,4</sup>

<sup>1</sup>GPMC. Dept. Física de Materiales. Facultad de Física. Universidad Complutense. 28040 Madrid, Spain, , , <sup>2</sup>Instituto de Ciencia de Materiales de Madrid ICMM-CSIC 28049 Cantoblanco. Spain, , ,

<sup>3</sup>Materials Research and Technology Department, Luxembourg Institute of Science and Technology (LIST), Avenue des Hauts-Fourneaux 5, L-4362 Esch/Alzette, Luxembourg, , , <sup>4</sup>Unidad Asociada UCM/CSIC, “Laboratorio de Heteroestructuras con aplicación en spintrónica”, , , <sup>5</sup>Department of

Physics and Materials Science, University of Luxembourg, 41 Rue du Brill, L-4422 Belvaux, Luxembourg, ,

Poster Group 1

Complex correlated oxides are quantum materials characterized by unshielded d-electrons. Their interaction across competing energy scales leads to diverse functionalities, which can be altered by slight changes of their structure, composition, or boundary conditions [1]. In this context, recent studies on ferroelectric oxides have shown the formation of complex polar topologies, which are related to a delicate interplay between the intrinsic tendency of the material towards a uniform polarization and the electrical and mechanical constraints placed upon them [2]. However, the cube-on-cube epitaxial structure of these materials forces the use of single crystalline substrates for their growth, which restricts the possible mechanical boundary conditions and, therefore, the formation of new topological structures. To overcome this limitation, we have isolated the ferroelectric materials from their parent substrate by a selective chemical exfoliation method, thus obtaining freestanding layers of just a few unit cells in thickness. This new approach vastly increases the potential for novel hetero-integration approaches by stacking various freestanding layers and avoiding the chemical, structural, or thermal limitations of conventional synthesis and growth processes [3].

In this work, we show how a polar vortex pattern is induced by stacking twisted freestanding ferroelectric BaTiO<sub>3</sub> layers [4]. We study the formation of these topological polar structures in relation to the twisted angle and layer thickness by aberration-corrected scanning transmission electron microscopy and density-functional theory calculations.

These results show an exciting opportunity to create novel polar topologies using the unique modulations that are possible in moiré bilayers and pave the way for potential applications in future high-density ferroelectric memory devices.

### Keywords:

ferroelectric, freestanding membranes, topological structures

### Reference:

- [1] Y. Tokura et al., Nature 13, 1056 (2017)
- [2] Yadav, A. K. et al. Observation of polar vortices in oxide superlattices, Nature, 2016, 530, 198–201.
- [3] S. Puebla et al., Nano Letters 22, 18 (2022)
- [4] G. Sánchez-Santolino, V. Rouco et al., Nature, 626, 529–534 (2024)
- [5] This work has been supported by the Regional Government of Madrid CAM through SINERGICO project CAIRO-CM (Y2020/NMT-6661). Authors acknowledge received funding from the EU FLAG-ERA project To2Dox (JTC-2019-009) and the Spanish Ministry of Science and Innovation (grant PID2020-

118078RB-I00 and fellowship PRE2018-084818). G.S.-S. acknowledges financial support from the Spanish MCI grant nos. RTI2018-099054-J-I00 (MCI/AEI/FEDER, UE) and IJC2018-038164-I. V.R. was supported by the V PRICIT (Regional Programme of Research and Technological Innovation).



958

## TEM studies of polarization nanodomains in (BaTiO<sub>3</sub>/SrTiO<sub>3</sub>)<sub>10</sub> superlattices on silicon

Dr Ines Haeusler<sup>1</sup>, Valentin Väinö Hevelke<sup>1</sup>, Adnan Hammud<sup>2</sup>, Prof. Dr. Christoph Koch<sup>3</sup>, Dong Jik Kim<sup>1</sup>, Prof. Dr. Catherine Dubourdieu<sup>1</sup>

<sup>1</sup>Helmholtz-Zentrum Berlin für Materialien und Energie, Institute Functional Oxides for Energy Efficient Information Technology, 14109 Berlin, Germany, <sup>2</sup>Fritz-Haber Institut der Max-Planck-Gesellschaft, 14195 Berlin, Germany, <sup>3</sup>Humboldt-Universität zu Berlin, Department of Physics, 12489 Berlin, Germany

Poster Group 1

Over the last decade, it has been recognized that different topological structures formed in ferroelectrics significantly influence the physical properties of the material system. Ferroelectric oxides deposited on a semiconductor substrate are of particular interest for applications in nanoelectronics or photonics. A particularly attractive candidate of ferroelectric materials is BaTiO<sub>3</sub>. We investigated the crystalline structure, defects and the polarization patterns in (BaTiO<sub>3</sub>/SrTiO<sub>3</sub>)<sub>10</sub> superlattices epitaxially grown by molecular beam epitaxy (MBE) on a silicon substrate. A thin epitaxial SrTiO<sub>3</sub> template directly grown on the substrate is mainly used to compensate for the lattice mismatch between BaTiO<sub>3</sub> and Si.

To determine the spontaneous polarization within the (BaTiO<sub>3</sub>/SrTiO<sub>3</sub>)<sub>10</sub> superlattice, the in-plane and out-of-plane strain components of the lattice were determined using Geometrical Phase Analysis (GPA) and using a direct peak finding method. Furthermore, a more refined peak finding algorithm was used to analyze the displacements of the Ti atoms relative to the center of their respective unit cells in real space. Therefore, high-resolution HAADF-STEM images, which show a direct visualization of the atom columns in a crystal, were recorded.

The analyses resulted in two-dimensional displacement maps of the Ti atoms, in which the areas of the BaTiO<sub>3</sub> layers revealed periodic, wave-like polarization patterns. These patterns are also partially continued in the SrTiO<sub>3</sub> layer. The two-dimensional strain maps show a strong modulation of the out-of-plane strain component and a periodic variation of the in-plane strain component in the region of the BaTiO<sub>3</sub> layers. The combination of the displacement maps and the strain maps shows a significant correlation between the two.

These investigations of (BaTiO<sub>3</sub>/SrTiO<sub>3</sub>)<sub>10</sub> superlattices contribute to the understanding of two-dimensional oxide ferroelectrics for the future integration of topological polar nanostructures in devices.

### Keywords:

BaTiO<sub>3</sub>, ferroelectrics, HAADF-STEM

978

## In situ growth and phase engineering of manganese arsenide nanostructures in environmental TEM

Hedda Christine Soland<sup>1,2</sup>, Mikelis Marnauza<sup>1,2</sup>, Pau Ternero<sup>2,3</sup>, Professor Kimberly A. Dick<sup>1,2</sup>

<sup>1</sup>Centre for Analysis and Synthesis, Lund University, Lund, Sweden, <sup>2</sup>NanoLund, Lund University, Lund, Sweden, <sup>3</sup>Solid State Physics, Lund University, Lund, Sweden

Poster Group 1

### Background incl. aims

For magnetic materials, in situ synthesis offers an additional advantage by enabling the exploration of the magneto-structural relationship. Understanding magneto-structural phase transitions is crucial for the development of materials such as those used for magnetocaloric applications. One such material is MnAs, in bulk known for the ferromagnetic transition around 315K coupled with a structural transition from hexagonal ( $\alpha$ -MnAs) to orthorhombic ( $\beta$ -MnAs). However, experimental studies of MnAs nanoparticles have shown discrepancies where the ferromagnetic transition occurs even in the absence of the structural transition.

Nanomaterial synthesis is usually done ex-situ, which can sometimes be tedious and time-inefficient, especially when exploring new or metastable materials. An environmental TEM (ETEM) specifically designed for exploring new material systems, allows for simultaneous exploration of synthesis parameters while observing the changing nanostructures with atomic resolution. Parameters can be fine-tuned, and even metastable material systems and crystal structures have been synthesized this way, showing promise for exploring not only new material systems but also those that have previously been discarded.

In this study, we focus on transition metal pnictides, particularly MnAs, due to their promising applications in spintronics, magnetic refrigeration, and data storage devices. During the preliminary work, the goal is to explore the diffusion behaviour of manganese, how to control the growth rate of MnAs and explore the various structural phase transitions, laying the groundwork for a deeper understanding of magnetic transition metal pnictides. In the long term, we would like to integrate Lorentz imaging techniques to also explore the magnetic properties. This way, material growth could be paired with atomic resolution imaging, chemical analysis, and even information about magnetic domains, and pave the way for a new approach to fundamental studies and phase engineering of magnetic nanomaterials.

### Methods

MnO<sub>2</sub> nanoparticles were prepared via spark ablation and sputtered directly onto a MEMS chip for further work in the Hitachi HF-3300S 300kV ETEM. In the ETEM, arsine (AsH<sub>3</sub>) was used as the precursor gas to facilitate the growth of MnAs nanostructures. Various parameters, including temperature, gas flow, and electron beam effects, were explored to map the parameter space of this material system and optimize the stability of both MnO<sub>2</sub> and MnAs. For analysis, HRTEM, FFT, SE and Z-contrast in STEM mode, and both TEM- and STEM-EDX were performed during the experiments.

### Results

It was observed that AsH<sub>3</sub> diluted with H<sub>2</sub> during electron beam irradiation causes MnAs to form outside of the MnO<sub>2</sub> particles. Together with the oxide reducing in size and eventually disappearing, this might indicate that the manganese atoms diffuse out of the oxide particles to crystallize into MnAs. This effect seems to be correlated with electron dose and is not observed in STEM mode. The fact that MnAs only form under a strong electron beam can be advantageous in the exploration of

the parameter space, as no changes were observed for the non-exposed oxide particles. However, using manganese oxide particles instead of pure manganese also introduces some limitations. At lower temperatures, around 200°C, the stability of the MnO<sub>2</sub> nanoparticles under the electron beam was compromised, even without any AsH<sub>3</sub> supplied. However, at higher temperatures, around 400°C, the MnO<sub>2</sub> particles were observed to be more stable and thus preferable for control of the diffusion of manganese into MnAs.

#### Conclusion

MnAs was successfully synthesized from MnO<sub>2</sub>-particles under AsH<sub>3</sub> atmosphere using an in situ ETEM due to what seems like an electron beam-activated process. These preliminary findings demonstrate the feasibility of synthesizing stable MnAs nanostructures in the ETEM environment and underscore the potential of this approach for exploring transition metal pnictides and similar material systems. The results show that this method is promising for future studies of magneto-structural relationships in transition metal pnictides, especially if magnetic imaging techniques are well integrated into the system. Additionally, the results are laying the foundation for further investigations into phase engineering and combinations with semiconducting III-V nanowires, such as GaAs and InAs, which already have been greatly explored in this system.

#### Keywords:

ETEM MnAs in-situ

#### Reference:

Motizuki, Kazuko, et al. "Electronic structure and magnetism of 3d-transition metal pnictides." (2010).

Tian, Peng, et al. "Diverse structural and magnetic properties of differently prepared MnAs nanoparticles." *ACS nano* 5.4 (2011): 2970-2978.

Tornberg, Marcus, et al. "Enabling in situ studies of metal-organic chemical vapor deposition in a transmission electron microscope." *Microscopy and Microanalysis* 28.5 (2022): 1484-1492.

Han, Ying, et al. "In Situ TEM Characterization and Modulation for Phase Engineering of Nanomaterials." *Chemical Reviews* 123.24 (2023): 14119-14184.

1028

## Characterizing Magnetic Properties of Nanoparticle Systems: Insights from Electron Tomography and Micromagnetic Simulations

Cristian Radu<sup>1,2</sup>, Andrei Cristian Kuncser<sup>1</sup>

<sup>1</sup>National Institute of Materials Physics, Atomistilor 405A, 077125, , Romania, <sup>2</sup>Faculty of Physics, University of Bucharest, Atomistilor 405, 077125, , Romania

Poster Group 1

### Background incl. aims

Nanoscale 3D imaging techniques, such as electron tomography, are increasingly essential in material science and engineering. Extracting quantitative information from these techniques requires robust processing methods. This study presents several approaches for evaluating magnetic properties, such as magnetic shape anisotropy energy and demagnetization factors, as well as of magnetic nanoparticle ensembles using electron tomography data.

### Methods

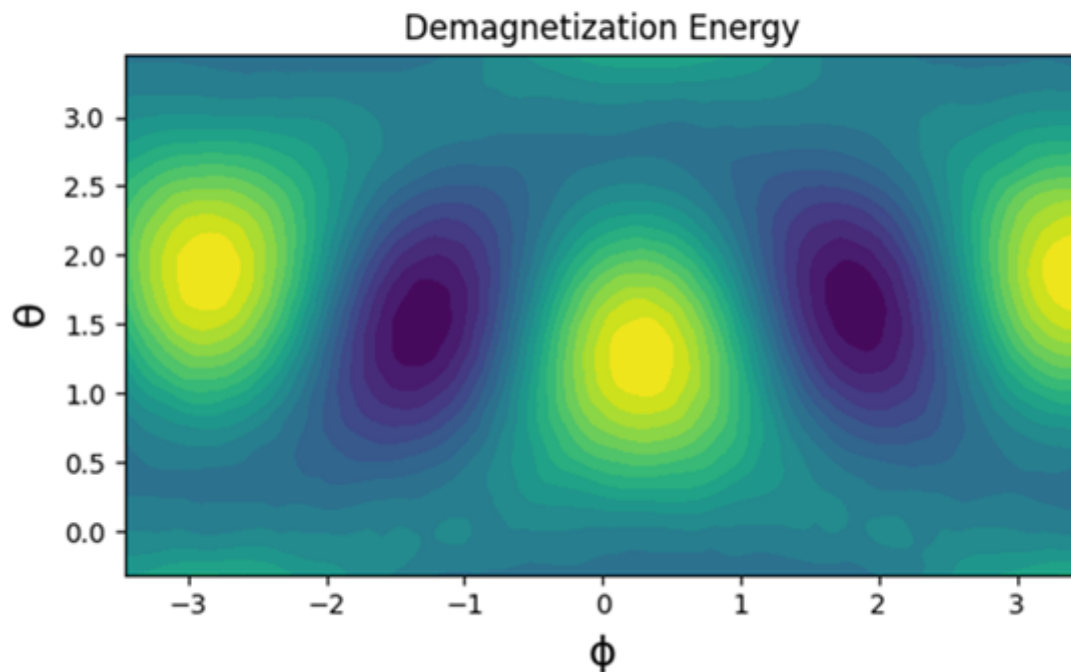
We extend a previously developed in-house software for processing 3D data to retrieve quantitative morphological information about nanoparticle systems [1]. Our focus is on iron oxide (magnetite) nanoparticle systems prepared via coprecipitation methods. Transmission electron microscopy (TEM) tomographic series were acquired using a JEOL 2100 TEM, and the reconstruction was performed using GENFIRE software. The raw 3D data is segmented with an in house developed software and the retrieved quantitative morphological information on nanoparticle size and shape is saved in a suitable format for use by the Object Oriented Micro Magnetic Framework (OOMMF) [2].

### Results

The micromagnetic simulations are employed to obtain several magnetic features including demagnetization energy maps of the nanoparticles as well as a statistical perspective of magnetic shape anisotropy energy and demagnetization factors of the studied system. By comparing magnetic information obtained from OOMMF simulations with approximation based morphological data, we seek a better understanding of how morphological features influence the magnetic phenomena.

### Conclusion

Morphological information, such as size and shape, coupled with magnetic parameters like demagnetization factors and shape anisotropy energy, holds significant importance in diverse fields such as gas sensing [3], catalysis, spintronics, and magnetic hyperthermia-based therapies [4]. By integrating electron tomography with micromagnetic simulations, this study aims to advance our understanding of the intricate relationships between morphology and magnetic behavior in nanoparticle systems.



**Keywords:**

Electron tomography, micromagnetic simulations

**Reference:**

- [1] Radu C, Vlaicu I.D., Kuncser A. C. (2022). A new method for obtaining the magnetic shape anisotropy directly from electron tomography images. *Beilstein J. Nanotechnol.* 13, 590–598.
- [2] M. J. Donahue and D. G. Porter (1999), *OOMMF User's Guide Version 1.0*. (National Institute of Standards and Technology, Gaithersburg, MD, 1999), <http://math.nist.gov/oommf/>
- [3] Cao, A., Hu, Y., & Lieber, C. M. (2013). Nanoparticles for gas sensing applications. *Nano Today*, 8(6), 690-702.
- [4] Das P, Colombo M, Prosperi D. (2019). Recent advances in magnetic fluid hyperthermia for cancer therapy. *Colloids Surf B Biointerfaces.*;174:42-55.



1053

## Exploring Local Order/Disorder in Relaxor Ferroelectric Materials via TEM and STEM Methods

Beatriz Vargas Carosi<sup>1</sup>, PRanjali Nandi<sup>1</sup>, Lluís Yedra<sup>1</sup>, Sonia Estradé<sup>1</sup>, Angélica M. Benitez-Castro<sup>2,3</sup>, Juan Muñoz-Saldaña<sup>3</sup>, Bernat Mundet<sup>4</sup>, Lluís López-Conesa<sup>1</sup>, Francesca Peiró<sup>1</sup>

<sup>1</sup>LENS, Department of Electronics and Biomedical Engineering and Institute of Nanoscience and Nanotechnology (IN2UB), University of Barcelona (UB), Barcelona, Spain, <sup>2</sup>Institute of Glass and Ceramics, Department of Materials Science and Engineering, Friedeich-Alexander-Universität Erlangen-Nürnberg, Erlangen, Germany, <sup>3</sup>Centro de Investigación y de Estudios Avanzados del IPN, Lib. Norponiente 2000, Querétaro, Mexico, <sup>4</sup>Catalan Institute of Nanoscience and Nanotechnology (ICN2), CSIC and BIST, Campus UAB, Bellaterra, Spain

Poster Group 1

### Background incl. aims

Perovskite relaxor ferroelectric materials are very interesting for a variety of applications due to their extraordinary piezoelectric properties. However, understanding the complicated local order/disorder phenomena within these materials is crucial for optimizing their performance. Transmission Electron Microscopy (TEM) and Scanning Transmission Electron Microscopy (STEM) techniques were employed to study the local order/disorder phenomena in  $(1-x)\text{Na}_{1/2}\text{Bi}_{1/2}\text{TiO}_3-x\text{BaTiO}_3$  (NBT-BT) compositions with varying  $\text{BaTiO}_3$  concentration ( $x = 2.5, 7.5, \text{ and } 15 \text{ mol}\%$ ).

### Methods

The samples with mol fractions of 0.025, 0.075, and 0.15 were prepared using conventional synthesis methods for mixed oxides. High-purity powders of  $\text{Bi}_2\text{O}_3$ ,  $\text{Ti}_2\text{O}$ ,  $\text{Na}_2\text{CO}_3$ ,  $\text{BaCO}_3$ , and  $\text{K}_2\text{CO}_3$  were combined in stoichiometric ratios and then milled in a planetary mill at 250 RPM for 2 hours. After drying, the mixture was calcined three times at  $920^\circ\text{C}$  for 5 hours to ensure the formation and purity of the perovskite-type phase. The resulting powder was ground again and passed through a  $100 \mu\text{m}$  sieve. Afterward, the powders were compacted uniaxially and isostatically at 180 Mpa pressure into discs, then sintered at  $1080^\circ\text{C}$  for 10 hours in a powder bed of the same composition to minimize element volatilization. Cross-sectional samples were prepared using the ThermoFischer Scios 2 DualBeam in the Scientific and Technical Resources Service of the Universitat Rovira i Virgili. Our research was aimed at understanding the chemical composition, domain configurations, and structural evolution of these materials. The crystalline structure was analyzed by selected area diffraction (SAED); local changes in lattice parameters were monitored using HAADF-STEM and the presence of polar nanodomains (PNRs) was assessed by iDPC imaging techniques. The samples were observed in a ThermoFisher SPECTRA (S)TEM 300 at 300 kV (ALBA synchrotron), in a JEOL 2010F TEM, and in a JEOL 2100 TEM, both working at 200 kV (Scientific and Technological Centers of the Universitat de Barcelona).

### Results

Our findings showed the presence of various phases within the samples. For lower  $x$  value,  $R3c$  symmetry coexisted with  $\text{Pm-}3m$ , but higher  $\text{BaTiO}_3$  ratios resulted in a transition from  $\text{Pm-}3m$  to  $\text{P}4bm$  symmetry. For the sample with  $x=0.15 \text{ mol}$ , only  $\text{P}4bm$  symmetry was observed. Conversely, for  $x=0.025 \text{ mol}$ ,  $R3c$  and  $\text{Pm-}3m$  symmetries were detected, and for  $x=0.075 \text{ mol}$ , all three symmetries were observed in distinct grains. The analysis of the lattice parameters through HAADF and iDPC images also showed the transition from a rhombohedral phase for  $x=0.025$ , to a cubic phase for  $x=0.075$ , and to the tetragonal phase for  $x=0.15 \text{ mol}$ . Polarization maps from iDPC technique will highlight the presence of PNRs. Electron Energy Loss Spectroscopy (EELS) also exhibited particular features in the spectra when increasing the  $\text{BaTiO}_3$  ratio. Low-loss energy loss spectroscopy was also

conducted to observe variations in the optical response and to compare them with Density Functional Theory (DFT) simulated data of  $\text{BaTiO}_3$ ,  $\text{BiTiO}_3$ , and  $\text{NaTiO}_3$  using the Vienna Ab initio Simulation Package (VASP).

### Conclusion

This study explores the general panorama of domain configurations and structural complexities in these materials, as well as the spectroscopic properties observed, including the dielectric function and ELF, as the  $\text{BaTiO}_3$  ratio is incrementally increased.

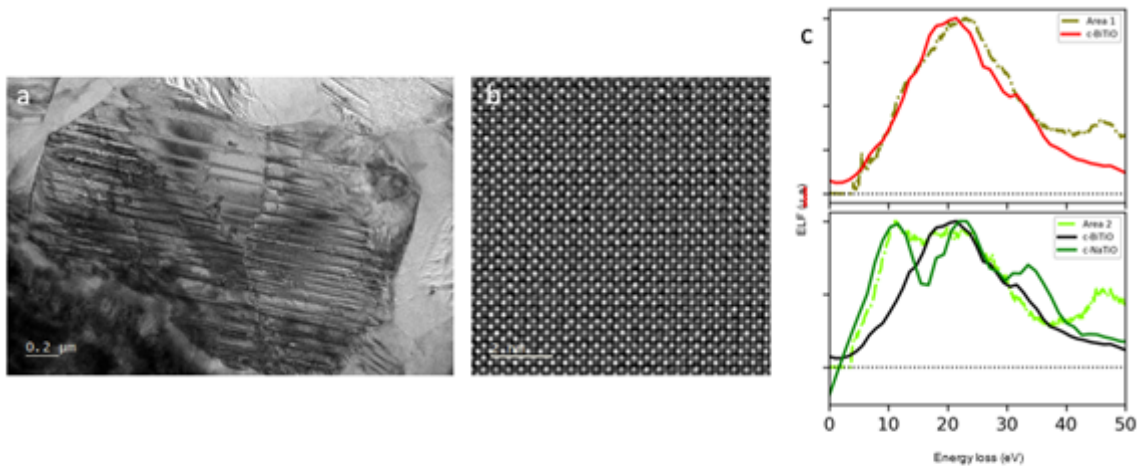


Figure 1: a) BF-TEM image of sample  $x=0.15\text{mol}$  in  $[310]$  zone axis. b) iDPC image of sample  $x=0.075\text{ mol}$  in  $[001]$ . c) ELF of experimental data obtained from Kramers-Kronig calculation and simulated data obtained from DFT simulation. The experimental data are from two different areas of sample  $x=0.025\text{ mol}$ , while the simulations data was obtained from the cubic structure of  $\text{BiTiO}_3$  and  $\text{NaTiO}_3$ .

### Keywords:

Relaxor-ferroelectrics, TEM, STEM, NBT-BT

### Reference:

1. Physical Review Materials 6, 064409 (2022). DOI: 10.1103/PhysRevMaterials.6.064409
2. Adv Struct Chem Imag 3, 9 (2017). DOI: 10.1186/s40679-017-0042-5
3. (2021). PinkShnack/TEMUL: (Version 0.1.3). Zenodo. DOI: 10.5281/zenodo.4543963
4. ACS Appl. Mater. Interfaces 14, 5525–5536 (2022). DOI: 10.1021/acsami.1c17383

1084

## Geometric phase analysis-based characterization of skyrmion lattice equilibria

M.Sc Vinko Sršan<sup>1,2</sup>, Asst. Prof. Matej Komelj<sup>2</sup>, Prof. Sašo Šturm<sup>1,2,3</sup>

<sup>1</sup>Jožef Stefan International Postgraduate School, Ljubljana, Slovenia, <sup>2</sup>Department for Nanostructured Materials, Jožef Stefan Institute, Ljubljana, Slovenia, <sup>3</sup>Department of Geology, Faculty of Natural Sciences and Engineering, University of Ljubljana, Ljubljana, Slovenia

Poster Group 1

Magnetic skyrmions are, topologically protected, vortex-like magnetization patterns which can form a two-dimensional lattice. Skyrmion lattices, just as crystal lattices, can be deformed by both internal and external influences, resulting in dislocations or skyrmion grain boundaries. Understanding the rise of skyrmion lattice deformations is important to find the correlation between local and external influences on skyrmion lattice formation and stability. We apply geometric phase analysis (GPA), a widespread image analysis technique for measurement of deformation fields in high-resolution transmission electron microscopy images (TEM), to simulated Lorentz TEM images. Lorentz TEM images have been calculated by means of micromagnetic simulations based on FeGe chiral magnet which supports stabilization of skyrmion lattice. We have simulated Lorentz TEM images with and without the application of the spin-polarized current. The strain and dislocation maps were obtained by applying GPA to all simulated images. Our findings suggest that applying spin-polarized currents can lead to further stabilization of skyrmion lattice compared to ground state. We demonstrate that GPA can be successfully used for the analysis of Lorentz TEM images both at static and dynamic conditions. Strain analysis of skyrmion lattice in Lorentz TEM images can further enhance the knowledge of deformation mechanisms and skyrmion lattice dynamics.

### Acknowledgements:

This work has been supported by the Slovenian Research Agency through the P2-0084 research program, J7-4637 project and European Union's Horizon Europe Research and Innovation Program REESILIENCE (grant agreement no. 101058598).

### Keywords:

GPA, LTEM, Magnetic skyrmions

1105

## Correlative microscopy for the discovery of novel nano-grains in spintronic materials.

Dr Adam Kerrigan<sup>1</sup>, Dr Irene Azaceta<sup>2</sup>, Dr Ercin Duran<sup>3</sup>, Dr Stuart Cavill<sup>2</sup>, Dr Alex Eggeman<sup>3</sup>, Prof Vlado Lazarov<sup>1,2</sup>

<sup>1</sup>The York-JEOL Nanocentre, University of York, York, United Kingdom, <sup>2</sup>School of Physics, Engineering and Technology, University of York, York, United Kingdom, <sup>3</sup>Department of Materials, University of Manchester, Manchester, United Kingdom

Poster Group 1

### Background incl. aims

Spintronics is an expanding field in nanoscience, attracting attention in the last decade due to its potential to revolutionize CMOS based logic and data devices by utilizing the spin of electrons. Spin manipulation via spin current generation, propagation, and spin injection and detection, are key steps for the realization of fast, non-volatile, and low power computational devices. The successful achievement of these goals is challenging as it requires atomic level control of interfaces and thin film structures in multi-layered heterostructures. The 100% spin polarization in ideal L21 structured Heusler alloys is very sensitive to both extended defects (i.e. dislocations) due to strain effects, as well as anti-site defects, and which results in variety of lower symmetry ordered Heusler phase, like B2, DO3, and A2. Hence methods that can detect differences between phases in nano-volumes is critical for optimizing performance of spintronic devices based on Heusler alloys.

### Methods

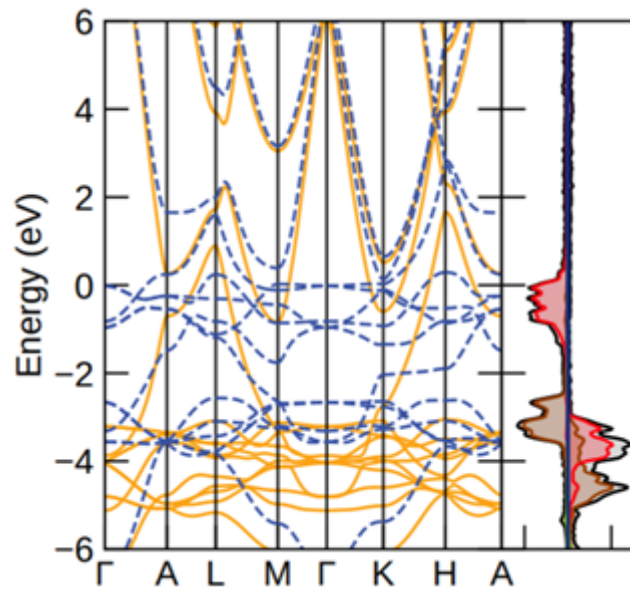
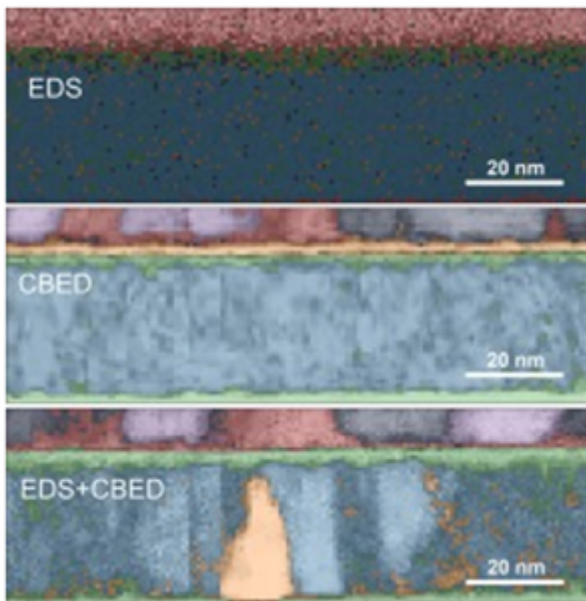
We have investigated the nano-grain structure of Co<sub>2</sub>FeSi films using correlative microscopy, fusing simultaneously acquired Energy Dispersive X-ray (EDX) spectroscopy and 4D-Scanning TEM datasets, on a Thermo Fisher Talos F200X operated at 200kV. The convergence angle achieved was 1.5 mrad, using a 10 μm C2 aperture. A Thermo Fisher Super-X SDD detector, with 0.9 srad collection angle, was used to acquire EDX. CBED patterns were recorded using a Quantum Detectors Merlin Quad detector with 512x512 pixels. For the scans used in this study a dwell time of 2–25 ms was used to scan regions with a step-size of 1–2 nm. Unsupervised machine learning algorithms have then been employed to identify nano-grains in the Heusler Co<sub>2</sub>FeSi thin films. Fuzzy C-means clustering, using a Gustafsson-Kessel approach allowing for elliptical clustering, was applied to a robustly scaled and dimensionally reduced combination of CBED and EDX data. The dimensional reduction was achieved using Principal Component Analysis. Density Functional Theory (DFT) studies were performed using the Vienna Ab-initio Simulation Package (VASP) using the SCAN functional with PAW pseudopotentials. A k-point mesh of 8 x 8 x 8 and planewave cut-off of 700eV were used for geometry optimisations with a finer density used for spectral calculations.

### Results

Clustering of individual signals from the 4D-STEM and EDX of Co<sub>2</sub>FeSi thin films was unable to identify any higher ordering within the Heusler structure. However when the signals were combined the finer details of the film texture became apparent. Specifically, the correlative acquisition has allowed the unsupervised clustering algorithm to separate regions inseparable via noncorrelative techniques. The analysis of the clustered nano-grains, of differing structural and chemical composition, revealed a novel phase of CoFeSi that has been confirmed via further HAADF imaging. The structure has been optimised using DFT calculations and shown to be more stable than other known CoFeSi phases, emphasising the structure's relevance. Further computational calculations have predicted the structure to be a semi-metal rather than a half-metal and as such it's inclusion in a Co<sub>2</sub>FeSi is potentially a, previously hidden, defect compromising spin polarisation.

## Conclusion

By combining Energy Dispersive X-ray (EDX) spectroscopy and 4D-Scanning TEM datasets, we have a unique structure and chemical composition that is invisible when the data is treated independently. Subsequent analysis of the identified nano-size secondary phase shows that it contains ordering peaks that overlap with the full-Heusler L21-ordering, making it difficult to detect via standard characterization techniques (e.g. X-Ray Diffraction). Furthermore, we show that this new phase has unique ordering not reported for Heusler phases in current literature. Additional magnetic measurements and density functional calculations have shown that the secondary phase is not fully spin polarized, has lower magnetic moment per unit cell, which can be detrimental when films with such inhomogeneities are incorporated in a device structure.



## Keywords:

4D-STEM Unsupervised Learning DFT



1165

## Exploring polar ordering in lead-free $K_{0.5}Na_{0.5}NbO_3$ ferroelectrics using in situ biasing and 4D STEM techniques

prof. Goran Dražić<sup>1,2,3</sup>, Ms. Katarina Žiberna<sup>2,3</sup>, Dr. Oana Condurache<sup>2,3</sup>, prof. Andreja Benčan Golob<sup>2,3</sup>

<sup>1</sup>Department for materials chemistry, National institute of chemistry, Ljubljana, Slovenia, <sup>2</sup>Electronic ceramics department, Jožef Stefan Institute, Ljubljana, Slovenia, <sup>3</sup>Jožef Stefan international postgraduate school, Ljubljana, Slovenia

Poster Group 1

The effectiveness of ferroelectric materials is fundamentally dependent on their ability to switch polarization, a process driven by complex dynamics that include the movement of ferroelectric domain walls (DWs), domain growth, and the nucleation of new domains. Traditionally, the behaviour of ferroelectric domains and DWs has been examined using indirect methods, such as nonlinear ferroelectric / piezoelectric measurements or in situ x-ray diffraction techniques. While these methods have significantly enhanced our understanding of the relationship between domain structures and functional properties, they only offer an averaged, collective response that may mask the details of individual events. In contrast, in situ transmission electron microscopy (TEM) provides a direct observation method for ferroelectric switching and domain dynamics. This approach reveals phenomena that are often concealed in macroscopic studies, offering a clearer, more detailed view of the microscale processes that govern the macroscopic properties of ferroelectric materials. One key aspect of ferroelectric research involves determining the direction and magnitude of polar ordering, typically achieved through precise measurements of atomic displacements from their equilibrium positions in centrosymmetric structures. The adoption of advanced atomic-scale Scanning Transmission Electron Microscopy (STEM) technologies, especially those equipped with 4D STEM pixelated detectors, combined with the insights from STEM image simulations and first-principles calculations, has not only enabled the direct determination of polar directions but has also expanded the research to include analysing various defect types such as oxygen vacancies, strain fields, and charge density distributions around defects. Moreover, the use of in-situ biasing/heating holders for structural examinations under applied external stimuli has enriched our understanding of the dynamic nature of ferroelectrics.

This presentation will focus on a series of structural studies exploring the dynamic properties of potassium sodium niobate. The STEM analyses were conducted using Jeol ARM 200CF and Thermo Fisher Scientific Spectra 300 Cs-corrected microscopes, both equipped with advanced Merlin and EMPAD pixelated detectors, respectively. Our studies of potassium sodium niobate materials focus on directly observing domain growth, coalescence, and interactions among different types of domain walls within the microscope's environment under applied voltage. Through these investigations, we aim to elucidate how the type, quantity, and dynamics of structural defects influence local material properties, offering opportunities for tailored manipulation and optimization.

In the study, we explore the voltage-driven dynamics of mobile, needle-like domains and DWs within a  $(K,Na)NbO_3$  single crystal (KNNsc) utilizing in situ Transmission Electron Microscopy (TEM) in a miniaturized capacitor setup [1]. Our findings suggest that the immobile DWs act as random bound pinning centres, capable of pinning larger regions while the edges of the sample facilitate the nucleation of new domains. The process of domain growth and coalescence is not consistently continuous; specific voltages can disrupt it, leading to fine domain splitting and the creation of nanoscale domains. Discontinuities in the functional response also occur when two orthogonal, needle-like domains intersect, resulting in soft-pinning events. These insights deepen our understanding of ferroelectric domain behaviour and may extend to other perovskite-based



ferroelectric materials that exhibit similar domain morphologies or coexistence of dynamic and stationary DWs.

Slovenian research and innovation agency (ARIS) is acknowledge for financial support through projects J2-3041, J7-4637, P2-0105 and P2-0421.

**Keywords:**

KNN, ferroelectrics, 4DSTEM

**Reference:**

[1]. O. Condurache et al., Applied physics letters, 2023, 20, 202902-1-202902-7

1272

## Unveiling the Mechanisms of Structural Reconstruction and Magnetic Evolution in NiFe<sub>2</sub>O<sub>4</sub> During Phase Transition

Dr. Qi Wang<sup>1,2,3</sup>, Prof. Xiaoyan ZHONG<sup>1,2,3</sup>

<sup>1</sup>Department of Materials Science and Engineering, City University of Hong Kong, Hong Kong, People's Republic of China, <sup>2</sup>City University of Hong Kong Matter Science Research Institute (Futian), Shenzhen, People's Republic of China, <sup>3</sup>Nanomanufacturing Laboratory (NML), City University of Hong Kong Shenzhen Research Institute, Shenzhen, People's Republic of China

Poster Group 1

The phase transition from spinel to rock salt structure has significant implications for information storage and energy conversion applications. Previous studies have employed various techniques, such as X-ray diffraction (XRD), neutron scattering, and X-ray absorption spectroscopy (XAS), to investigate the mechanism and pathway of this transition.[1] However, due to technical constraints, a comprehensive understanding of the transformation of local structures during this transition remains elusive, particularly regarding how local lattice and chemical environments influence the process. Moreover, the role of local structural order and chemical environment in this transition process has not been fully elucidated.[2] To bridge this knowledge gap, our study utilizes advanced transmission electron microscopy (TEM) and electron energy loss spectroscopy (EELS) techniques to monitor atomic migration and electronic structure alterations in real-time during the phase transition. By employing TEM and EELS, we aim to provide new insights into the mechanism and pathway of the spinel to rock salt phase transition, shedding light on the influence of local lattice and chemical environments on the process. These enable us to gain a deeper understanding of the local structural and chemical changes occurring during the transition, which have not been fully explored in previous studies.

### Methods

This study employs a combination of advanced scanning transmission electron microscopy (STEM) techniques to investigate the phase transition in NiFe<sub>2</sub>O<sub>4</sub>'s spinel structure under electron beam irradiation. Specifically, we utilize high-angle annular dark-field scanning transmission electron microscopy (HAADF-STEM) and annular bright-field scanning transmission electron microscopy (ABF-STEM) to dynamically observe the migration of Fe atoms within the spinel structure. In addition to the structural analysis, we employ a nanobeam electron magnetic circular dichroism (nanobeam-EMCD) method to observe the variation in magnetic information during the phase transition. This technique enables us to probe the local magnetic properties at the nanoscale and correlate them with the structural changes observed through HAADF-STEM and ABF-STEM.

### Results

Through the integration of STEM image simulations and quantitative image analysis, we have unraveled the reconstruction dynamics of octahedrally-coordinated Fe/Ni atoms during the phase transition in NiFe<sub>2</sub>O<sub>4</sub>. Our findings provide valuable insights into the lattice dynamics and Fe atom rearrangement pathways across varying coordination environments. By tracking the movement of these atoms in real-time, we have gained a deeper understanding of the atomic-level mechanisms driving the phase transition. Simultaneously, we have employed real-time electron energy loss spectroscopy (EELS) to monitor the changes in the chemical valence states of Fe, Ni, and O throughout the various stages of the phase transition. This approach has allowed us to correlate the structural changes observed through STEM with the electronic structure evolution, providing a comprehensive picture of the phase transition process. Furthermore, we have investigated the magnetism evolution during the phase transition using EMCD.[3] By correlating the structural information obtained from STEM with the magnetic information derived from EMCD, we have gained

insights into the interplay between the atomic structure and magnetic properties of NiFe<sub>2</sub>O<sub>4</sub> during the phase transition.[4]

**Keywords:**

Dynamic atomic study, NiFe<sub>2</sub>O<sub>4</sub>, EMCD

**Reference:**

[1] Choi, Hyun Woo, et al. APL Materials 4.11 (2016).

[2] Hwang, Sooyeon, et al. Chemistry of Materials 26. 1084-1092 (2014).

[3] Li Z, Lu J, Jin L, et al. Advanced Functional Materials, 2021, 31(21): 2008306.

[4] Acknowledge: This work was financially supported by NSFC (52171014), Science, Technology and Innovation Commission of Shenzhen Municipality (JCYJ20210324134402007), Guangdong Provincial Department of Science and Technology (2024A1515012303), Sino-German Center for Research Promotion (M-0265), RGC (C1013-23EF, C1018-22E, CityU 11302121, CityU 11309822), European Research Council (856538, "3D MAGiC"), and CityU (9610484, 9680291, 9678288, 9610607 · 7020043).